

AN INVESTIGATION INTO THE EFFECT OF FUEL PELLET ECCENTRICITY
ON FUEL-CLADDING GAP HEAT TRANSFER

A THESIS

Presented to

The Faculty of the Division of Graduate
Studies and Research

By

Marc David Goldberg

In Partial Fulfillment
of the Requirements for the Degree
Master of Science in Nuclear Engineering

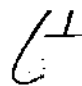
Georgia Institute of Technology

August, 1974

AN INVESTIGATION INTO THE EFFECT OF FUEL PELLETT ECCENTRICITY
ON FUEL-CLADDING GAP HEAT TRANSFER

Approved:


James H. Rust, Chairman


G. G. Eichholz


R. A. Karam

Date approved by Chairman: Aug 19, 1974

ACKNOWLEDGMENT

The author wishes to express his thanks to his thesis advisor, Dr. James H. Rust, for his never-ending encouragement. His experience and expert critical suggestions provided inspiration and incentive during the preparation of this paper.

Thanks are also due to Dr. G. G. Eichholz and Dr. R. A. Karam. Their critical suggestions as members of the Reading Committee were very helpful.

Finally, the author wishes to thank Susie for her patience and support, without which this travail would have become unbearable.

TABLE OF CONTENTS

	Page
ACKNOWLEDGMENTS.	ii
LIST OF TABLES	iv
LIST OF ILLUSTRATIONS.	v
ABSTRACT	vii
Chapter	
I. INTRODUCTION.	1
II. FORMULATION OF MODEL.	6
III. COMPUTER ANALYSIS	16
IV. DISCUSSION OF RESULTS	20
V. CONCLUSIONS	58
APPENDICES	60
A. DERIVATION OF EQUATIONS	61
B. DETERMINATION OF GAP.	70
C. COMPUTER PROGRAM.	74
D. DATA FOR CHAPTER V.	94
E. NOMENCLATURE.	102
BIBLIOGRAPHY	104

LIST OF TABLES

Table		Page
1.	Temperature Jump Distances.	9
2.	Initial and Final Values for Non-dimensional Parameter Ranges.	15
3.	Summary of Computer Runs.	17
4.	Comparison of Normalized Heat Flux for Boiling and Non-boiling Heat-Transfer Coefficient	21
5.	Comparison of Normalized Heat Flux for Boiling and Non-boiling Heat-Transfer Coefficient	23
6.	Maximum Temperature and Heat Flux Ratios for Varying Temperature Jump Distances.	24
7.	Maximum Temperature and Heat Flux Ratios for Varying Temperature Jump Distances.	24
8.	Fuel Surface Temperatures for Concentric Fuel Pellets	43
9.	Comparison Between Actual Values and Approximation Values of Gap Size.	72

LIST OF ILLUSTRATIONS

Figure	Page
1. Geometry of Problem	2
2. Thermal Conductivity of Mixtures.	13
3. Radial Fuel Temperature Distribution.	26
4. Radial Fuel Temperature Distribution.	28
5. Radial Fuel Temperature Distribution as a Function of $\Delta r/R_f$	29
6. Radial Fuel Temperature Distribution as a Function of $\Delta r/R_f$	30
7. Isotherms in Concentric Fuel Pellet	31
8. Isotherms in Eccentric Fuel Pellet.	32
9. Isotherms in Eccentric Fuel Pellet.	33
10. $\phi_f = 1.0$ Isotherm in Eccentric Fuel Pellet.	34
11. Fuel Surface Temperature as a Function of $\Delta r/R_f$	36
12. Cladding Outside Temperature as a Function of $\Delta r/R_f$	37
13. Normalized Wall Heat Flux as a Function of $\Delta r/R_f$	38
14. Fuel Surface Temperature as a Function of $\Delta r/R_f$	39
15. Cladding Surface Temperature as a Function of $\Delta r/R_f$	40
16. Normalized Wall Heat Flux as a Function of $\Delta r/R_f$	41
17. Normalized Wall Heat Flux	44

LIST OF ILLUSTRATIONS (Concluded)

Figure	Page
18. Normalized Wall Heat Flux	45
19. Normalized Wall Heat Flux	46
20. Normalized Fuel Surface Temperature	48
21. Normalized Wall Heat Flux	49
22. Normalized Temperature.	50
23. Normalized Wall Heat Flux	51
24. Normalized Wall Heat Flux	52
25. Normalized Wall Heat Flux	53
26. Normalized Wall Heat Flux	54
27. Normalized Wall Heat Flux	56
28. Normalized Wall Heat Flux	57
29. Gap Geometry.	71

ABSTRACT

Current nuclear reactor technology relies heavily on computer codes to calculate heat fluxes and temperature distributions in fuel and cladding. Temperature distributions are usually assumed to depend only upon the radial coordinate. This assumption is reasonable when intimate contact exists between fuel and cladding, forming concentric cylinders. A gap will exist between the fuel and cladding due to radial differences or fuel densification. The fuel pellet now can be eccentrically located in the cladding causing the temperature distributions to depend on the angular coordinate as well as radial. This thesis investigates the error in heat flux and temperature distributions incurred by assuming concentric geometry for situations involving eccentric fuel pellets.

A computer program was written to solve for temperature distributions and heat fluxes in the fuel and cladding. The major parameters include thermal conductivity ratio of gas to fuel, relative radial difference of fuel and cladding, and degree of relative eccentricity.

The study indicated that diametrical clearance and relative eccentricity (given by $\epsilon = e/R_f$) were important parameters in determining the degree of asymmetry in temperature and heat flux distributions. In addition, a decrease in gas thermal conductivity, which is due to the dilution of helium with fission product gases, increased the amount of asymmetry when keeping other parameters fixed. The effect of varying convection heat transfer coefficients was negligible. Maximum fuel temperatures were

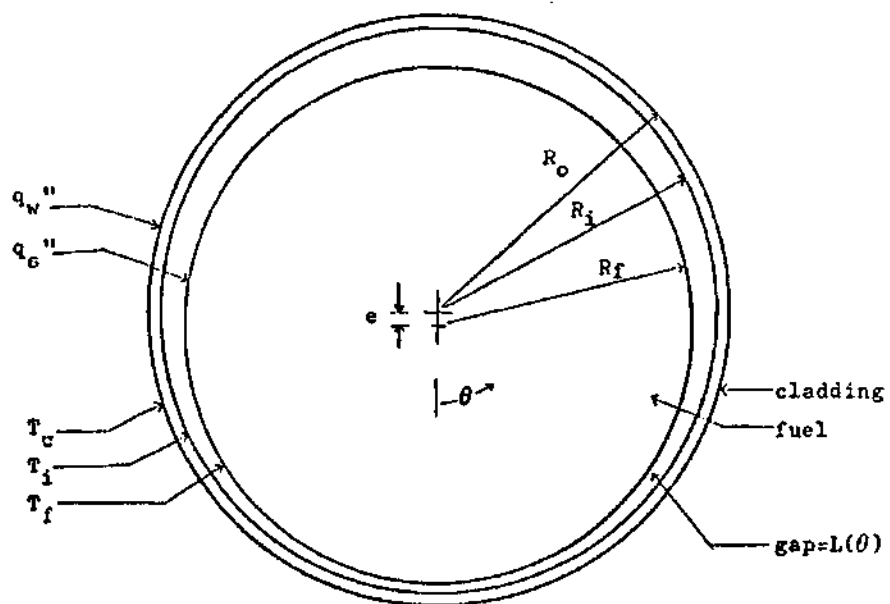
unchanged or smaller when comparing eccentric fuel pellets with concentric fuel pellets.

CHAPTER I

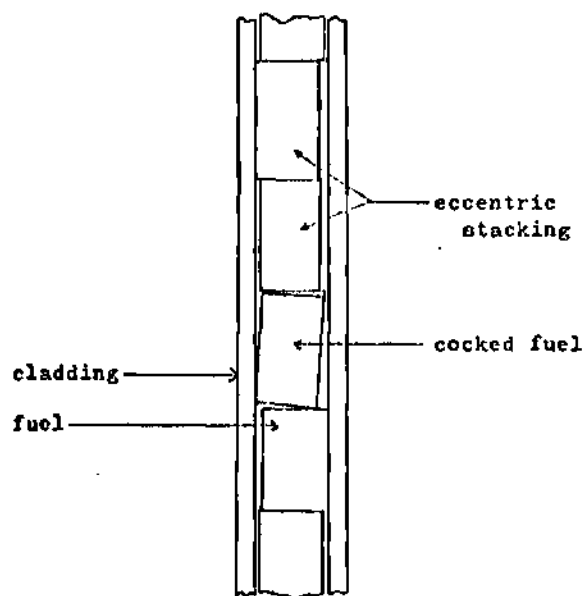
INTRODUCTION

Current nuclear reactor technology depends heavily on the proper design of reactor fuels and on an accurate analysis of the thermodynamic aspects of heat generation. Water-cooled reactor fuel elements commonly consist of uranium-dioxide (UO_2) fuel pellets contained within a thin-walled cladding of stainless steel or zirconium alloy. A gas-filled gap normally exists between the fuel pellet and inside cladding wall at room temperature. Helium is most often chosen for this fill because of its non-corrosive behavior and its excellent heat transfer properties.

In order to analyze fuel temperature distributions in reactor cores, computer codes, such as CYGRO,¹ FIGRO,² FMODEL,³ TAFY,⁴ and others are used. These codes assume that temperatures are a function of only the radial coordinate, which implies that the fuel pellet is concentrically located within the cladding. This assumption is reasonable at the beginning of operation where, due to thermal expansion of the fuel at operating temperatures, the fuel and cladding are in intimate contact. Recent investigations have discovered in some fuel elements the occurrence of significant densification towards end of life operations.^{5,6} Intimate contact then no longer exists at all points on the fuel surface. More likely, the fuel pellets will be stacked eccentrically or cocked within the cladding, as shown in Figure 1. Should either



a. Fuel-Cladding Geometry



b. Fuel Stacking

Figure 1. Geometry of Problem

of these cases occur, neither temperatures nor heat fluxes are independent of the angular coordinate and significant errors in code calculation may occur.

The purpose of this investigation is to examine heat transfer in fuel elements with fuel pellets located eccentrically within the cladding and determine the extent of error in those calculations that assume concentric behavior. To this end, an analytical solution was obtained for fuel temperature distributions and heat fluxes for the situations described above. Accurate determination of these quantities is essential for further analysis of reactor fuel behavior. Thermal stresses, fuel or cladding melting, and departure from nucleate boiling (DNB) are examples of calculations that rely on accurate calculation of heat fluxes and temperature distributions. A parametric study was performed by varying major variables over values that could reasonably be expected during the operation of a reactor. Among these parameters are the ratio of gas-to-fuel thermal conductivity (K_g/K_f), the degree of relative pellet eccentricity ($\epsilon = e/R_f$), and the ratio of average gap width to pellet radius ($\Delta r/R_f$). Results of this study were compared to equivalent systems with concentric loading so as to evaluate errors that arise due to the one-dimensional assumptions.

Few heat transfer investigations have been published studying fuel pellets located eccentrically in the cladding. A study by R. Nijssing⁷ examined non-uniform heat fluxes and temperature distributions due to variable internal heat generation, non-uniform heat-transfer coefficient, as well as eccentrically located fuel pellets. He obtained an infinite

series solution for temperature distributions similar in form to the one obtained in Appendix A, though with some notable differences. The contact heat-transfer coefficient was based on accommodation factors and not on the thermal conductivity of the gas in the gap. As will be discussed in Chapter II, data for accommodation factors are not plentiful and cannot be relied on with the same confidence as the experimentally determined values used in this study. Nijsing's study arbitrarily increased the nominal value of the contact resistances, but without regard for changes in fill gas thermal conductivity. The major thrust of his investigation examined temperature changes and not cladding heat flux distributions. The solution was not normalized to be independent of volumetric heat generation, q''' . The results of Nijsing's analysis showed up to 10% variations in heat fluxes due to fuel pellet eccentricity.

A second investigator, A. J. Brook,⁸ took a portion of Nijsing's analysis to discuss the problems of fuel pellets mounted eccentrically in the cladding. Brook maintained that his temperature and heat flux variations were not as severe as the data indicated because high temperature and the accompanying thermal expansion would cause intimate contact between fuel and cladding, thus diminishing the degree of eccentricity. As mentioned, this is not a reasonable assumption with densified fuel since gaps do appear. Like Nijsing's, Brook's values were not normalized to include independence from the power level term q''' . Brook reported 61% temperature variations around the pellet surface with the pellet in the maximum eccentric position.

A later investigation by Grillo and Testa⁹ was directed towards

variations in temperature and heat flux due to non-homogeneity of pressed and vibrationally compacted mixed oxide ($\text{UO}_2\text{-PuO}_2$) fuels. They briefly considered the effects of cladding ovality and pellet eccentricity. The solution used only an approximation for the gap heat-transfer coefficient and failed to indicate the method used for obtaining heat fluxes. The solution assumed perfect contact between fuel and cladding and does not appear to have been normalized either dimensionally or to power levels. Although they considered an end of exposure situation, the nominal values of contact resistance were assigned rather than calculated on the basis of fission gas content. They reported a value of 1.255 for maximum-to-average ratio of heat flux at end of exposure of the fuel.

Another approach to the problem of angular dependence was performed by Wolf and Johannsen.¹⁰ This mathematical analysis was directed toward solution of temperature distributions in sodium-bonded fuel pellets located eccentrically within the cladding. The heat conduction equation was solved for hollow cylinders using bipolar coordinates. These coordinates were defined by:

$$\xi = \{ [(x-c)^2 + y^2] [(x+c)^2 + y^2]^{-1} \}^{\frac{1}{2}} \quad 0 \leq \xi \leq 1$$

$$\eta = \arctan \frac{2cy}{x^2 + y^2 + c^2}$$

where $c = x$ coordinate of center of the cylinder. They obtained a series solution, but it was mainly concerned with η -dependent contact coefficient of the bonding and q''' . However, with proper adjustment for geometry and normalization, the solution could be applied to a gas-filled element.

CHAPTER II

FORMULATION OF MODEL

The basis for the parametric study is a computer program written by the author to solve the equation

$$\Phi(\xi, \theta) = -\xi^2 + \sum_{\nu=0}^{\infty} a_{\nu} \xi^{\nu} \cos \nu \theta \quad (2.1)$$

This equation solves for the non-dimensional fuel temperature distributions for a pellet as shown in Figure 1a. The term ξ is the non-dimensional radius (r/R_f) and Φ is the non-dimensional temperature given

by $(T-T_b) / \frac{q'''R_f}{4K_f}$,

where T_b = bulk temperature of coolant
 R_f = pellet radius
 K_f = thermal conductivity of fuel
 q''' = volumetric heat generation

The expression assumes negligible axial heat conduction and constant K_f and q''' . The set of constants a_{ν} arises from the application of the surface boundary condition of the problem. The derivation of this equation can be found in Appendix A along with the application of the surface boundary condition for the solution of the set of constants a_{ν} .

The major objective of this investigation is a parametric study to determine the effect of various parameters on heat transfer in eccentric-

ally loaded fuel pellets. The major non-dimensional parameters that affect the system are:

ϵ = relative eccentricity factor (e/R_f)

G = temperature jump distance (g_1+g_2/R_f)

$\Delta r/R_f$ = difference in radii (R_i-R_f/R_f)

K_g/K_f = thermal conductivity ratio (gas to fuel)

K_c/K_f = thermal conductivity ratio (clad to fuel)

$R_f h_w / K_f$ = cladding surface Nusselt number

An important quantity in the calculation of the constants is the value of the "contact" heat-transfer coefficient $h_c(\theta)$ in $\text{Btu/hr-ft}^2\text{-}^\circ\text{F}$. The major heat transfer mechanism in the gas-filled gap is conduction, since there would be little free convection across such a small gap width. However, the use of an effective $h_c(\theta)$ at the fuel boundary allows a method of calculation to be applied. As will be seen, the values of $h_c(\theta)$ are strongly dependent upon the gas thermal conductivity, K_g .

Two expressions for the heat-transfer coefficient that have reasonable agreement with actual experimental values were proposed by R. Nijsing¹¹ and by A. M. Ross and R. L. Stoute.¹² Both are similar in form. Nijsing uses

$$h_c(\theta) \propto \frac{1}{L(\theta)} \quad (2.2)$$

where $L(\theta)$ = gap width = $(R_i - R_f)(1 + \epsilon \cos \theta)$

provided a nominal gap $R_i - R_f$ corresponds to a nominal contact resistance for the fuel, β_o . So,

$$h_c(\theta) = \frac{1}{\beta_o(1+\epsilon\cos\theta)} \quad (2.3)$$

The coefficient is rewritten in the form $h_c(\theta) = 1/v+w \cos\theta$. An average heat-transfer coefficient is found by

$$\bar{h}_c = \frac{1}{\pi} \int_0^\pi h_c(\theta) d\theta$$

which leads to a modified heat transfer coefficient

$$h_c(\theta) = \bar{h}_c \frac{v^2+w^2}{v+w\cos\theta} \quad (2.4)$$

The Nijssing expression for $h_c(\theta)$ was not used in this analysis, because experimental data for values of β_o were not readily available. Additionally, this factor was proposed as a function of fuel material where, actually, contact resistances depend on the surrounding gas as well as the fuel material.

The Ross and Stoute correlation for heat transfer coefficient is given by¹²

$$h_c(\theta) = \frac{K_g}{L(\theta) + (g_1 + g_2)} + \frac{K_m P}{a_o R^2 H} \quad (2.5)$$

where K_g = thermal conductivity of gas in gap
 L = actual gap at θ
 $g_1 + g_2$ = temperature jump distance
 P = contact pressure

The contact pressure will always be assumed negligible in this investigation and, consequently, the second term will be zero. The jump distances, g_1+g_2 , are functions of the gas in the gap and represent the increase in gap at each surface due to accommodation effects. Values for g_1+g_2 have been experimentally determined by Ross and Stoute and are shown in Table 1.

Table 1. Temperature Jump Distances¹²

Gas	(g_1+g_2) (cm)	Temperature Range (°C)
Helium	10×10^{-4}	150-250
Argon	5×10^{-4}	180-230
Krypton	1×10^{-4}	180-330
Xenon	$< 1 \times 10^{-4}$	180-330

$L(\theta)$ for this problem, as indicated in Figure 1a, is closely approximated by

$$L(\theta) = (R_i - R_f) - e \cos \theta \quad (2.6)$$

This determination was made by comparing hand calculated values from the above statement to a computer trigonometric solution for the exact gap at discrete θ 's. The correlation was always within a 1% error for all θ . A computer program for this calculation was written by the author in FOCOL-F and is listed in Appendix B along with a sample output of results.

The Ross and Stoute heat-transfer coefficient was used in this

investigation because of its dependency on the gas conductivity as well as the surface condition in the determination of g_1+g_2 .

It should be noted here that data for temperature jump distances were not available at each temperature and gas composition used in the parametric study and this could have an effect on the results of this study. It was ultimately decided that the data would be affected equally by the available g_1+g_2 values since a parametric study is as much interested in comparison of the variables as it is with exact values. The Ross and Stoute expression for $h_c(\theta)$ has become widely accepted because of its ease of application and the high quality of experimental investigation from which it was derived. In this light, the author chose Eq. 2.5 as being the best available. Other expressions have been proposed by Tong and Weisman¹³ and by R. A. Dean¹⁴; however, these were not considered as accurate as the Ross and Stoute expression.

Large variations in the ratio K_g/K_f arise from changes in the thermal conductivities of the gas and fuel. At the beginning of service, the gas fill can be assumed to be pure helium. K_g can be obtained at operating conditions from tables of physical data. However, as noted in the introduction, the eccentricity problems affect the system more significantly towards the end of the fuel rod life. At this point, the gas is certain to be contaminated with gaseous fission products making the calculation of gas thermal conductivity a more difficult task. The important factor is that the thermal conductivities of pure xenon and krypton, two major gaseous fission products, are several orders of magnitude lower than helium.

Physical properties of gaseous mixtures have been studied extensively

through use of the kinetic theory of gases. Numerous analytical solutions are available which agree adequately with experimental observations. An early correlation by A. Wassiljewa¹⁵ gave the thermal conductivity of a gaseous mixture as

$$K_{\text{mix}} = \frac{K_1}{1 + A_{12} \left(\frac{x_1}{x_2}\right)} + \frac{K_2}{1 + A_{21} \left(\frac{x_1}{x_2}\right)} \quad (2.7)$$

where x_1, x_2 = mole fraction of components 1 and 2

A_{12}, A_{21} = constants dependent on mixture and temperature

Other expressions have been proposed by Hirschfelder, et al.,¹⁶ Lindsay and Bromley,¹⁷ and Srivastava and Saxena.^{18,19}

Von Ubisch, Hall, and Srivastav²⁰ have presented data for the thermal conductivity of helium mixed with krypton and xenon. Their analysis assumed the fission gas composition in the gap to be 15.3% krypton and 84.7% xenon. Iodine and others were disregarded since, although they may have high production rates, they do not escape the fuel to the gap in sufficient quantities to affect the thermal conductivity. The relative quantities of krypton and xenon produced are supported by data reported by Russian scientists Zysin, Lbov, and Sel'chenkov.²¹ Actual fission gases in the gap will probably be higher in krypton concentration since, being the lighter gas, it will more easily diffuse through the fuel material. However, at longer burnup times, the concentrations will closely approach the values reported above. Von Ubisch, et al. used atmospheric gases and not fission gases in their experiments. Although isotopic compositions are different, thermal conductivities would vary by about 1%.

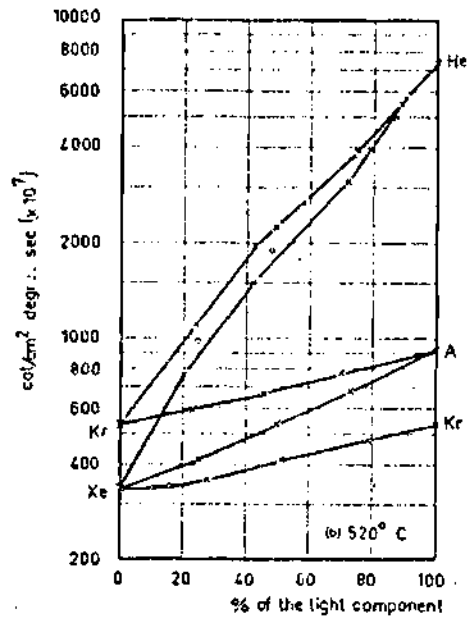
According to kinetic theory, thermal conductivities vary inversely as the square root of the molecular weight of the species. Figure 2 shows some results of the von Ubisch investigations.

From the von Ubisch results, the range of values for K_g for use in the parametric study was determined. This range is $K_g = 0.16$ Btu/hr-ft-°F for beginning of life to $K_g = 0.016$ Btu/hr-ft-°F at large burnup conditions. These values represent the range of possible values of interest in a nuclear reactor and correspond to about 100% He and 10% He as the gas concentrations at the beginning and end of life, respectively.

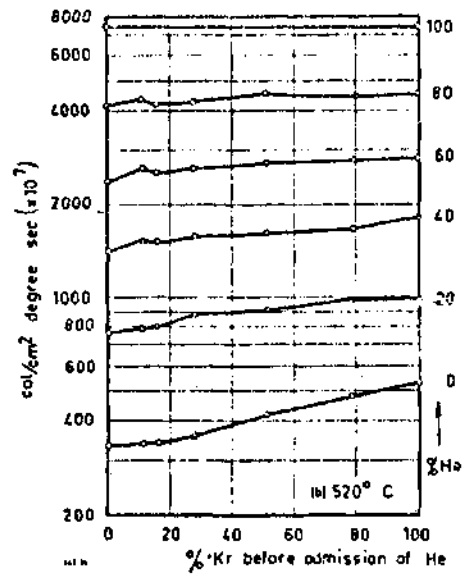
For the purposes of this investigation, the value of e ranged from zero for the concentric case to a value within 0.001 inch of the difference in radii. This latter value accounted for an assumed average surface roughness of cladding and fuel. It is unwarranted to assume smooth, metallurgically perfect surfaces so that e would equal Δr . To do so would lead to unrealistically large heat-transfer coefficients across the gap.

The range of values of K_f at operating conditions is of the order of 1.8 - 2.2 Btu/hr-ft-°F. To calculate the quantity of interest, which is the ratio K_g/K_f , the value for K_f for UO_2 was held constant at 2.0 Btu/hr-ft-°F. Then K_g can be calculated and will determine the ratio value. Similarly, the value for thermal conductivity of the cladding K_c was assigned the value of 8.0 Btu/hr-ft-°F. It was found that the ratio K_c/K_f had almost no effect on temperature distributions as compared to K_g/K_f , and thus was not varied as a parameter.

The study was also concerned with variations in the diametral clearance. This value will vary with design and manufacturers' tolerances. For the purpose of the parametric study, the diametral clearance was varied



a. Binary Mixture of Gases at 520°C ²⁰



b. Ternary Mixture of He-Kr-Xe at 520°C ²⁰

Figure 2. Thermal Conductivity of Mixtures

from 0.0 to 0.012 inch. This value appears in the quantity $\Delta r/R_f$.

As indicated in Table 1, data for the temperature jump distances are not plentiful. It is clear that the values depend on the gas in question, but not clear how variations of the mixtures will affect them. For the purposes of this study, the jump distances, g_1+g_2 , will be assumed to vary in the same manner as the thermal conductivity varies for a mixture of helium with fission gases. The range of values used for g_1+g_2 is from 3.281×10^{-5} ft to 3.281×10^{-6} ft.

The heat-transfer coefficient from the cladding to the coolant, h_w , is another term that can vary. The main concern with this study will be comparison between boiling and non-boiling heat transfer. For the purposes of this parametric study, the non-boiling heat transfer coefficient, $h_w(NB)$, was assumed as $5000 \text{ Btu/hr-ft}^2\text{-}^\circ\text{F}$ and for boiling heat-transfer coefficient, $h_w(B)$, was assumed as $50,000 \text{ Btu/hr-ft}^2\text{-}^\circ\text{F}$. These are typical values encountered in nuclear reactors.²²

It should be noted that, due to the normalization of the variables, temperature distributions are independent of the volumetric heat generation rate. Hence they apply at all power levels. With these ranges for parameters, the proper non-dimensional quantities were determined for use by the computer program. Table 2 indicates the initial and final values used for ranges of the non-dimensional parameters. The value for R_f was assumed as 0.185 inch, a typical value for pressurized water reactors.

Table 2. Initial and Final Values for Non-dimensional
Parameter Ranges

Parameter	Initial Value	Final Value
ϵ	0.0	0.032432
G	2.1282×10^{-3}	2.1282×10^{-4}
$\Delta r/R_f$	0.0	0.032432
K_g/K_f	0.08	0.008
K_c/K_f	4.0	constant
$R_{fw}^h(NB)/K_f$	38.542	constant
$R_{fw}^h(B)/K_f$	385.42	constant

CHAPTER III

COMPUTER ANALYSIS

Computer Program

A computer program was written to provide numerical solutions to the non-dimensional temperature distribution of Eq. 2.1 by solving Eq. A.20 for the set of constants a_v . Equation A.20 uses the Ross and Stoute expression of Eq. 2.5. The listing of the program and a sample output are included in Appendix C. The program was written for use on the UNIVAC 1108 at the Georgia Institute of Technology in modified Fortran IV and can be easily adapted to any high level system.

The basic flow of the program begins with solving for the coefficients a_v in subroutine INTEG. The function STEPNI is a Simpson's rule integration routine packaged in the UNIVAC system library. Once the a_v values are obtained, calculation of fuel surface temperatures, wall heat fluxes, and maximum fuel temperatures can be accomplished. Temperature maps can also be obtained in order to show isotherms in a fuel pellet cross section. The maps are obtained by using NEWTIT, a Newton-Raphson iteration technique which is also a packaged library program. This routine solves the roots of Eq. 2.1 to give radius as a function of temperature and angle.

As can be noted from the program, only a_0 through a_7 were used in the calculations. In a strict sense, a mathematical convergence criterion was not employed. However, the series in Eq. 2.1 quickly converged, and

the constants a_n rapidly approached zero. The general procedure used solved the equations using a_0 and adding a successive term each time. The values obtained each time were compared with preceding values to check for convergence. It was found that by including a_7 , the value of $\psi(\xi, \theta)$ changed by less than 0.01% in all cases. A similar procedure was used in the analysis by Nijsing.²³

The computer program calculated temperature and heat flux distributions for a wide variety of parameter values. Table 3 lists the conditions for each run. The individual run represents either a boiling or non-boiling case, as determined by h_w , and a single value of G . The parameters ϵ , K_g/K_f , and $\Delta r/R_f$ are varied over the full range of values.

Table 3. Summary of Computer Runs

Run No.	Surface	G
1	Non-boiling	3.2810×10^{-5}
2	Boiling	3.2810×10^{-5}
3	Non-boiling	3.2810×10^{-6}
4	Boiling	3.2810×10^{-6}
5	Non-boiling	2.5428×10^{-5}
6	Boiling	2.5428×10^{-5}
7	Non-boiling	1.8046×10^{-5}
8	Boiling	1.8046×10^{-5}
9	Non-boiling	1.0663×10^{-5}
10	Boiling	1.0663×10^{-5}

Data from the program were obtained in three distinct forms:

1. Distributions--these include:

- a. Fuel surface temperature as a function of $\theta[\bar{\phi}_f]$
- b. Fuel surface temperature relative to the concentric case
 $[\bar{\phi}_f/\bar{\phi}_f(\text{conc})]$
- c. Cladding surface temperature as a function of $\theta[\bar{\phi}_c]$
- d. Cladding surface temperature relative to the concentric case
 $[\bar{\phi}_c/\bar{\phi}_c(\text{conc})]$
- e. Cladding surface heat flux relative to the concentric case
 $[q_w''/q_w''(\text{conc})]$
- f. Cladding surface heat flux relative to the concentric case
 $[\text{Nu} \times \bar{\phi}_c/q_w''(\text{conc})]$
- g. Maximum fuel temperature $[\bar{\phi}_{\text{max}}]$

2. Temperature profiles

This gives fuel temperatures as a function of radius on a cross section through the 0° and 180° points, which are the cold and hot spots on the fuel surface, respectively.

3. Temperature maps

This gives data in the form of radii as a function of temperature and angle and for use in plotting isotherms in the fuel.

In the cases of 1e and 1f above, the two values represent independent determinations of cladding surface heat flux and serve to check each other.

Input Instructions

For the computer program used, all of the constants were included in element MAIN with the exception of those parameters that had a range of values and those that changed frequently. These were input in "read"

statements from element DATA. The instructions for the four data cards are as follows.

Card 1--

I2	M999	A two digit number indicating the run code
I2	KJJ	1 for non-boiling, 2 for boiling

Card 2--

F10.7	CF1	Thermal conductivity of fuel (K_f)
F10.7	CG1	Initial thermal conductivity of gas (K_g)
F10.7	CCL1	Thermal conductivity of cladding (K_c)
F10.7	GG1	Temperature jump distance (G)
F10.7	DR1	Initial value for $\Delta r/R_f$

Card 3--

F10.7	CG4	Final thermal conductivity of gas (K_g)
F10.7	DR4	Final value of $\Delta r/R_f$

Card 4--

F5.4	CG99	Number of increments between CG1 and CG4
F5.4	DR99	Number of increments between DR1 and DR4

A sample listing of DATA is included in Appendix C at the end of the program listing.

It should be noted that the eccentricity factor (ϵ) is varied from 0.0 to the value of $\Delta r/R_f$ at each parameter setting. Its value is set by control from MAIN and not from data cards.

CHAPTER IV

DISCUSSION OF RESULTS

Data for the parametric study were obtained in normalized form from computer calculations described in Chapter III. They were analyzed by observing how parameter values and combinations of parameter values affected temperature and heat flux distributions in the fuel and cladding.

Dependence on Cladding Outside Heat-transfer Coefficient

For this study, h_w was assigned values representative of boiling and non-boiling heat transfer at the cladding surface. The calculations showed that changing this surface condition had almost no effect on the system except for causing different cladding surface temperatures.

Table 4 compares normalized heat fluxes for a medium burnup ($K_g/K_f = 0.044$), medium eccentric ($e = 0.016216$) case for boiling and non-boiling heat-transfer coefficients. The results show an almost negligible (less than 1%) difference between the boiling and non-boiling cases. From the printouts for these cases, pages 95 and 96 in Appendix D, the effect of changing h_w on cladding surface temperatures can be seen. As expected, the values of $\bar{\Phi}_c$ show considerable variation due to h_w . However, one should note the close agreement between the ratio $\bar{\Phi}_c/\bar{\Phi}_c(\text{conc})$ in the two cases. The fuel surface temperatures, $\bar{\Phi}_f$, show slightly lower values in the boiling case. This is to be expected since $\bar{\Phi}_c$ is smaller. However, the eccentricity effect which is observable in the ratio

Table 4. Comparison of Normalized Heat Flux for Boiling and Non-boiling Heat-Transfer Coefficient

Theta	$q_w''/q_w''(\text{conc})$ (non-boiling)	$q_w''/q_w''(\text{conc})$ (boiling)
0	1.285045	1.290463
10	1.276965	1.281998
20	1.254266	1.258378
30	1.220589	1.223699
40	1.179769	1.182012
50	1.134795	1.136191
60	1.088163	1.088612
70	1.042438	1.041991
80	0.999884	0.998874
90	0.961584	0.960382
100	0.927339	0.926032
110	0.896697	0.895107
120	0.869934	0.867954
130	0.847829	0.845650
140	0.830622	0.828548
150	0.817596	0.815692
160	0.807890	0.805929
170	0.801508	0.799291
180	0.799223	0.796861

Parameters:

$$e = 0.016216$$

$$K_g/K_f = 0.044$$

$$\Delta x/R_f = 0.024324$$

$\phi_f/\phi_f(\text{conc})$ shows almost no change when comparing the boiling and non-boiling values. One should further note from those pages that the maximum fuel temperature for the boiling case differed by less than 2% from the non-boiling value.

The conclusions drawn from the above comparison apply equally well in the case of greater burnup ($K_g/K_f = 0.026$) and medium eccentricity ($\epsilon = 0.010811$). Table 5 shows the normalized wall heat flux comparison for these parameters and pages 97 and 98 of Appendix D show the temperature comparison. From the data for these two cases, and others not shown, it was determined that the cladding surface heat-transfer mechanism had little effect on heat transfer from eccentric pellets as opposed to concentric ones. Further analysis in this chapter will deal solely with non-boiling heat-transfer coefficients.

Dependence on Temperature Jump Distances

The temperature jump distance is a quantity found in the denominator of $h_c(\theta)$. It serves to increase $\Delta r/R_f$ in varying amounts to account for surface effects of cladding and fuel. From the data obtained, it was determined that the values used for the quantity g_1+g_2 (G in non-dimensional form) had little effect on the temperature and heat flux ratios. Five values were used for G and five for $\Delta r/R_f$. The effect of changing G only produced a set of 25 $\Delta r/R_f$ values that were spaced together with smaller intervals. Table 6 shows the effect of varying G on the maximum values of $q_w''/q_w''(\text{conc})$ and $T_f/T_f(\text{conc})$. This case used values of $\Delta r/R_f = 0.024324$, $K_g/K_f = 0.044$, and eccentricity $\epsilon = 0.021622$. As the table shows, there is only a few percent of change in the maximum values over the entire range of G . Table 7 shows a similar comparison for $\Delta r/R_f = 0.016216$, $K_g/K_f =$

Table 5. Comparison of Normalized Heat Flux for Boiling
and Non-boiling Heat-Transfer Coefficient

Theta	$q_w''/q_w''(\text{conc})$ (non-boiling)	$q_w''/q_w''(\text{conc})$ (boiling)
0	1.297963	1.303081
10	1.289705	1.294531
20	1.266275	1.270349
30	1.231033	1.234160
40	1.187943	1.190121
50	1.140551	1.418240
60	1.091803	1.092220
70	1.044212	1.043886
80	0.999721	0.998863
90	0.959375	0.958199
100	0.923354	0.921959
110	0.891541	0.889914
120	0.864062	0.862201
130	0.841240	0.839241
140	0.823125	0.821116
150	0.809302	0.807324
160	0.799293	0.797275
170	0.793043	0.790923
180	0.790888	0.788713

Parameters:

$$e = 0.010811$$

$$K_g/K_f = 0.026$$

$$\Delta x/R_f = 0.016216$$

Table 6. Maximum Temperature and Heat Flux Ratios
for Varying Temperature Jump Distances

Run	G	q''_w/q''_w (conc) (maximum)	ϕ_f/ϕ_f (conc) (maximum)
1	0.00212821	1.407575	1.311244
5	0.00164938	1.412778	1.318591
7	0.00117055	1.418279	1.326269
9	0.00069165	1.427633	1.338811
3	0.00021282	1.430405	1.342777

Parameters:

$$\epsilon = 0.021622$$

$$K_g/K_f = 0.044$$

$$\Delta r/R_f = 0.024324$$

Table 7. Maximum Temperature and Heat Flux Ratios
for Varying Temperature Jump Distances

Run	G	q''_w/q''_w (conc) (maximum)	ϕ_f/ϕ_f (conc) (maximum)
1	0.00212821	1.232924	1.052909
5	0.0014938	1.238030	1.055208
7	0.00117055	1.243374	1.057664
9	0.00069165	1.249101	1.060373
3	0.00021282	1.254856	1.063104

Parameters:

$$\epsilon = 0.005405$$

$$K_g/K_f = 0.008$$

$$\Delta r/R_f = 0.016216$$

0.008, and $\epsilon = 0.005405$. The same behavior appears over the range used for G . These and other data indicate a much stronger dependence on $\Delta r/R_f$ and only a minor dependence on G . Also, the maximum ratio values in these two tables always occur at the lowest G value ($G = 0.0212821 \times 10^{-3}$). For this reason, all subsequent discussion of eccentric distributions will use this minimum value for G . This will provide a limiting upper value on reported ratios with respect to the temperature jump distances.

Effect of Parameter Values on Maximum Fuel Temperature

The quantity that affects maximum fuel temperatures the most noticeably is the gas thermal conductivity in the ratio K_g/K_f . As this ratio is decreased, the maximum fuel temperature rises. At any given value for K_g/K_f , the maximum fuel temperature is affected markedly by the degree of eccentricity ϵ . The results of this study indicate that, for a constant K_g/K_f , the maximum fuel temperature occurs in the concentric configuration. Eccentricity tends to lower the maximum temperature and move its location from the pellet center along the 180° line.

Figure 3 shows fuel temperature profiles for $K_g/K_f = 0.062$ and $\Delta r/R_f = 0.016216$ and three values for pellet eccentricity. The 0 - 180° cross section was chosen for the profiles because of gap sizes at these locations. For 0° , the gap is smallest and temperatures are lowest due to high $h_c(\theta)$ values. For $\theta = 180^\circ$, the gap has its maximum value and, consequently, $h_c(\theta)$ has its lowest value and the fuel surface temperature has its maximum value. Maximum fuel temperatures for $\epsilon > 0$ are less than that for the concentric case and displaced towards the side with smallest

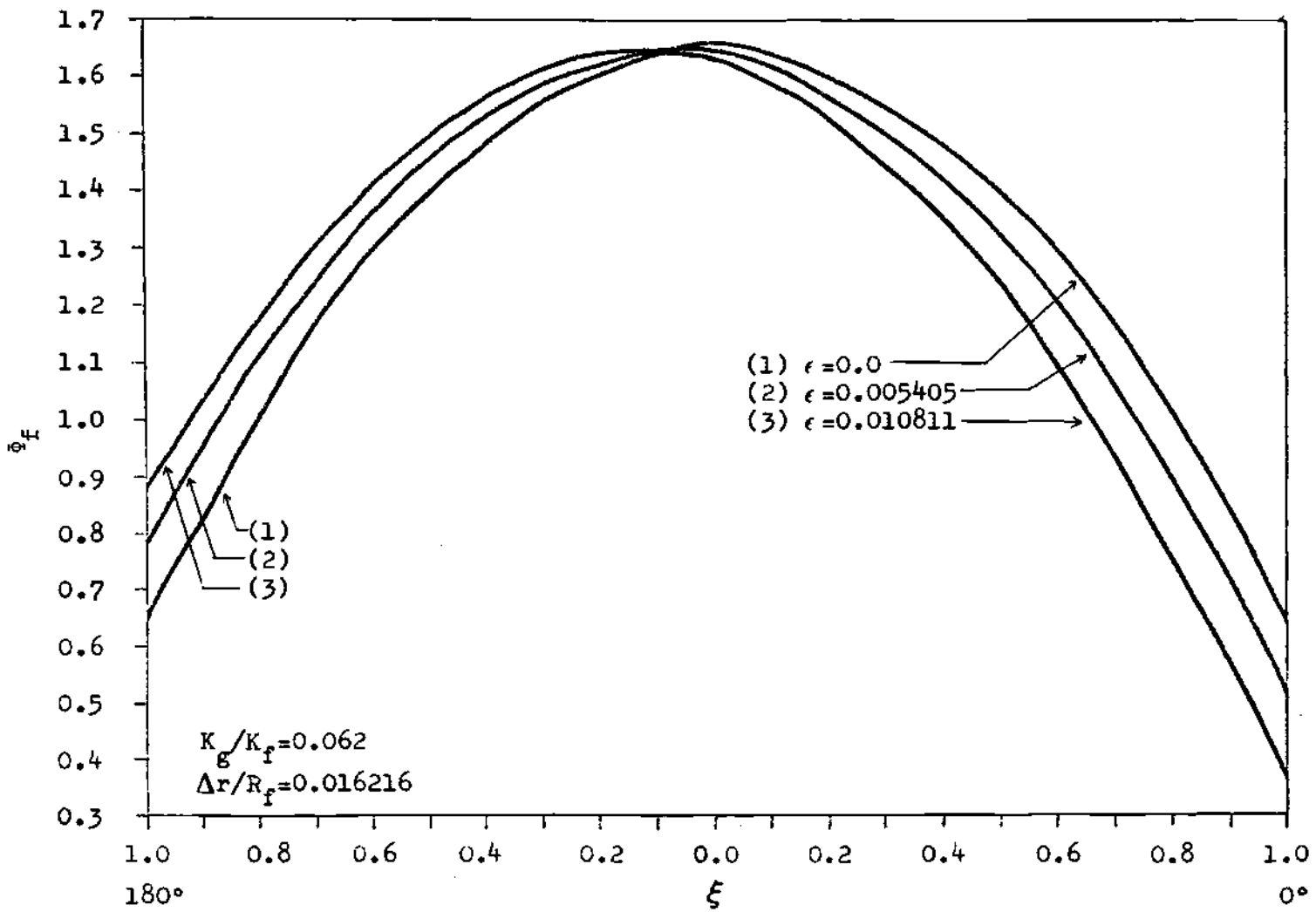


Figure 3. Radial Fuel Temperature Distribution

contact heat-transfer coefficient ($\theta = 180^\circ$). Figure 4 shows identical behavior for $K_g/K_f = 0.026$ and $\Delta r/R_f = 0.016216$. Temperatures are higher than in the previous example because of the higher fuel surface temperature caused by smaller contact heat-transfer coefficient.

Figure 5 shows the effect of varying $\Delta r/R_f$ for a constant eccentricity $\epsilon = 0.005405$ and $K_g/K_f = 0.08$. The profile shows a steady increase in temperature with increases in $\Delta r/R_f$. Maximum temperatures are still displaced slightly toward 180° due to the eccentricity. Figure 6 shows the same behavior for a conductivity ratio $K_g/K_f = 0.044$.

Effect of Eccentricity on Isotherms

Another way to illustrate fuel temperature distributions is by plots of lines of constant temperature (isotherms). For concentric fuel pellets, the isotherms would be concentric circles. Figure 7 illustrates isotherms for a concentric fuel pellet in which $K_g/K_f = 0.062$ and $\Delta r/R_f = 0.024324$. For these same parameters and $\epsilon = 0.010811$, Figure 8 shows the isotherms for the fuel. One should note how the isotherms have migrated away from the center towards the hot side of the fuel. A similar plot for higher burnups ($K_g/K_f = 0.008$) and $\Delta r/R_f = 0.016216$ with eccentricity of $\epsilon = 0.005405$ appears in Figure 9. The temperatures are higher and the migration towards the fuel hot side is greater in this plot due to the sharp decrease in K_g/K_f .

Figure 10 shows a plot of the $\phi_f = 1.0$ isotherm for three pellet eccentricities. For this case, $K_g/K_f = 0.062$ and $\Delta r/R_f = 0.016216$. This figure gives a good indication of how an individual isotherm changes position with changing eccentricity.

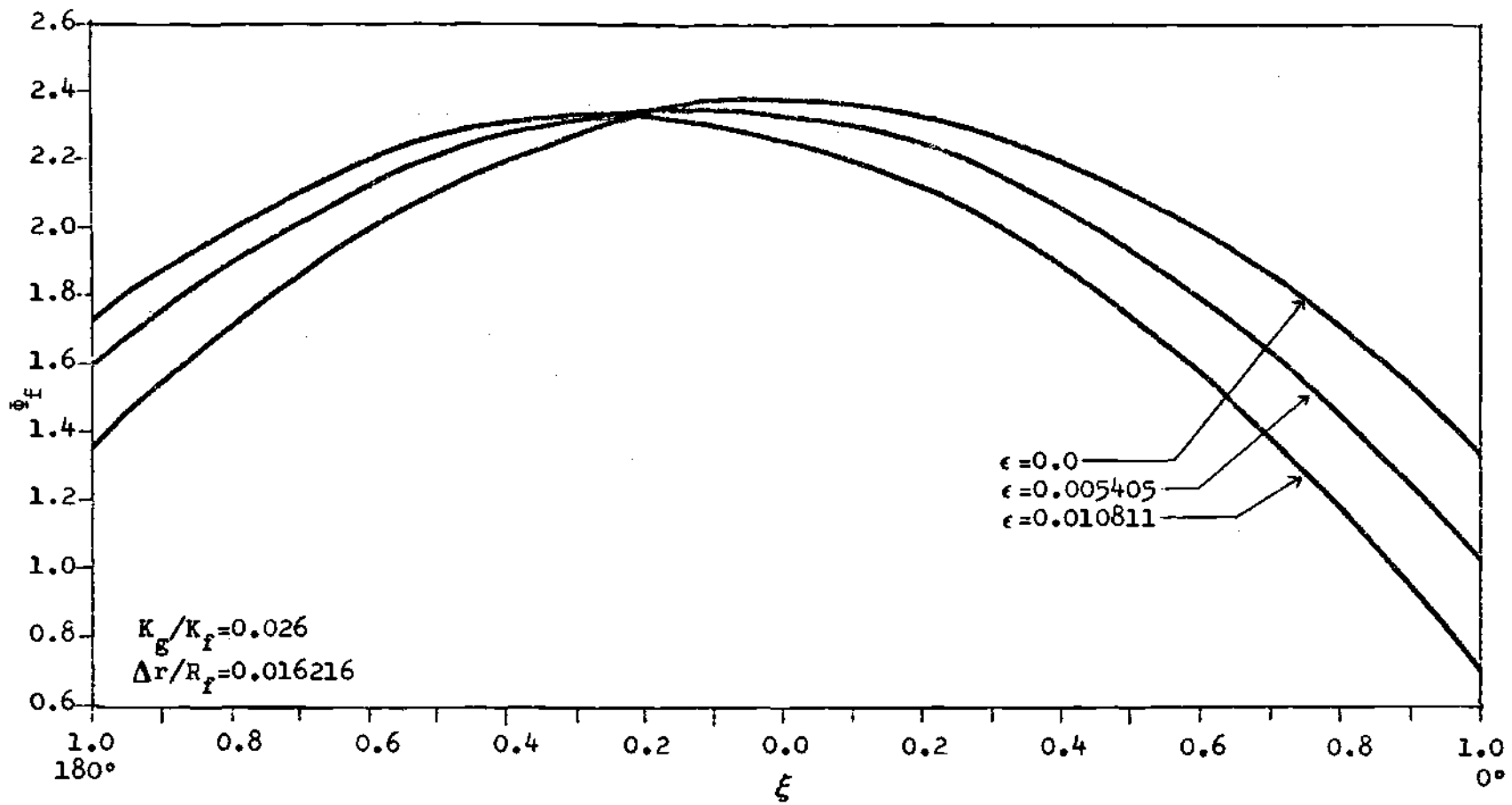


Figure 4. Radial Fuel Temperature Distribution

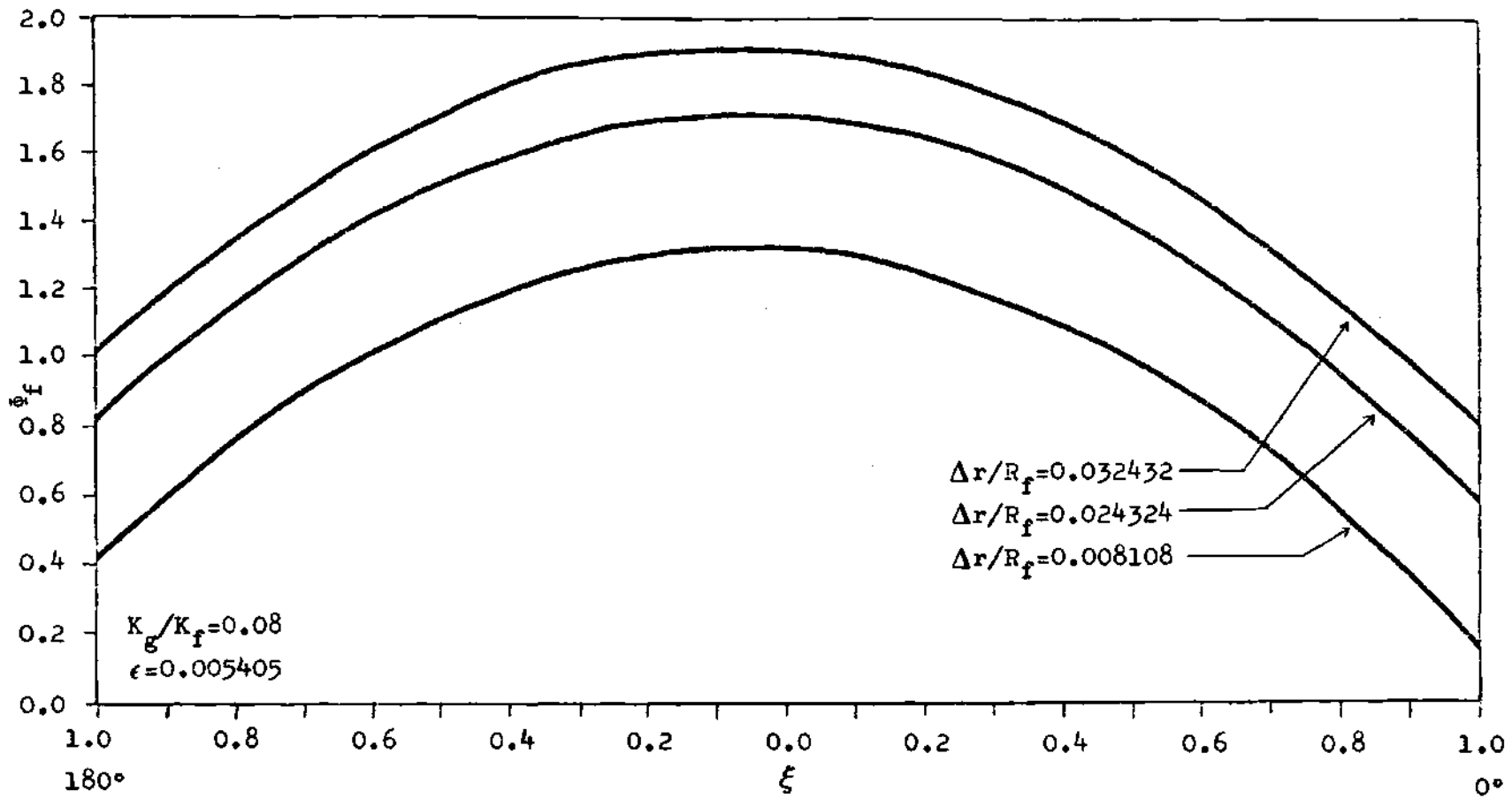


Figure 5. Radial Fuel Temperature Distribution as a Function of $\Delta r/R_f$

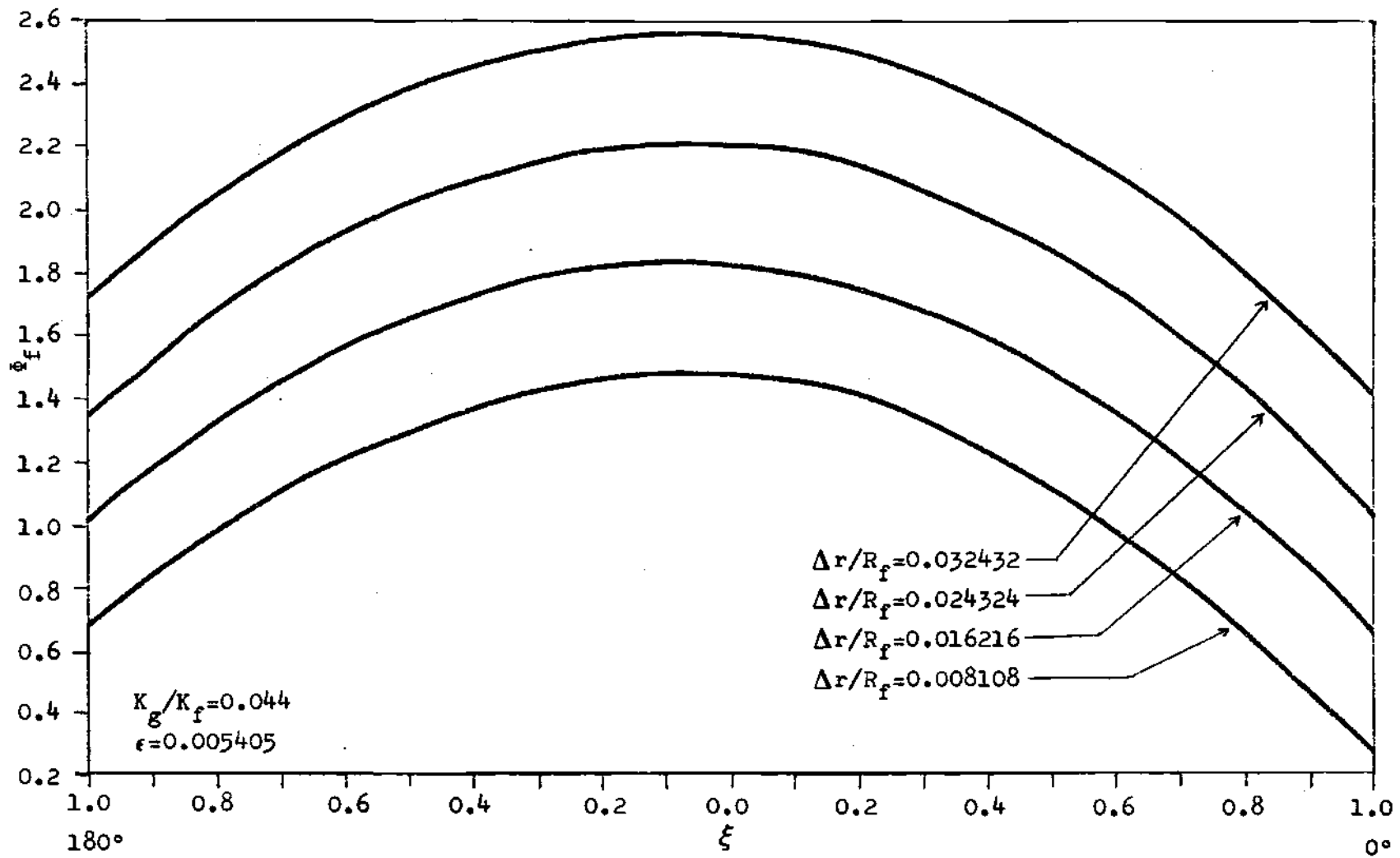


Figure 6. Radial Fuel Temperature Distribution as a Function of $\Delta r/R_f$

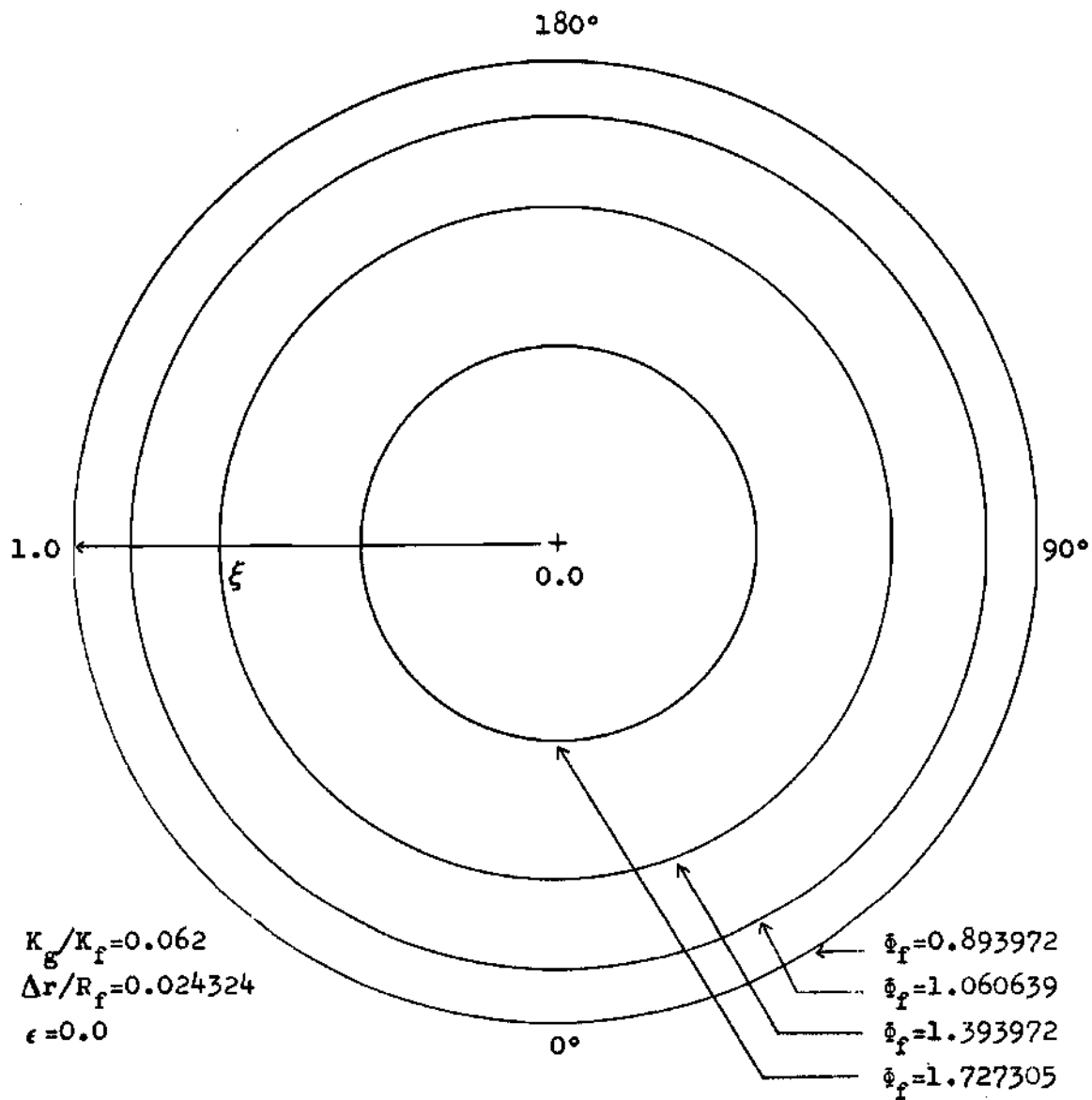


Figure 7. Isotherms in Concentric Fuel Pellet .

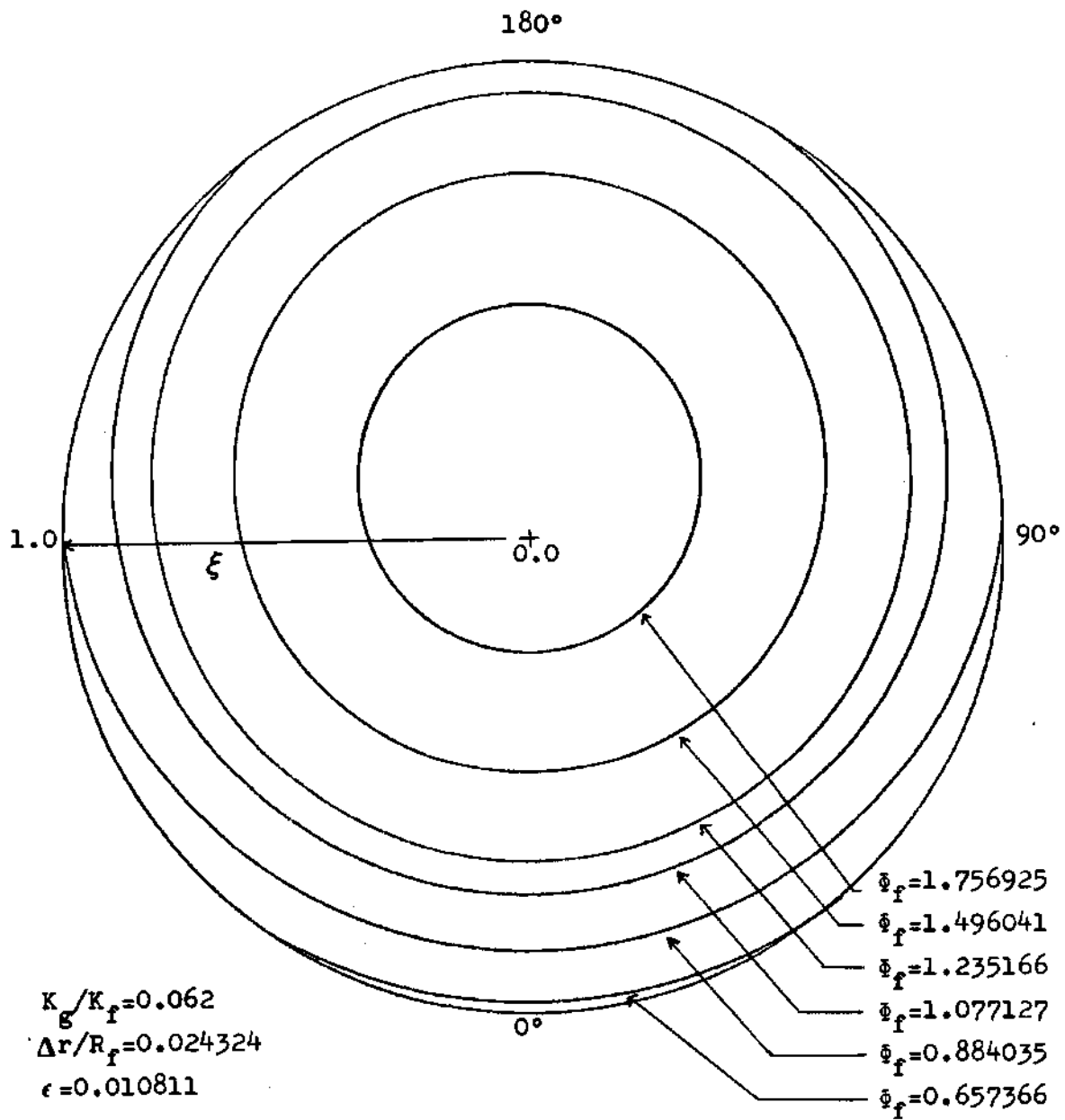


Figure 8. Isotherms in Eccentric Fuel Pellet

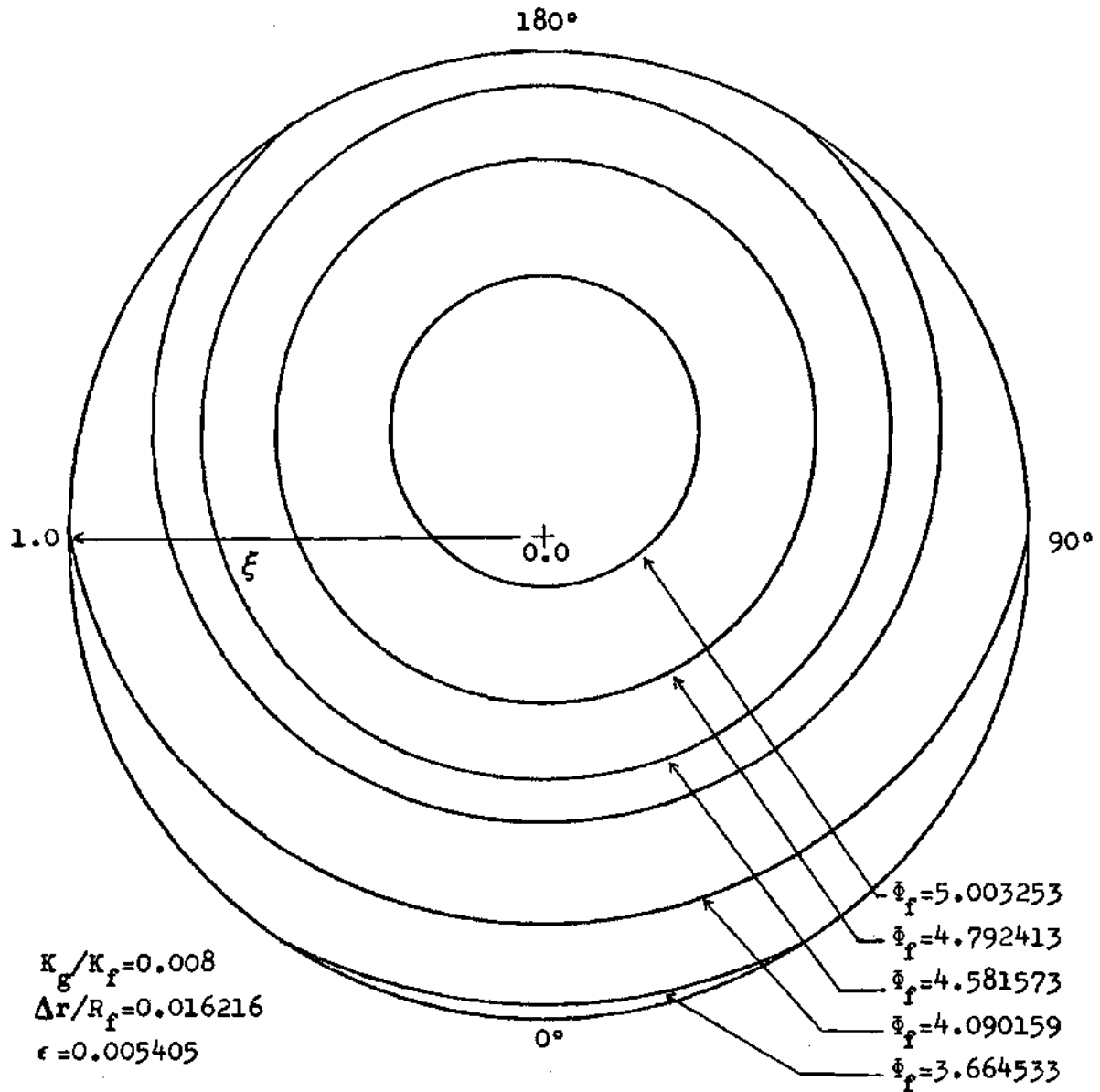


Figure 9. Isotherms in Eccentric Fuel Pellet

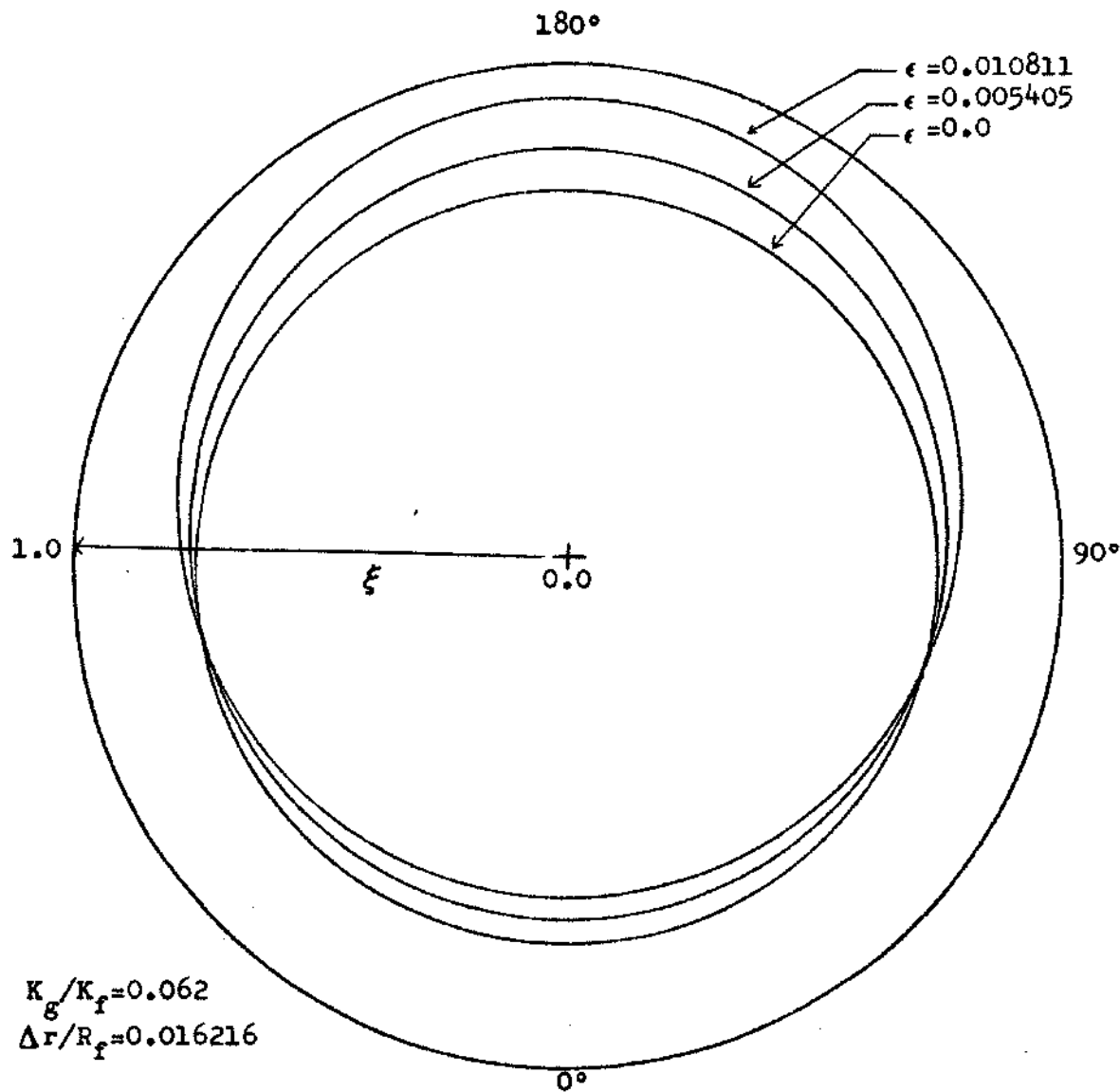


Figure 10. $\phi_f = 1.0$ Isotherm in Eccentric Fuel Pellet

1
f
tu
No
val
of
heat
appear
come m
Figure 1
Figure 1
Figure 16
 $\Delta r/R_f$ are

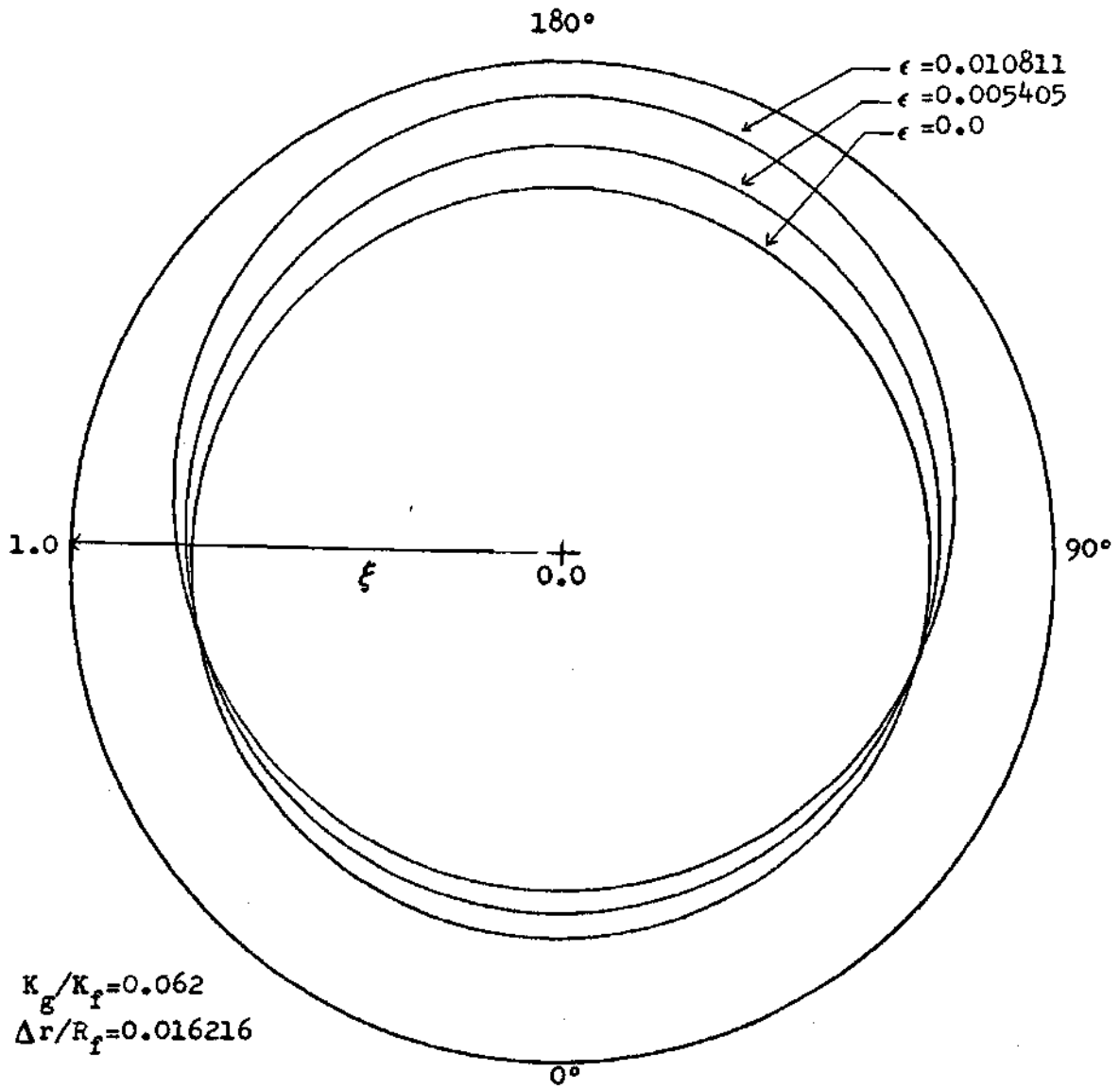


Figure 10. $\phi_f = 1.0$ Isotherm in Eccentric Fuel Pellet

Dependence on $\Delta r/R_f$

Fuel temperatures are strongly influenced by the magnitude of $\Delta r/R_f$. As $\Delta r/R_f$ goes from zero to its maximum value, fuel temperatures continually increase as the contact heat-transfer coefficient decreases. The situation where $\Delta r/R_f = 0.0$ is equivalent to intimate contact between fuel and cladding. As $\Delta r/R_f$ increases, the gap increases causing the value of $h_c(\theta)$ to fall. Thus, the temperatures rise.

The eccentric condition is of more interest. For $K_g/K_f = 0.08$ and $\epsilon = 0.005405$, Figure 11 shows how fuel surface temperatures vary with increases in $\Delta r/R_f$. One should note the trend of increased fuel surface temperature with increasing $\Delta r/R_f$ and compare this to Figures 5 and 6 for fuel temperature profiles. Figure 12 shows how cladding surface temperatures vary with increasing $\Delta r/R_f$ for the same parameters as in Figure 11. Normalized wall heat fluxes are shown in Figure 13 for the three $\Delta r/R_f$ values indicated in the previous figure. One should note that the effect of increasing $\Delta r/R_f$ for the same ϵ tends to decrease the asymmetry in the heat flux ratio. As $\Delta r/R_f$ increases, the gap widens making the pellet appear less severely eccentric, thus causing the heat flux ratios to become more uniform.

A second case was examined for $K_g/K_f = 0.026$ and $\epsilon = 0.010811$. Figure 14 shows fuel surface temperature variations as $\Delta r/R_f$ increases. Figure 15 shows the same comparison for cladding surface temperatures and Figure 16 shows normalized wall heat fluxes. The trends with increasing $\Delta r/R_f$ are similar to the example when $K_g/K_f = 0.08$.

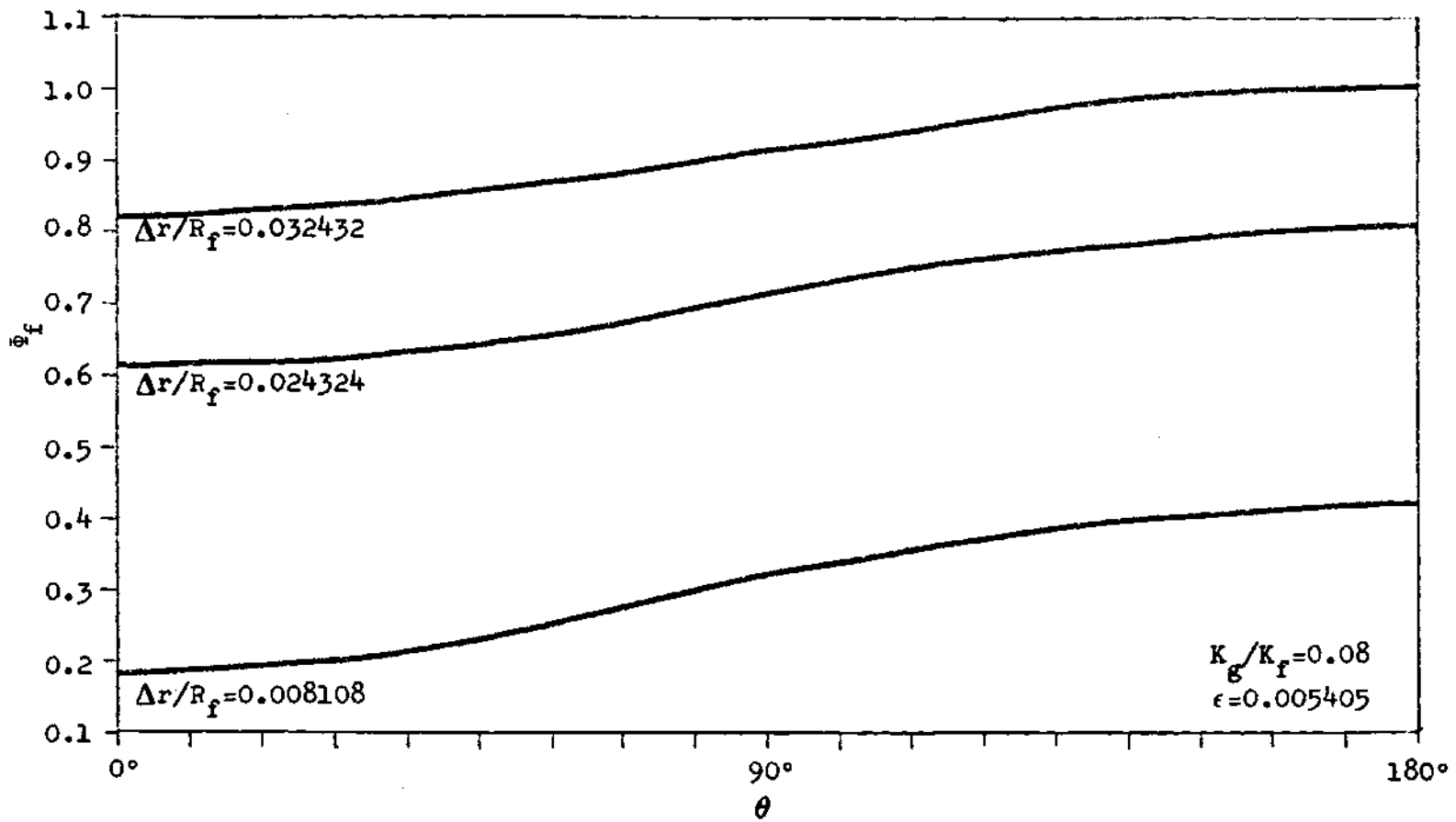


Figure 11. Fuel Surface Temperature as a Function of $\Delta r/R_f$

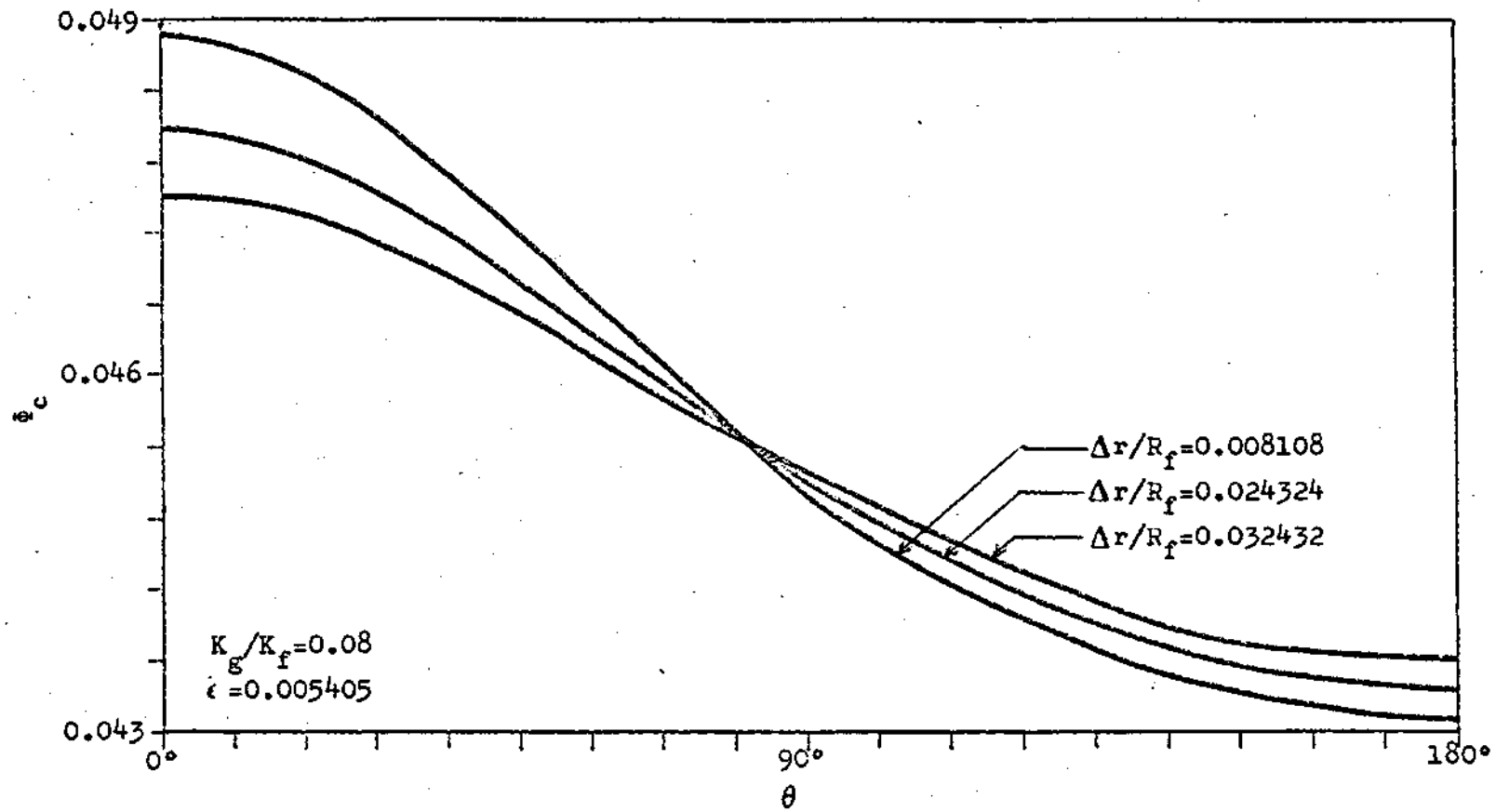


Figure 12. Cladding Outside Temperature as a Function of $\Delta r / R_f$



Figure 13. Normalized Wall Heat Flux as a Function of $\Delta r/R_f$

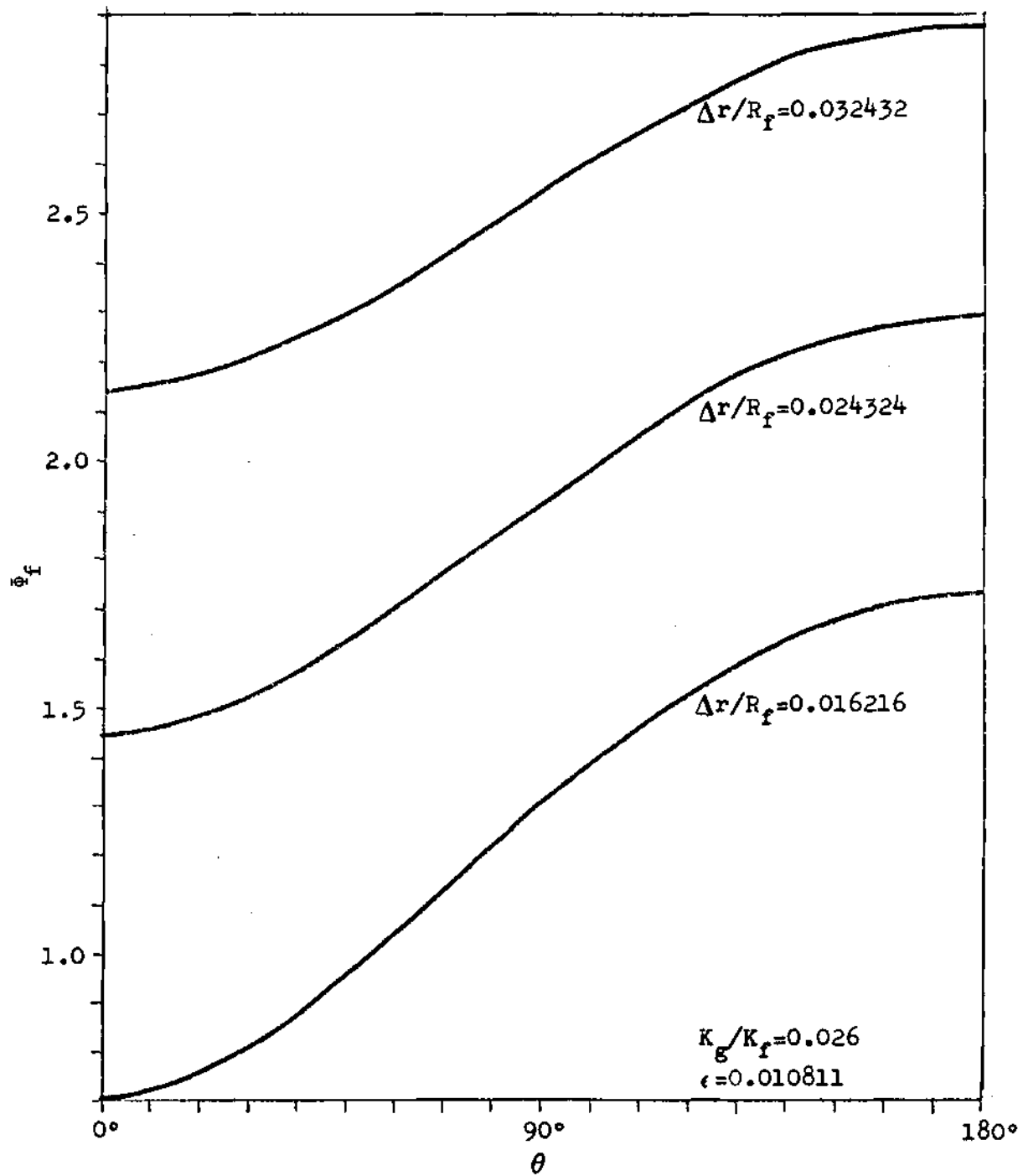


Figure 14. Fuel Surface Temperature as a Function of $\Delta r/R_f$

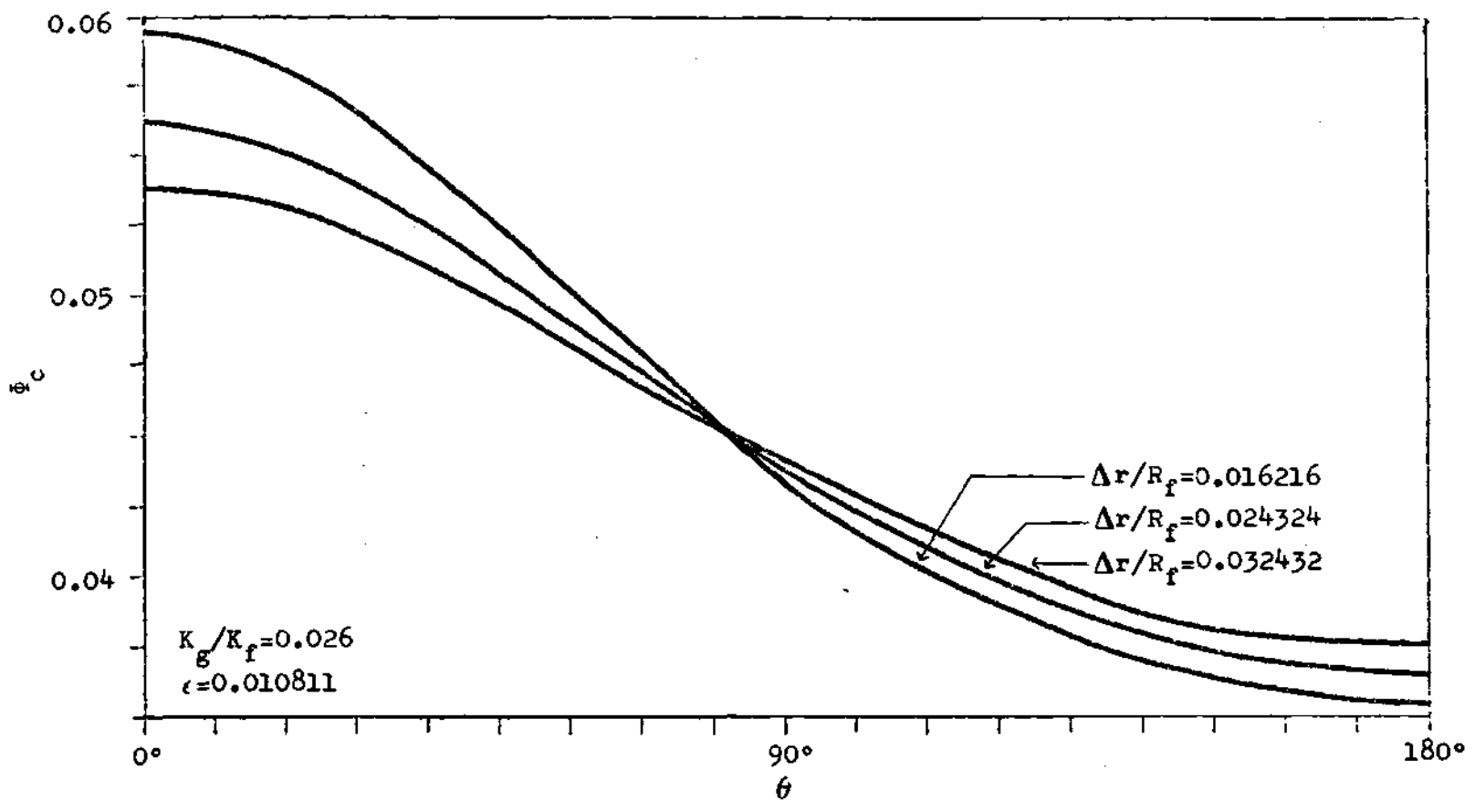


Figure 15. Cladding Surface Temperature as a Function of $\Delta r / R_f$

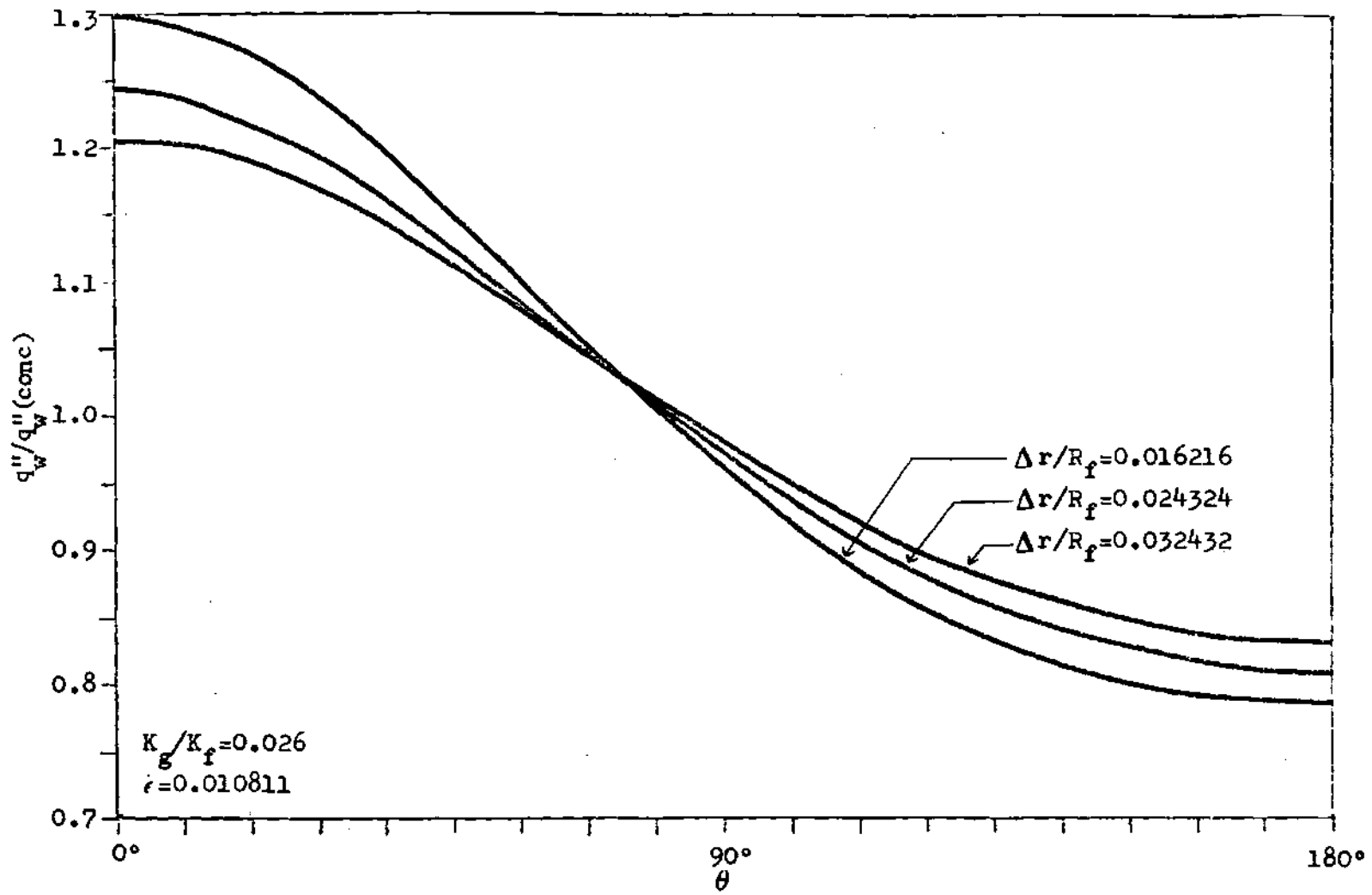


Figure 16. Normalized Wall Heat Flux as a Function of $\Delta r/R_f$

Dependence on K_g/K_f

For concentric fuel pellets, lowering the conductivity ratio due to contamination of the helium with fission gases has the effect of raising fuel temperatures significantly. This temperature rise is especially noticeable at higher $\Delta r/R_f$ values. Table 8 shows fuel surface temperatures, ϕ_f , for concentric fuel pellets for a variety of $\Delta r/R_f$ and K_g/K_f . One should note the large effect at small K_g/K_f values and the trend of temperature rise caused by the interdependence of conductivity ratio and $\Delta r/R_f$.

In order to observe the effect of varying K_g/K_f for eccentric fuel pellets, normalized heat flux and temperature plots are presented in the figures that follow. These illustrations show, with all other parameters fixed, an increasing non-uniformity in temperature and heat flux distributions with decreasing K_g/K_f .

Figure 17 shows normalized wall heat fluxes for varying eccentricity with $K_g/K_f = 0.08$ and $\Delta r/R_f = 0.024324$. Heat flux ratios vary from 1.0 for the concentric case to 1.25 at $\epsilon = 0.021622$.

Figure 18 illustrates normalized wall heat fluxes for $K_g/K_f = 0.062$ and the same $\Delta r/R_f$. The eccentric curves in this table indicate a higher maximum value of heat flux ratio than the corresponding eccentricities in Figure 17. The $\epsilon = 0.010811$ curve, for example, shows a maximum $q_w''/q_w''(\text{conc})$ of 1.13 in Figure 18 and only 1.11 in Figure 17. Thus, decreasing the conductivity ratio tends to increase the non-uniformity of the heat fluxes. Figure 19 shows an even further decrease to $K_g/K_f = 0.026$ and illustrates an even higher degree of heat flux non-uniformity.

Table 8. Fuel Surface Temperatures for Concentric Fuel Pellets

K_g/K_f	$\Delta r/R_f$	$\bar{\theta}_f$
0.08	0.0	0.110065
	0.008108	0.311992
	0.016216	0.513931
	0.024324	0.715880
	0.32432	0.917841
0.062	0.0	0.111610
	0.008108	0.372386
	0.016216	0.633173
	0.024324	0.893972
	0.32432	1.154781
0.044	0.0	0.114419
	0.008108	0.482193
	0.016216	0.849978
	0.024324	1.217775
	0.032432	1.585583
0.026	0.0	0.121116
	0.008108	0.744040
	0.016216	1.366975
	0.024324	1.989922
	0.032432	2.612879
0.008	0.0	0.157950
	0.008108	2.184198
	0.016216	4.210456
	0.024324	6.236726
	0.032432	8.263007

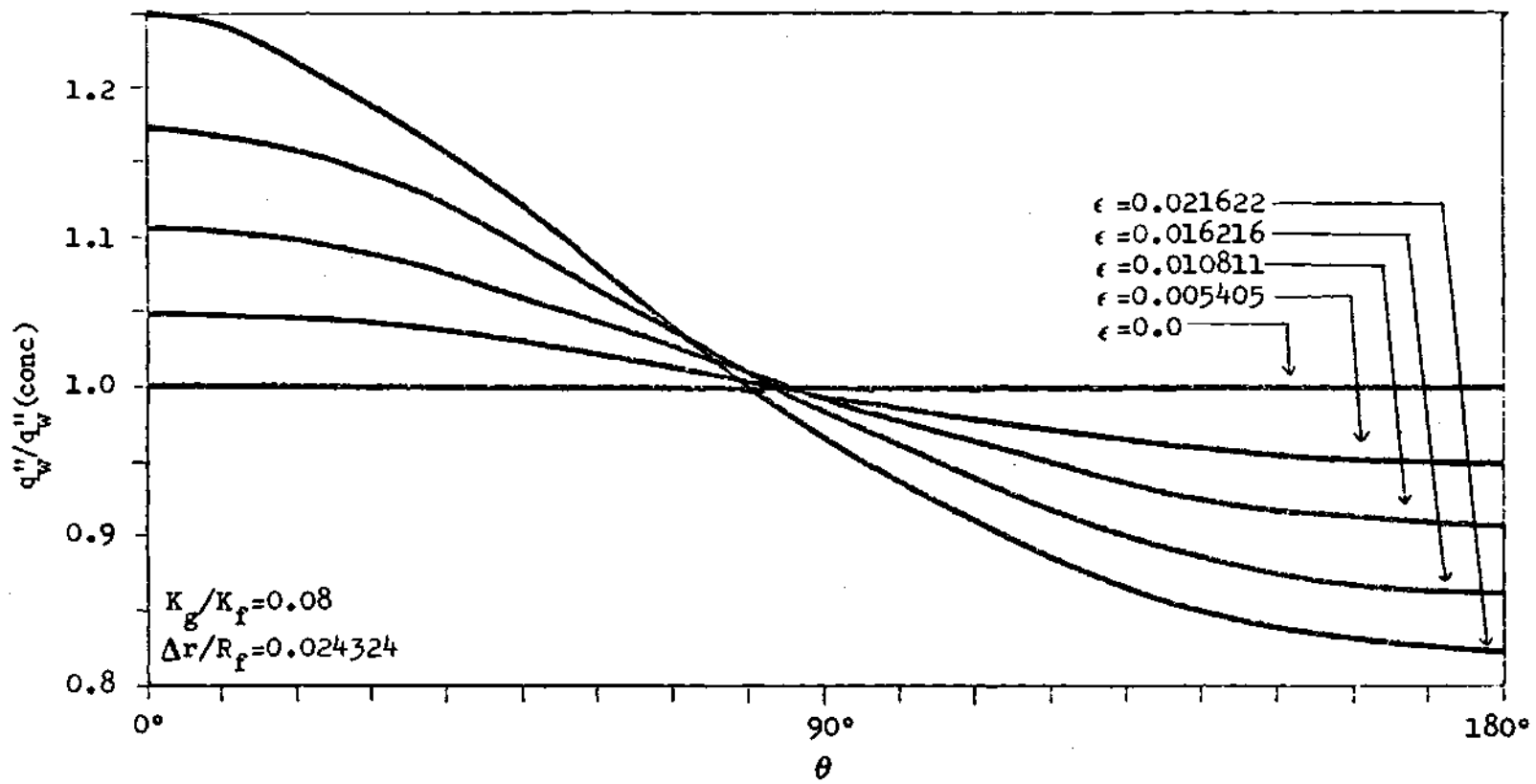


Figure 17. Normalized Wall Heat Flux

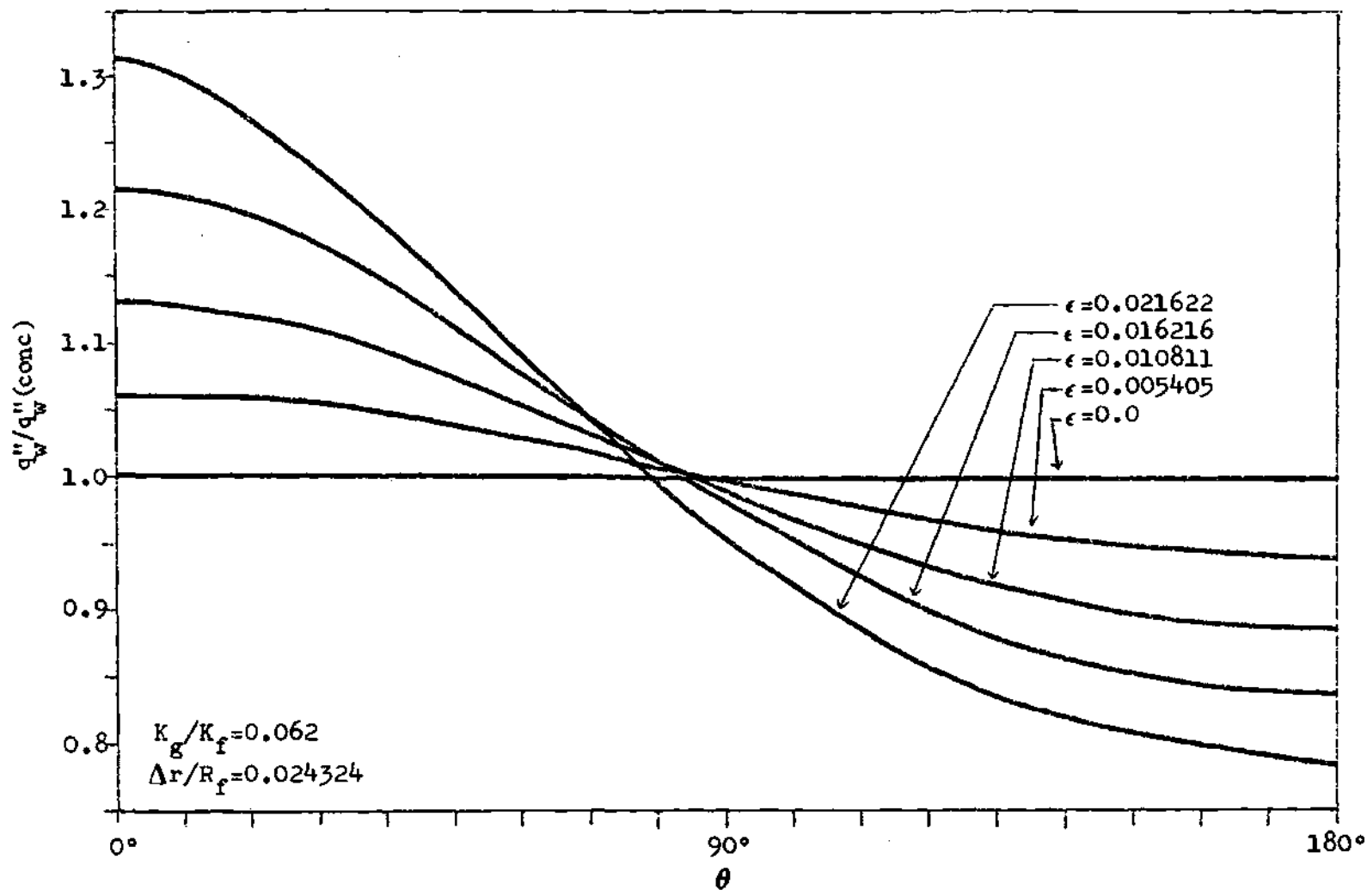


Figure 18. Normalized Wall Heat Flux

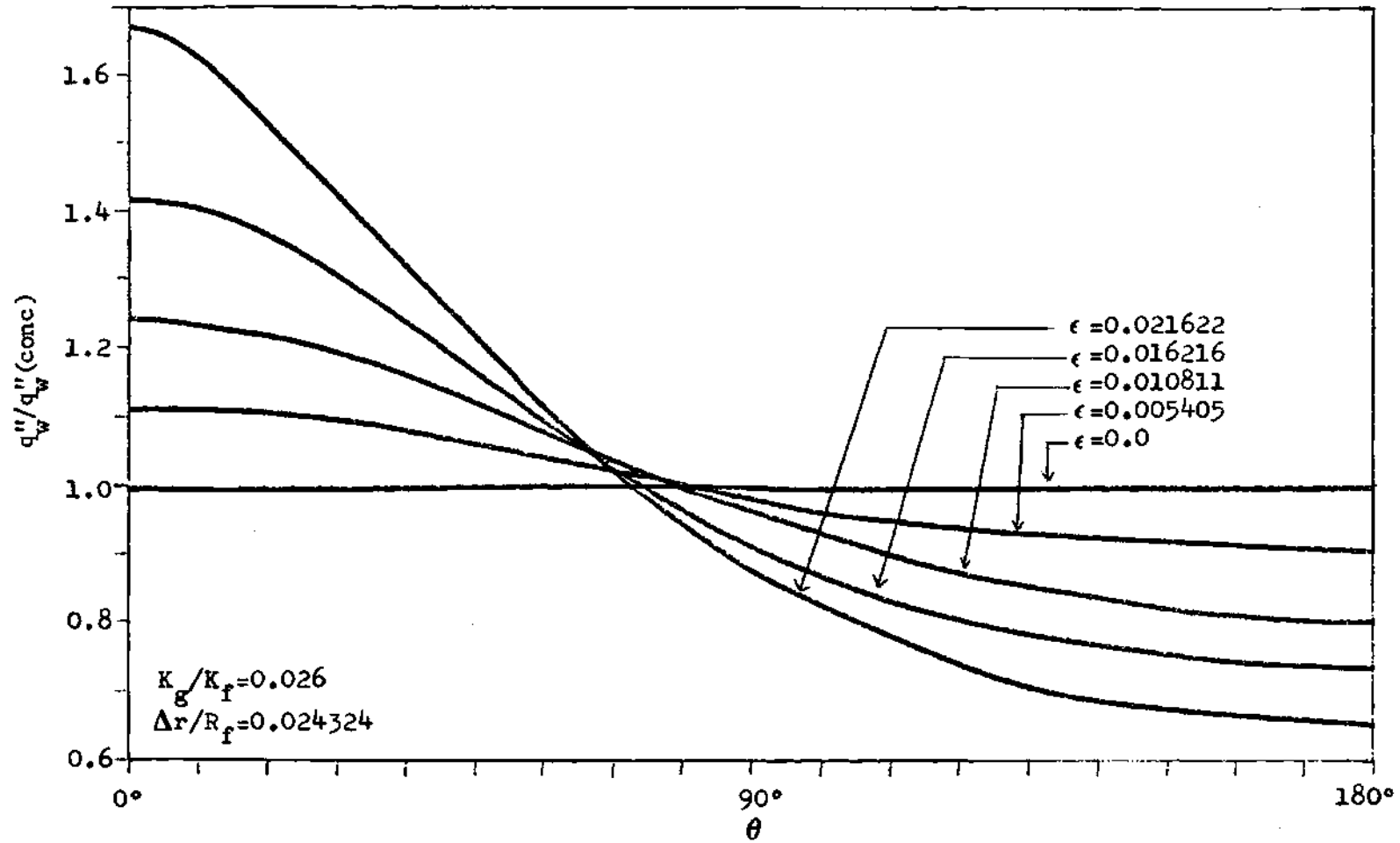


Figure 19. Normalized Wall Heat Flux

Figure 20 illustrates the behavior of fuel surface temperatures for this $\Delta r/R_f$ and $K_g/K_f = 0.044$.

Figure 18 can be compared to Figure 21 ($\Delta r/R_f = 0.016216$) to observe changes in $\Delta r/R_f$ for $K_g/K_f = 0.062$. The $\epsilon = 0.001081$ curve has a maximum heat flux ratio of 1.15 in Figure 21 and 1.13 in Figure 18. The trend shows the decrease in non-uniformity as $\Delta r/R_f$ increases.

The normalized wall heat fluxes in Figure 21 can be compared to Figure 23, where $K_g/K_f = 0.008$ and $\Delta r/R_f = 0.016216$. Again, one can see that lowering the conductivity ratio causes increased non-uniformity in heat flux ratios. Temperature comparisons appear in Figure 22 for the same case as Figure 21.

One can also observe the effect of eccentricity in Figure 24. Here, $K_g/K_f = 0.044$ and $\Delta r/R_f = 0.032432$. The effect shows a rise in heat flux ratios as eccentricity increases. Figure 25 shows normalized heat flux ratios for $K_g/K_f = 0.026$ and $\Delta r/R_f = 0.008108$ for both the concentric ($\epsilon = 0.0$) and eccentric ($\epsilon = 0.005405$) cases.

Combined Effects

This chapter has stressed the effect of variations in parameter values on fuel pellet heat transfer. Overall effects may arise due to interaction of many parameters. One should keep in mind that results such as temperature and heat flux ratios only compare the values for eccentric pellets to that value for the same parameters for a concentric fuel pellet.

Of all the combinations of parameter values, one of the worst cases obtained, shown in Figure 26, shows a 78% increase in q_w'' over the

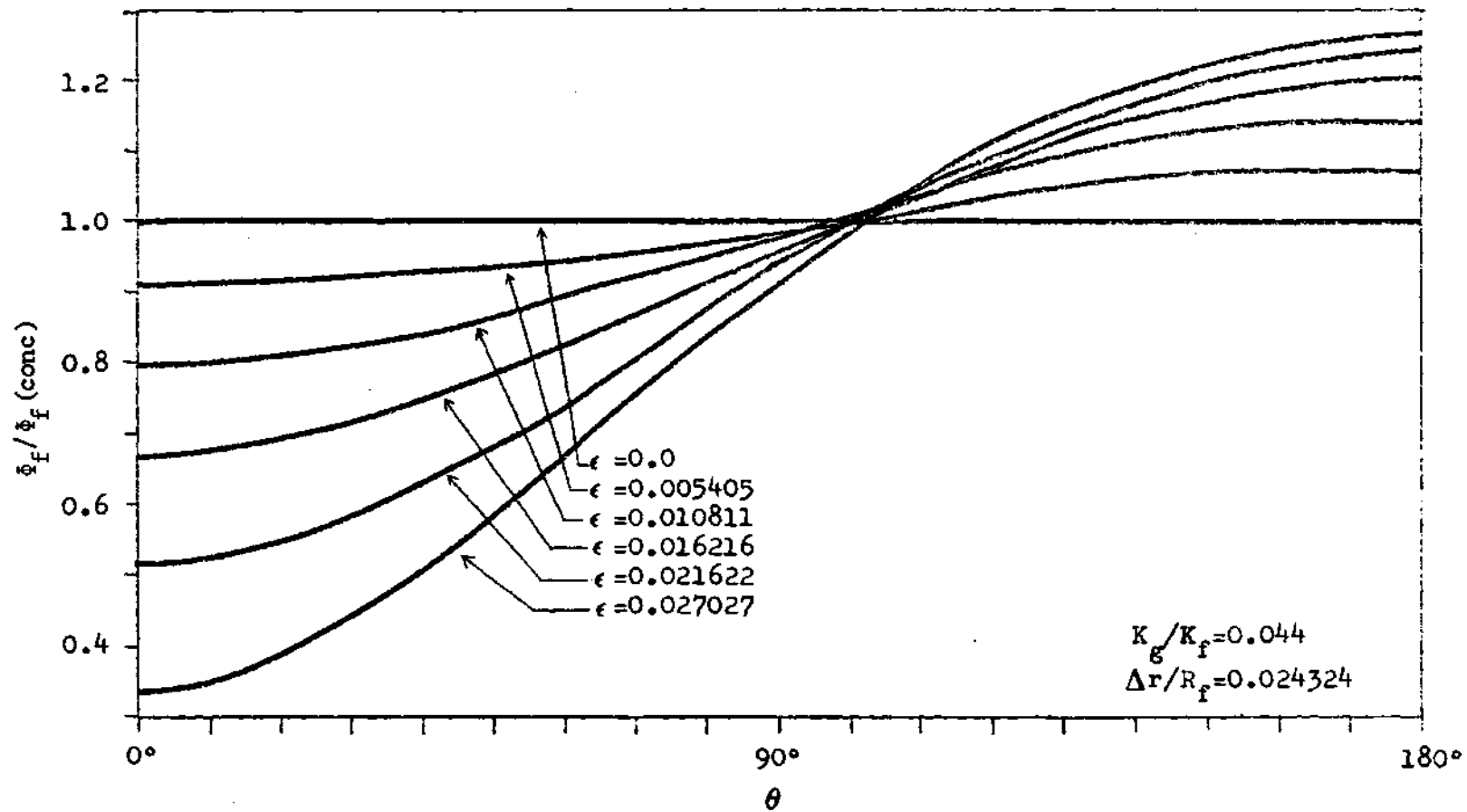


Figure 20. Normalized Fuel Surface Temperature

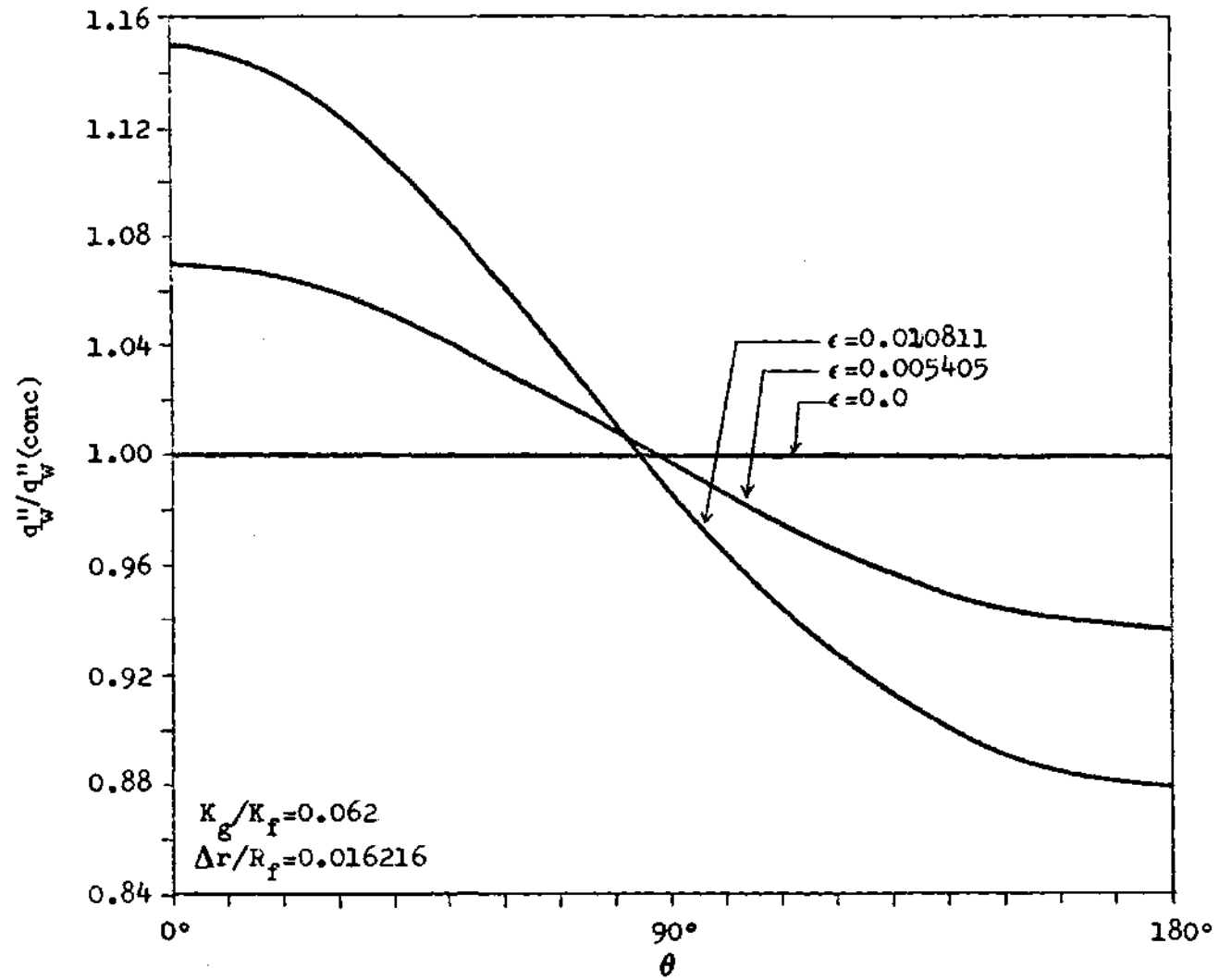


Figure 21. Normalized Wall Heat Flux

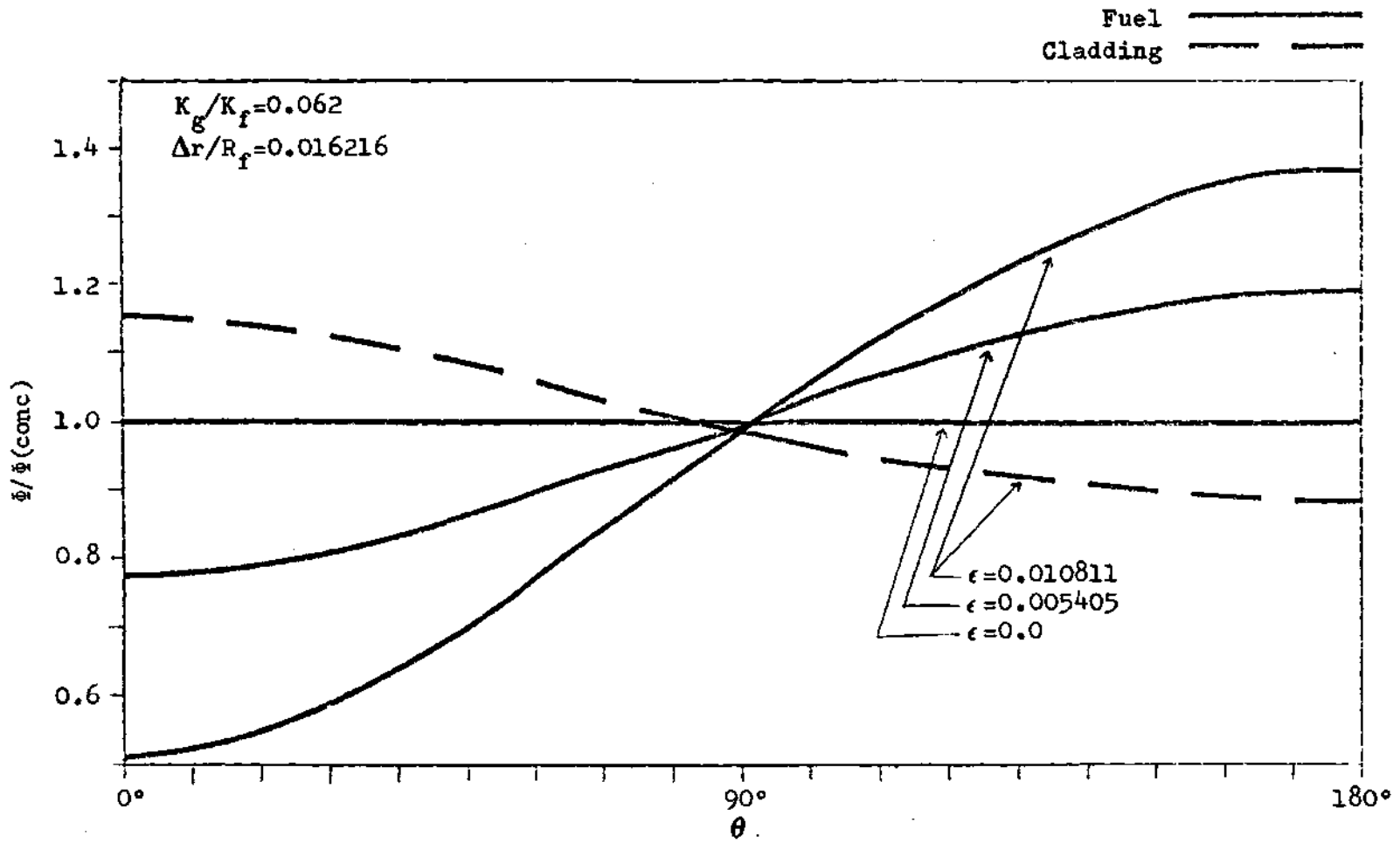


Figure 22. Normalized Temperature

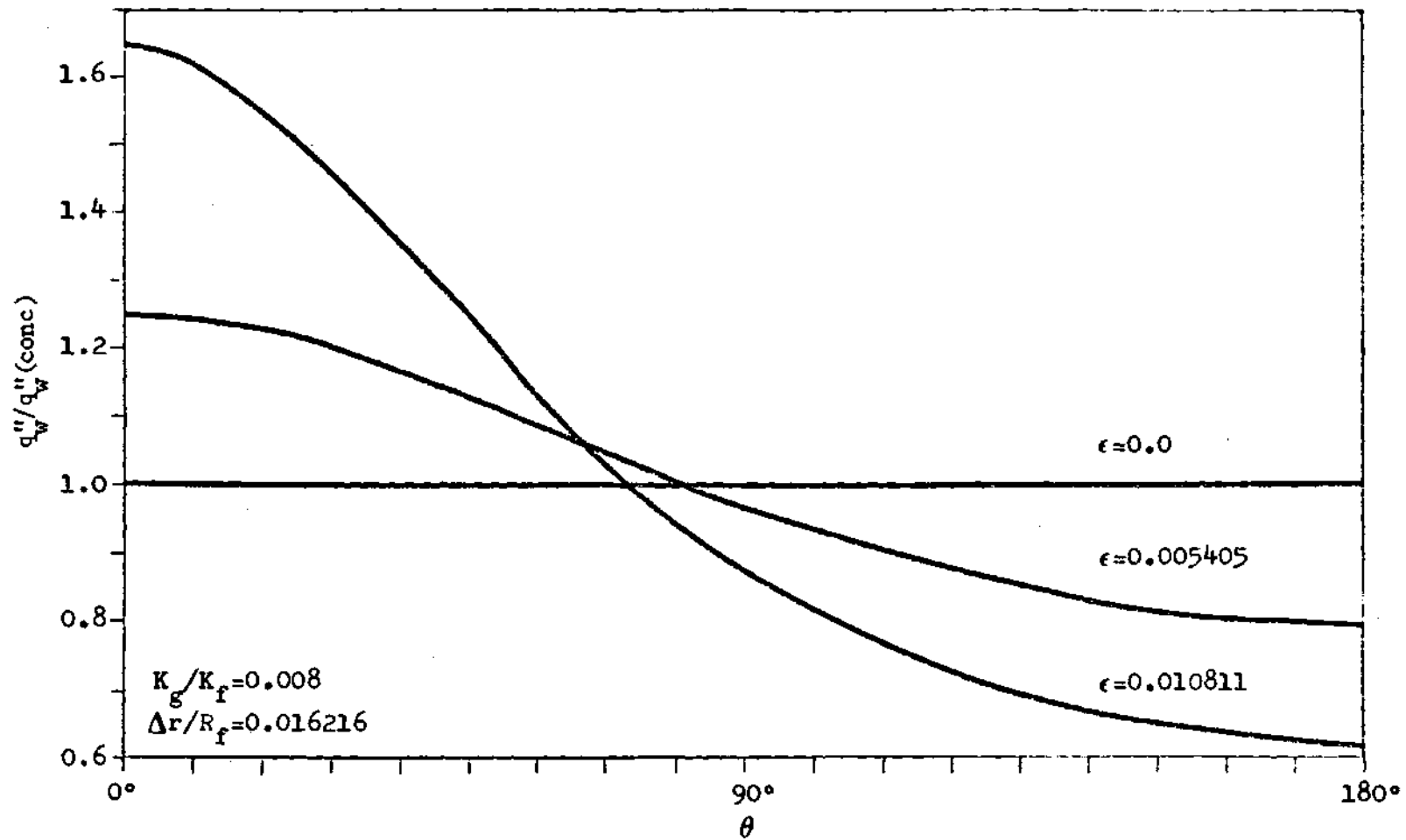


Figure 23. Normalized Wall Heat Flux

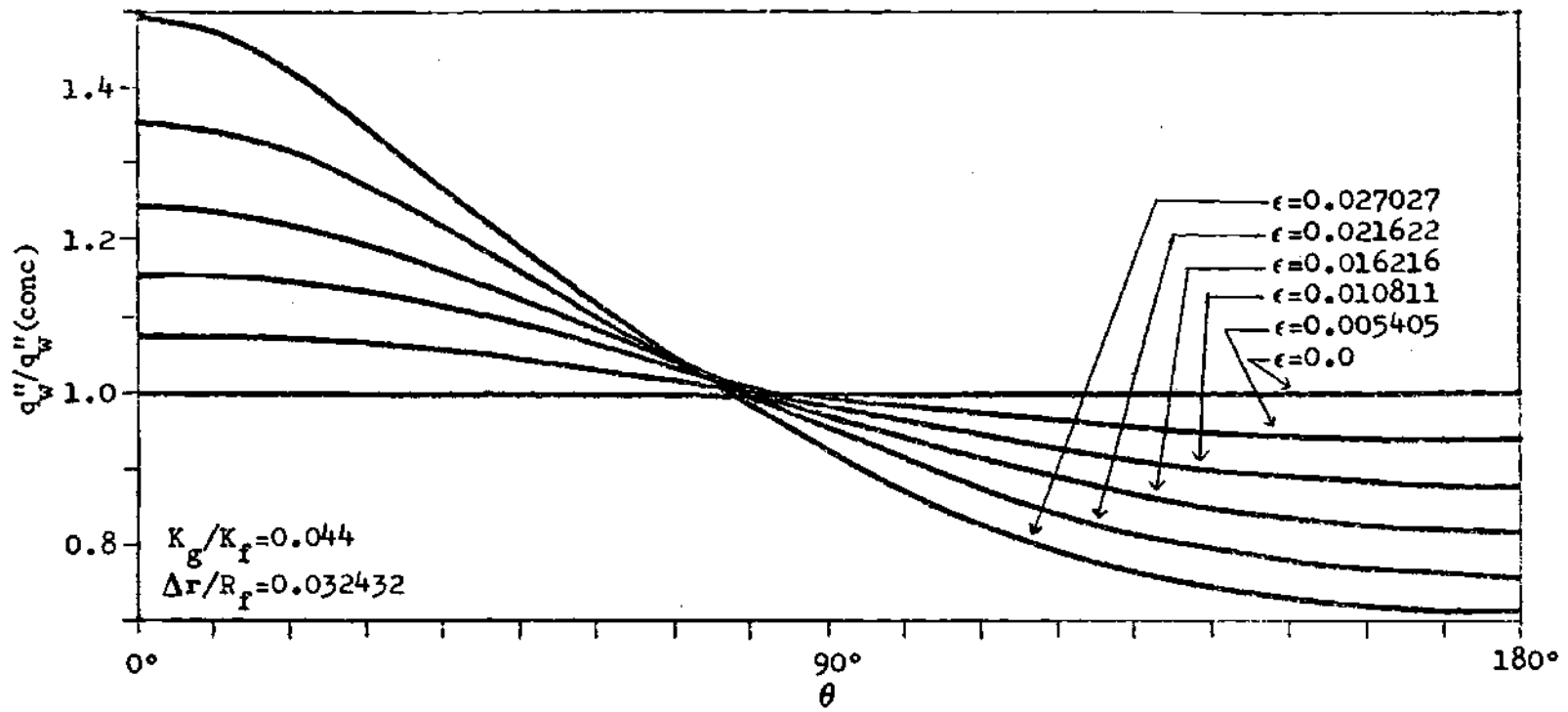


Figure 24. Normalized Wall Heat Flux

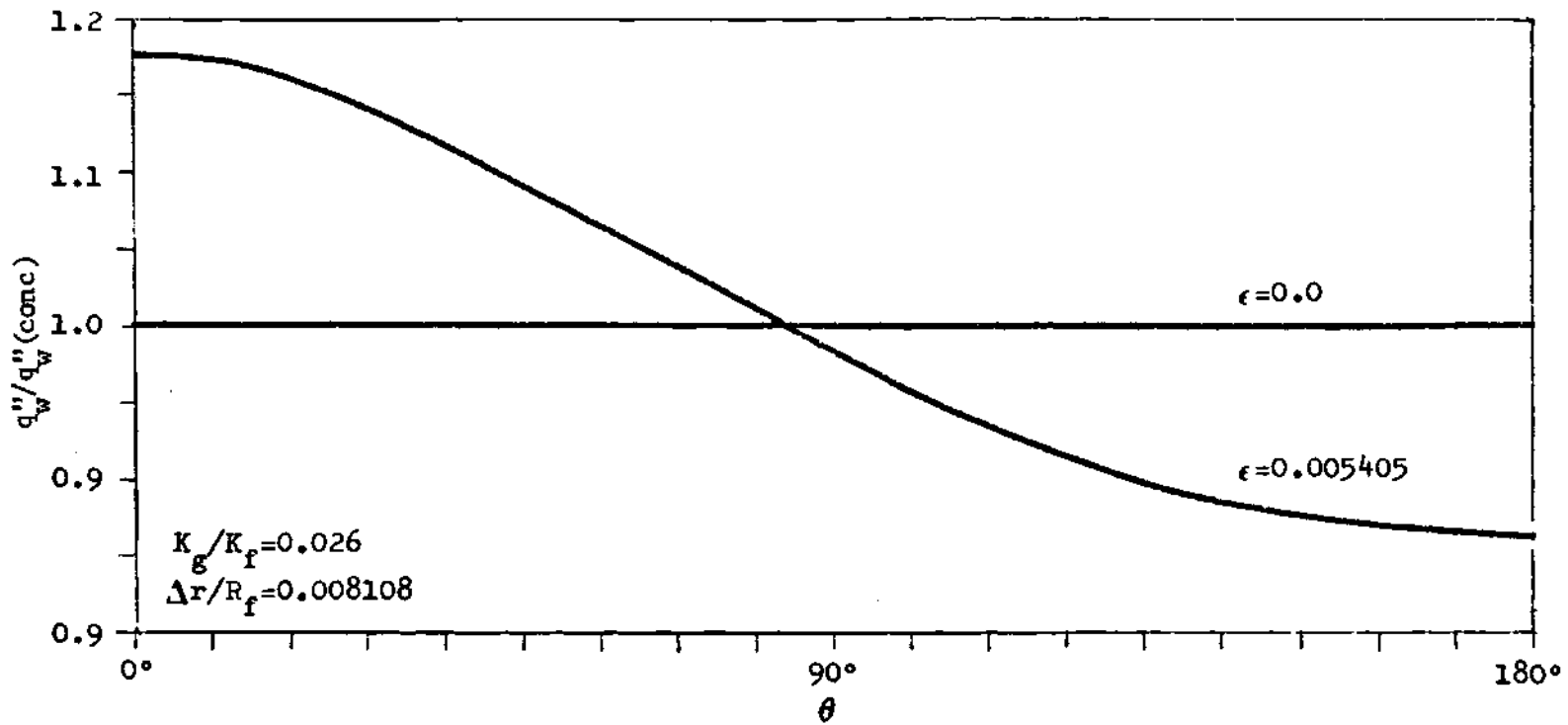


Figure 25. Normalized Wall Heat Flux

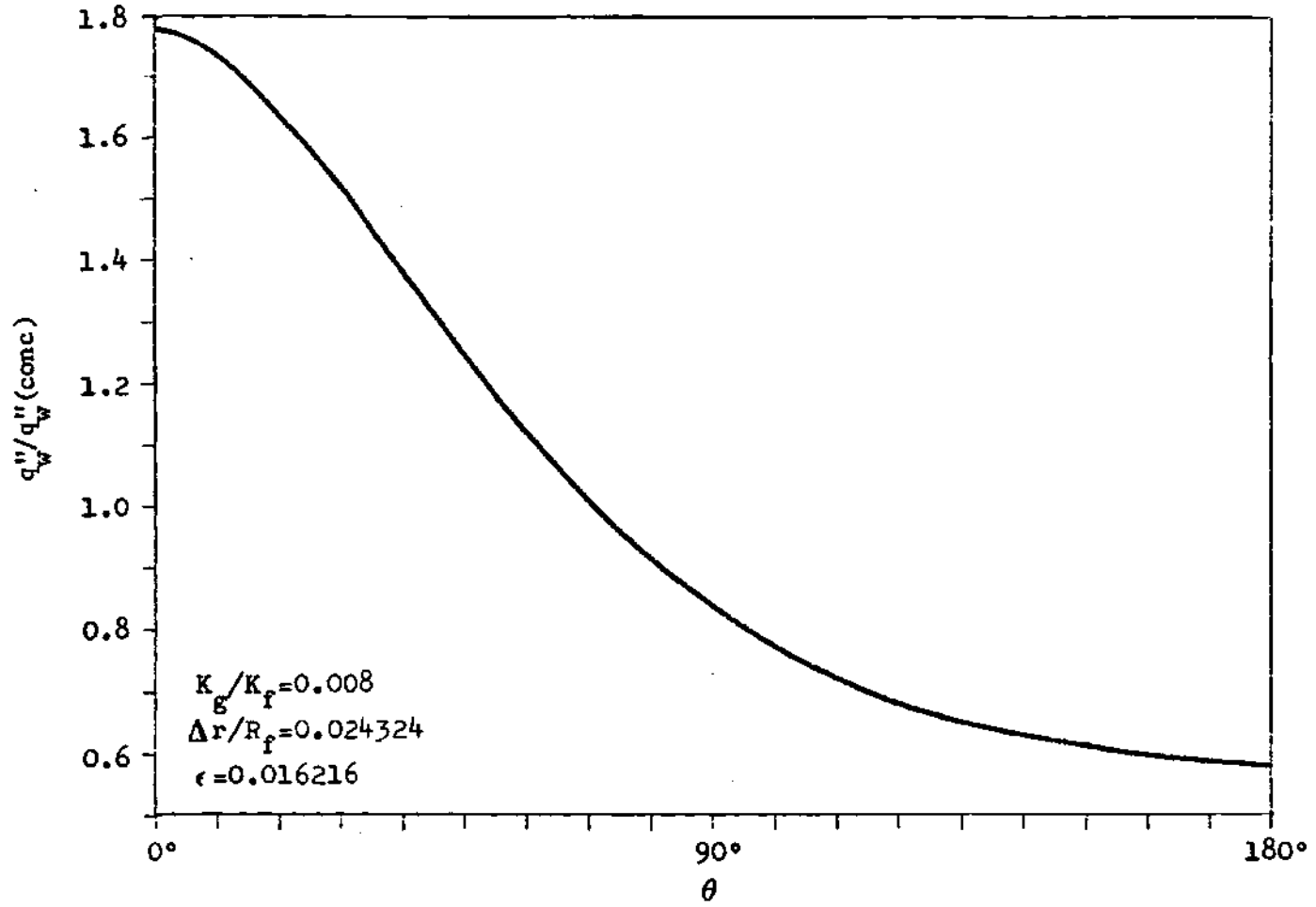


Figure 26. Normalized Wall Heat Flux

concentric case. Temperatures also were extremely high in this case. For this example, the conductivity ratio was taken at advanced burnup, $K_g/K_f = 0.008$, $\Delta r/R_f = 0.024324$, and $\epsilon = 0.016216$. Temperature data can be found on page 100 of Appendix D. The non-uniformity in heat flux ratios is very high, but it must be remembered that all the parameters represent extreme conditions.

Another case, shown on page 99 of Appendix D, is considered a reasonable "worst case" that one might expect for a power reactor. This shows high burnup, $K_g/K_f = 0.026$, $\Delta r/R_f = 0.024324$, and $\epsilon = 0.016216$. Figure 27 shows normalized heat fluxes and indicates a maximum of 42% rise in heat flux over the concentric case.

With less fuel densification ($\Delta r/R_f = 0.016216$) and shorter burnup times ($K_g/K_f = 0.044$), Figure 28 shows a rise of only 20% in heat flux over the concentric case for $\epsilon = 0.010811$. Temperature data for this case appear on page 101 of Appendix D. In a situation represented by this case, there will be hot spots on one side of the cladding.

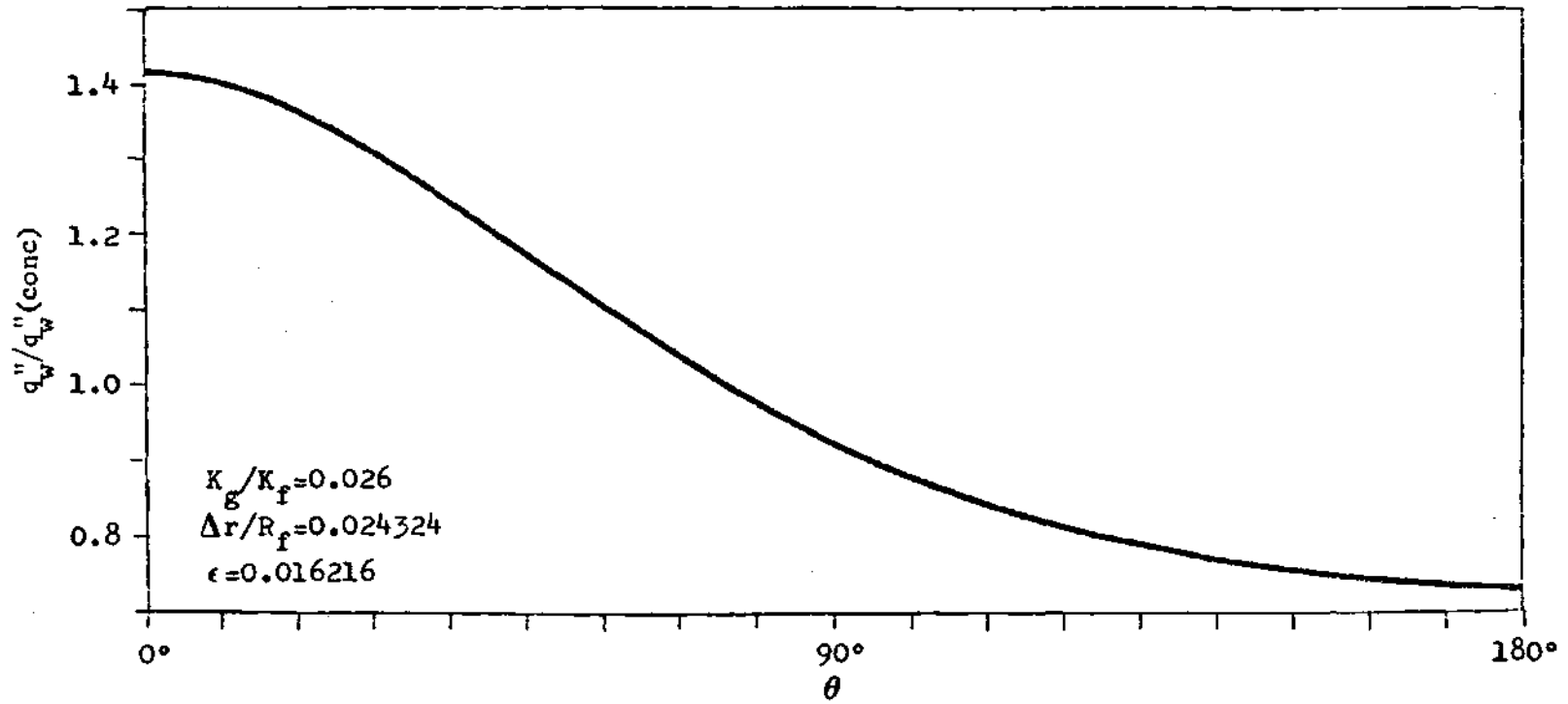


Figure 27. Normalized Wall Heat Flux

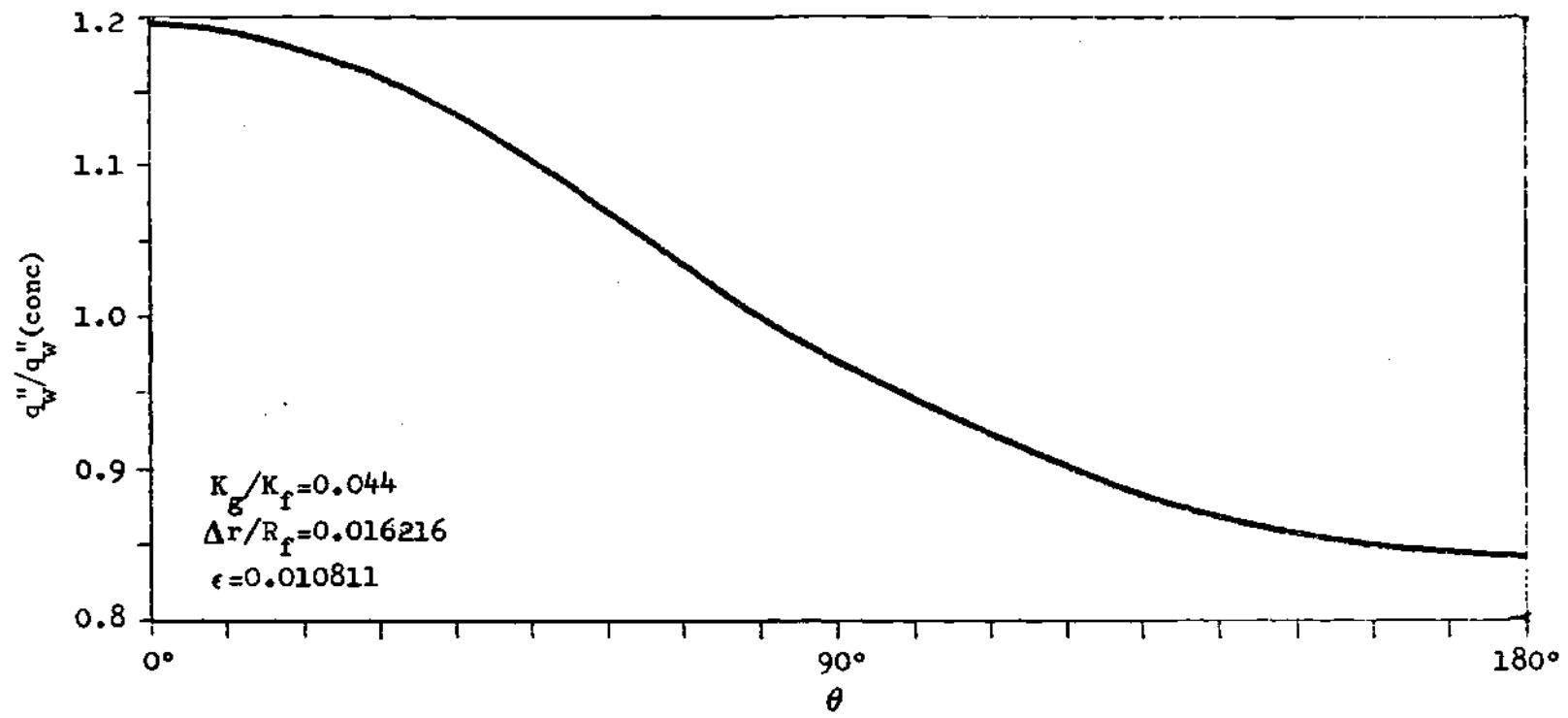


Figure 28. Normalized Wall Heat Flux

CHAPTER V

CONCLUSIONS

The results of the calculations must be taken in the proper perspective. The data reported are for individual fuel pellets of different eccentricities. Neighbors to this pellet may be eccentric relative to another angular position or may not be eccentric at all. For cocked pellets, the top and bottom will effectively have maximum eccentricity while the center will have zero eccentricity. Other parts of the fuel will have in between values of ϵ . All of these circumstances will tend to reduce the effects of fuel pellet eccentricity on local heat fluxes and temperature changes over the length of the fuel rod,

However, the reactor designer must be concerned with what happens to individual fuel pellets. Factors, such as eccentricity, can cause heat fluxes to exceed critical heat fluxes leading to film boiling and cladding failure. Heat fluxes based upon concentric fuel pellets may indicate a safety margin during operation. Local effects caused by eccentricity may result in operation dangerously close to or outside of the safety margin.

The important conclusions of this parametric study are as follows:

1. The ratios $\phi_f/\phi_f(\text{conc})$, $\phi_c/\phi_c(\text{conc})$, and $q_w''/q_w''(\text{conc})$ undergo little variation with changes in cladding outside heat-transfer coefficient.
2. Changes in $g_1 + g_2$ have negligible effect on the system compared to the quantity they supplement, $\Delta r/R_f$.
3. For a given condition, the maximum fuel temperature occurs in

the concentric case and tends to decrease with increasing eccentricity.

4. Cladding heat fluxes depend strongly on the eccentricity of the pellet, thermal conductivity ratio, and radial differences; generally, maximum values of the heat flux ratio increase as ϵ and K_g/K_f increase and decrease as $\Delta r/R_f$ increases.

In nuclear reactor design, the DNB ratio is defined as the predicted DNB heat flux divided by the cladding operating heat flux. During steady state and normal transient operations of a power reactor, this ratio is not allowed to fall anywhere within the core value greater than unity, i.e., 1.3. Consequently, a heat transfer analysis of fuel rods with fuel pellets located concentrically within the cladding will show DNB ratios to be equal or greater than the allowable minimum value. However, the highly non-uniform cladding heat fluxes, stated for eccentrically located fuel pellets in conclusion four, may cause local DNB ratios on the cladding periphery to be less than the minimum allowable design value and possibly be less than unity. It is not clear at this time that this will cause cladding failure. The experiments used to develop correlations for predicting DNB in fuel rods are based upon measurements taken from rods heated uniformly around the cladding periphery. Consequently, it is necessary to perform DNB experiments in heated fuel rods with non-uniform peripheral heat fluxes in order to determine whether rod failures occur if local DNB ratios based upon uniform heat flux correlations fall below unity or some other minimum value.

APPENDICES

APPENDIX A

DERIVATION OF EQUATIONS

Temperature Distribution in Fuel

The steady state heat conduction equation in cylindrical coordinates (r, θ, z) is given by²⁴

$$\frac{\partial^2 T}{\partial r^2} + \frac{1}{r} \frac{\partial T}{\partial r} + \frac{1}{r^2} \frac{\partial^2 T}{\partial \theta^2} + \frac{\partial^2 T}{\partial z^2} = - \frac{q'''}{K_f} \quad (\text{A.1})$$

The expression assumes an isotropic medium with constant thermal conductivity K_f and a uniform rate of internal heat generation q''' . The temperature T at a given point is $T(r, \theta, z)$. This problem assumes negligible heat transfer vertically through the fuel rod, so $\frac{\partial^2 T}{\partial z^2} = 0$. Now, $T = T(r, \theta)$. An analysis by Thorpe showed neglecting axial heat conduction will produce errors of less than 0.5%.²⁵ Should greater accuracy than this be required, the axial heat conduction term could be included.²⁶

In order to solve this differential equation, A.1 is first made homogeneous by defining

$$T(r, \theta) = \theta_1(r, \theta) + P(r, \theta) \quad (\text{A.2})$$

such that

$$\nabla^2 \theta_1(r, \theta) = 0 \quad (\text{A.3})$$

For r and θ dependency, $P(r,\theta)$ has been shown to be²⁷

$$P(r,\theta) = - \frac{q''' r^2}{4K_f} \quad (\text{A.4})$$

This expression for P serves as the basis for the non-dimensionalization of this problem. Define

$$\Phi(r,\theta) = \frac{T(r,\theta) - T_b}{q''' R_f^2 / 4K_f}$$

where T_b = temperature of the coolant. Define a non-dimensional radius as

$$\xi = \frac{r}{R_f} \quad \text{such that } 0 \leq \xi \leq 1$$

Normalizing P in the same fashion gives

$$P(\xi,\theta) = - \xi^2$$

Φ_1 is also normalized.

$$\Phi(\xi,\theta) = \frac{\Phi_1(r,\theta)}{q''' R_f^2 / 4K_f}$$

Now

$$\Phi(\xi,\theta) = - \xi^2 + \Phi(\xi,\theta) \quad (\text{A.5})$$

Since Eq. A.3 is now a homogeneous differential equation, a separation of

variable method of solution can be performed. Define

$$\emptyset(\xi, \theta) = R(\xi)Z(\theta) \quad (\text{A.6})$$

So,

$$\nabla^2 \emptyset(\xi, \theta) = \frac{\partial^2 \emptyset}{\partial \xi^2} + \frac{1}{\xi} \frac{\partial \emptyset}{\partial \xi} + \frac{1}{\xi^2} \frac{\partial^2 \emptyset}{\partial \theta^2} = 0 \quad (\text{A.7})$$

or,

$$\frac{\partial^2 (RZ)}{\partial \xi^2} + \frac{1}{\xi} \frac{\partial (RZ)}{\partial \xi} + \frac{1}{\xi^2} \frac{\partial^2 (RZ)}{\partial \theta^2} = 0 \quad (\text{A.8})$$

which yields,

$$\frac{R''}{R} + \frac{1}{\xi} \frac{R'}{R} + \frac{1}{\xi^2} \frac{Z''}{Z} = 0 \quad (\text{A.9})$$

where $R'' = \frac{\partial^2 R}{\partial \xi^2}$, $R' = \frac{\partial R}{\partial \xi}$, and $Z'' = \frac{\partial^2 Z}{\partial \theta^2}$.

Let $\frac{Z''}{Z} = -\nu^2$. This gives a differential equation

$$\frac{\partial^2 Z(\theta)}{\partial \theta^2} + \nu^2 Z(\theta) = 0 \quad (\text{A.10})$$

the solution of which is

$$Z(\theta) = A \cos \nu \theta + B \sin \nu \theta \quad (\text{A.11})$$

Equation A.5 is now written as

$$\frac{R''}{R} + \frac{1}{\xi} \frac{R'}{R} - \frac{\nu^2}{\xi^2} = 0 \quad (\text{A.12})$$

The solution of this equation is

$$R(\xi) = \begin{cases} C_1 + D_1 \ln \xi & \text{for } \nu = 0 \\ C_2 \xi^\nu + D_2 \xi^{-\nu} & \text{for } \nu \geq 1 \end{cases} \quad (\text{A.13})$$

The boundary conditions imposed on the temperature are:

$$\text{Symmetry} \quad \Phi(\xi, \theta) = \Phi(\xi, -\theta) \quad (\text{A.14})$$

$$\text{Cyclic} \quad \Phi(\xi, \theta) = \Phi(\xi, \theta + 2\pi) \quad (\text{A.15})$$

$$\text{Finiteness} \quad \Phi(0, \theta) \text{ is finite} \quad (\text{A.16})$$

The condition imposed by Eq. A.14 sets $B = 0$ in Eq. A.11 because only an even function is an acceptable solution.

$$Z(\theta) = A \cos \nu \theta \quad (\text{A.17})$$

The condition imposed by Eq. A.15 requires the values of ν to be integers, $\nu = 0, 1, 2, 3, \dots$

Since the temperature must be finite at $\xi = 0$, the values of D_1 and

D_2 in Eq. A.13 are zero, for both $\ln \xi$ and $1/\xi^\nu$ equal ∞ at $\xi = 0$. And since C_2 equals a constant C for $\nu = 0$, Eq. A.13 becomes

$$R(\xi) = C\xi^\nu \quad \nu = 0, 1, 2, \dots \quad (\text{A.18})$$

Equation A.6 now becomes .

$$\phi(\xi, \theta)_\nu = R(\xi)Z(\theta) = (C\xi^\nu)A \cos \nu \theta$$

or

$$\phi(\xi, \theta) = \sum_{\nu=0}^{\infty} a_\nu \xi^\nu \cos \nu \theta \quad (\text{A.19})$$

The temperature in the fuel can now be expressed from Eq. A.5 as

$$\bar{\phi}(\xi, \theta) = -\xi^2 + \sum_{\nu=0}^{\infty} a_\nu \xi^\nu \cos \nu \theta \quad (\text{A.20})$$

The values of a_ν are obtained from the boundary condition imposed on the fuel surface, as indicated in the next section.

Applying Fuel Surface Boundary Condition

This derivation further assumes negligible radiation across the gap. This term depends on

$$q'' = \sigma(T_s^4 - T_i^4)$$

where $\sigma = 0.1714 \times 10^{-8}$ Btu/hr-ft²-°R⁴ (Stefan's constant). Even with the

fourth power on temperature, the constant σ will keep the heat flux due to radiation quite low at the temperatures considered.

A reasonable assumption for a final boundary condition is to equate surface heat fluxes using constant bulk coolant temperature T_b surrounding the cladding. T_b will be a function of radial and axial positions in the core. But at any axial location, T_b surrounding any one fuel rod can generally be assumed constant. In terms of fuel surface and bulk coolant temperature, the heat flux is expressed by

$$(T_s - T_b) = q_s'' \left[\frac{1}{h_c(\theta)} + \frac{R_f}{K_c} \ln\left(\frac{R_o}{R_i}\right) + \frac{R_f}{R_o h_w} \right] \quad (\text{A.21})$$

or

$$q_s'' = \frac{(T_s - T_b)}{\left[\frac{1}{h_c(\theta)} + \frac{R_f}{K_c} \ln\left(\frac{R_o}{R_i}\right) + \frac{R_f}{R_o h_w} \right]} \quad (\text{A.22})$$

In addition, the fuel surface heat flux is given by

$$q_s'' = - K_f \left. \frac{dT}{dr} \right|_{r=R_f} \quad (\text{A.23})$$

so,

$$- K_f \left. \frac{dT}{dr} \right|_{r=R_f} = \frac{T_s - T_b}{\left[\frac{1}{h_c(\theta)} + \frac{R_f}{K_c} \ln\left(\frac{R_o}{R_i}\right) + \frac{R_f}{R_o h_w} \right]}$$

Normalizing this equation as in the preceding section

$$-\left. \frac{d\phi}{d\xi} \right|_{\xi=1} = \frac{\phi(1, \theta)}{\left[\frac{K_f}{R_f h_c(\theta)} + \frac{K_f}{K_c} \ln\left(\frac{R_o}{R_i}\right) + \frac{K_f}{R_o h_w} \right]}$$

Inserting Eq. A.20 yields

$$2 - \sum_{v=0}^{\infty} v a_v \cos v \theta = \frac{-1 + \sum_{v=0}^{\infty} a_v \cos v \theta}{\left[\frac{K_f}{R_f h_c(\theta)} + \frac{K_f}{K_c} \ln\left(\frac{R_o}{R_i}\right) + \frac{K_f}{R_o h_w} \right]} \quad (\text{A.24})$$

In order to solve for a_v , Eq. A.24 is multiplied by $\cos \lambda \theta$ and integrated from $-\pi$ to π taking advantage of the orthogonality of the cosine function.

$$\sum_{v=0}^{\infty} v a_v \int_{-\pi}^{\pi} \cos v \theta \cos \lambda \theta d\theta + \sum_{v=0}^{\infty} a_v \int_{-\pi}^{\pi} \frac{\cos v \theta \cos \lambda \theta d\theta}{\left[\frac{K_f}{R_f h_c(\theta)} + \frac{K_f}{K_c} \ln\left(\frac{R_o}{R_i}\right) + \frac{K_f}{R_o h_w} \right]} - \int_{-\pi}^{\pi} 2 \cos \lambda \theta d\theta - \int_{-\pi}^{\pi} \frac{\cos \lambda \theta d\theta}{\left[\frac{K_f}{R_f h_c(\theta)} + \frac{K_f}{K_c} \ln\left(\frac{R_o}{R_i}\right) + \frac{K_f}{R_o h_w} \right]} = 0 \quad (\text{A.25})$$

This equation yields n equations in n unknowns ($a_0 \rightarrow a_n$). Simultaneous solution of these n equations gives the values for a_v for use in Eq.

A.20.

Cladding Surface Temperature and Heat Flux

From the previous section, the method is discussed for determining the set of constants a_ν . Once they are obtained, the fuel temperature distribution by solving Eq. A.20. Heat flux at the fuel surface is obtained by

$$q_s'' = - \frac{K_f}{R_f} \left. \frac{d\phi}{d\xi} \right|_{\xi=1} = \frac{2 K_f}{R_f} - \sum_{\nu=0}^{\infty} \frac{K_f}{R_f} \nu a_\nu \cos \nu \theta \quad (\text{A.26})$$

To obtain the heat flux at the cladding surface, the geometry factor R_f/R_o is used.

$$q_w'' = q_s'' \frac{R_f}{R_o} \quad (\text{A.27})$$

Also,

$$q_w'' = h_w (T_c - T_b) \quad (\text{A.28})$$

So,

$$\left(\frac{R_f}{R_o} \right) \left[- K_f \left. \frac{d(T - T_b)}{dr} \right|_{r=R_f} \right] = h_w (T_c - T_b) \quad (\text{A.29})$$

In non-dimensional form, Eq. A.29 is given by

$$- \frac{K_f}{R_o} \left. \frac{d\phi}{d\xi} \right|_{\xi=1} = h_w \phi_c \quad (\text{A.30})$$

The cladding surface temperature can be calculated from Eq. A.30 in the form

$$\phi_c = \left(\frac{-K_f}{R_o h_w} \right) \left(-2 + \sum_{v=0}^{\infty} v a_v \cos v\theta \right) \quad (\text{A.31})$$

APPENDIX B

DETERMINATION OF GAP WIDTH

The expression used in this study for the angular dependent gap size is

$$L(\theta) = (R_i - R_f) - e \cos \theta \quad (\text{B.1})$$

This expression is an approximation derived by comparison with the exact values of $L(\theta)$ as determined by a computer program. This program was written in FOOL-F for use on the PDP-8 computer at Georgia Institute of Technology. The listing of this program appears at the end of this Appendix.

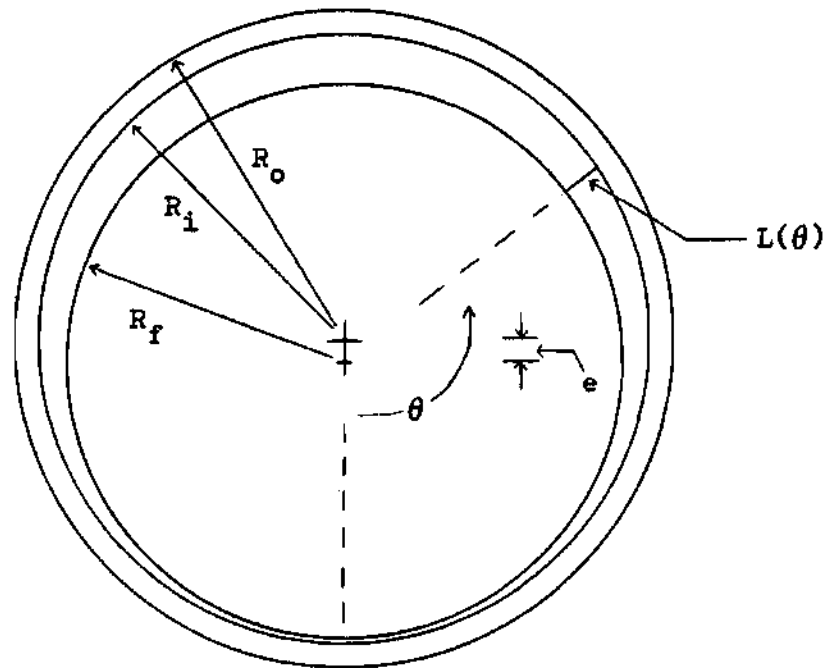
The solution for $L(\theta)$, as shown in Figure 29 is best obtained by using the Law of Cosines. The expression obtained is

$$L(\theta) = -R_f + \left(e^2 + R_i^2 - 2eR_i \cos \gamma \right)^{\frac{1}{2}} \quad (\text{B.2})$$

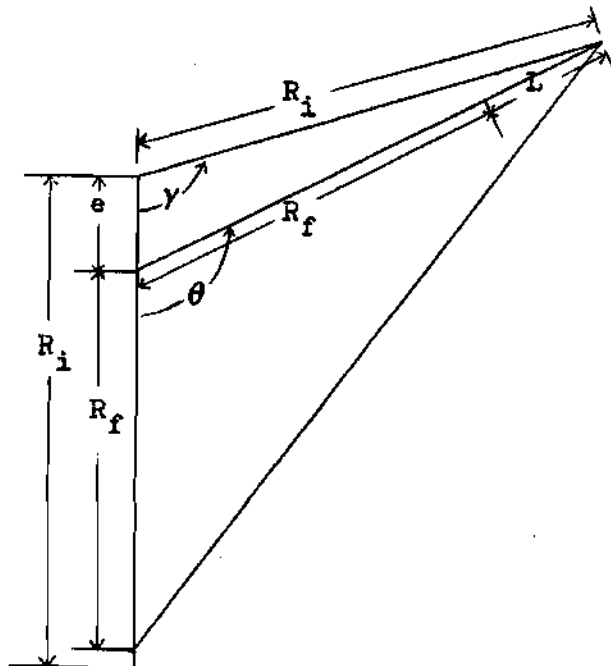
where

$$\cos \gamma = \frac{e \sin^2 \theta}{R_i} \pm \frac{1}{2} \left[\frac{4e^2 \sin^4 \theta}{R_i^2} - 4 \left(\frac{e^2 \sin^2 \theta}{R_i^2} + \sin^2 \theta - 1 \right) \right]^{\frac{1}{2}} \quad (\text{B.3})$$

Results for a sample run of this program appears in Table 9. Comparisons are made between Eq. B.1 and the exact value for $L(\theta)$.



a. Fuel-Cladding Cross Section



b. Angular Relationships

Figure 29. Gap Geometry

Table 9. Comparison Between Actual Values and Approximation Values of Gap Size

Theta	Exact $I(\theta)$	Equation (B.1)
0	1.5000	1.5000
10	1.5067	1.5072
20	1.5265	1.5301
30	1.5592	1.5669
40	1.6041	1.6160
50	1.6602	1.6726
60	1.7265	1.7304
70	1.8013	1.8142
80	1.8828	1.8917
90	1.9672	2.0000
100	2.0564	2.0852
110	2.1433	2.1610
120	2.2265	2.2388
130	2.3030	2.3213
140	2.3701	2.3830
150	2.4252	2.4331
160	2.4662	2.4698
170	2.4915	2.4924
180	2.5000	2.5000
190	2.4915	2.4924
200	2.4662	2.4698
210	2.4252	2.4331
220	2.3701	2.3830
230	2.3030	2.3213
240	2.2265	2.2388
250	2.1433	2.1610
260	2.0564	2.0852
270	1.9701	2.0000
280	1.8828	1.8917
290	1.8013	1.8142
300	1.7265	1.7304
310	1.6602	1.6726
320	1.6041	1.6160
330	1.5592	1.5669
340	1.5265	1.5301
350	1.5067	1.5072
360	1.5000	1.5000

As seen in all cases the agreement is within 1%. The program was run for numerous additional cases and consistently obtained accurate results.

The FOCOL program for gap-width determination follows. It solves Eq. B.2 for $L(\theta)$.

```

01.10 S E=.5
01.20 S RF=2; S RC=4
01.30 T%8.04
01.40 T"      T      A",!!!

02.10 FOR T=0,10,360;S TR=T*3.14159/180; DO 3
02.20 GOTO 4.1

03.10 S V1=(E )*(FSIN(TR) 4)/(RC 2)
03.11 S V2=(E 2)*(FSIN(TR) 2)/(RC 2)
03.12 S V3=(FSIN(TR) 2)
03.13 S V4=V1-V2-V3+1
03.14 S V9=FO(V4)
03.15 S V6=E*(FSIN(TR) 2)/RC
03.16 S V5=V9*FCOS(TR)/FABS(FCOS(TR))
03.20 S V7=(E 2)+(RC 2)
03.30 S A=-RF+FO(V7-2*E*RC*(V6+V5))
03.40 T T,"      ",A,!

04.10 QUIT
30.10 S Z'=FEXP(FLOG(A')/2)
30.20 LET FO=30

```

APPENDIX C

COMPUTER PROGRAM

The following is a listing of the computer program used for obtaining data for this investigation. Following the listing is a sample of the output that results from the program.

TEMP,MAIN
 07/24-13:32:25
 07)

```

000      FDD=1
000      READ(5,700)M999,KJJ
000      DIMENSION T(19),I(19),TF(19),A(10),TP(21),DW(19)
000      COMMON Z,DELR,G,E,F,V,CCC,CLK,CCH,RI,PO,PF
000      C      PRINT INTRODUCTION HERE
000      C      DATA INPUT
000      TF=0.0152167
000      CCLAD=1.01667E-3
000      M999=5000.0
000      DW=50000.0
000      M999=0
000      C      INITIALIZATION
000      C      INITIAL PARAMETER VALUES
000      READ(5,710)CG1,CG4,CCL1,GG1,DR1
000      C      FINAL PARAMETER VALUES
000      READ(5,720)CG4,DR4
000      C      PARAMETER RANGES
000      CG9=ABS(CG1-CG4)
000      DR9=ABS(DR1-DR4)
000      C      NUMBER OF POINTS
000      READ(5,730)CG99,DR99
000      C      INCREMENTS
000      CG88=CG9/CG99
000      DR88=DR9/DR99
000      JJJJ2=IFIX(CG99)+1
000      JJJJ4=IFIX(DR99)+1
000      DO 300 J2=1,JJJJ2
000      DO 500 J4=1,JJJJ4
000      J2=J2-1
000      J4=J4-1
000      R2=FLOAT(JJ2)
000      R4=FLOAT(JJ4)
000      C      PARAMETER VALUES
000      CG=CG1-CG88*R2
000      GG=GG1
000      DR=DR1+DR88*R4
000      CF=CG1
000      CCL=CCL1
000      CCC=CG/CF
000      CLK=CCL/CF
000      GO TO (2,4),KJJ
000      2 HW=HM93
000      GO TO 5
000      4 HW=HM5
000      5 CCH=HW/CF
000      RI=RT+DR
000      RW=RT+DCLAD
000      G=GG/HF
000      DELR=DIC/CF
000      FE=0.0

```

```

000 GO TO (6,11),N000
000 WRITE(6,7)M099
000 FORMAT(//////////,,'RUN CODE-',I2)
000 WRITE(6,9)HW
000 FORMAT(//,,'HW=',F12.6)
000 WRITE(6,9)G
000 FORMAT(//,,'G1+G2=',F12.6)
000 CONTINUE
000 WRITE(6,15)
000 FORMAT(14,1,'* * *')
000 N0002
000 M0000=MM0000+1
000 WRITE(6,20)M099,MM0000
000 FORMAT(5,,'RUN NUMBER',I3,1-',',I3)
000 F0000=10.0
000 F0000/RF
000 C FIND VALUES FOR INTEGRALS AND A(NU)
000 CALL INTEG(A)
000 C SOLVE THE SERIES
000 CALL SERIES(A,T1)
000 C SOLVE FOR TF(THETA)
000 CALL SUMS(T1,TF,TCENT)
000 C SOLVE FOR CLADDING OUTSIDE TEMPERATURE
000 CALL TCLA(TC,CCH,RO,A,TCENT,PE)
000 C SOLVE FOR CLADDING WALL HEAT FLUX
000 CALL FLUX(A,QCENT,OW)
000 C SOLVE FOR MAXIMUM TEMPERATURE
000 CALL TMX(A,IM,SOU)
000 C SOLVE FOR TEMPERATURE PROFILE
000 CALL PRFL(A,TP)
000 C PRINT RESULTS
000 CALL PRINT(TF,OW,TFCENT,QCENT,TC,TM,SOU,TP,TCENT)
000 PRINT TP,MAPS
000 C CALL TMAP(TF,A,TM)
000 N0000=12.0
000 F0000=0.001
000 TFEET=JRN)52,60,60
000 GO TO 10
000 CONTINUE
000 CONTINUE
000 CONTINUE
000 CONTINUE
000 FORMAT(2I2)
000 FORMAT(5F10.7)
000 FORMAT(3F10.7)
000 FORMAT(3E5.4)
000 FND
TFMP,F2
07/24-13:32:50
000 FUNCTION F2(THETA)
000 COMMON Z,DEL,R,G,E,V,CC,CCK,CCI,RI,RO,PE
000 Y1=(DEL+G-F+CC*(THETA))/CC
000 Y2=ALQ*(RO/RI)/CCK
000 Y3=1.0/(CCH+RO)
000 F2=(COS(7*THETA)+COS(V*THETA))/(X2+X3+X1)
000 RETURN
000 FND

```

```

TFMP,F4
RLI:60-G 07/24-13:32:37
(11)
000 FUNC=J0) F4(THETA)
000 COMMON Z,DELTA,G,E,V,CCC,CCK,CCH,RI,RO,RF
000 X1=(REL:16-E+COS(THETA))/CCC
000 X2=ALCG(RO/PI)/CCK
000 X3=1.0/(CCH+PO)
000 F4=CCS(7*THETA)/(X2+X3+Y1)
000 RETURN
000 FND

TFMP,INTFS
RLI:60-G 07/24-13:32:42
(12)
000 SUBROUTINE INTEG(A)
000 COMMON Z,DELTA,G,E,V,CCC,CCK,CCH,RI,RO,RF
000 EXTERNAL F4,F2
000 TIME=SI(A,A(10),FS(5),Sc(4)
000 AA=-3.14159
000 R=3.14159
000 HINTL=0.25
000 HMIN=0.00001
000 FPS=0.000001
000 N=0
000 Z=Z
000 V=V
000 TF(1)=30,30,50
000 V=0.0
000 V=0.0
000 S2=STEPIT(F2,AA,B,THETA,HINTL,HMIN,EPG,N,$100,FS,Sc)
000 S4=STEPIT(F4,AA,B,THETA,HINTL,HMIN,EPG,N,$100,FS,Sc)
000 A(1)=1(4,0=3.14159)+S4)/S2
000 A(2)=0.0
000 A(3)=0.0
000 A(4)=0.0
000 A(5)=0.0
000 A(6)=0.0
000 A(7)=0.0
000 A(8)=0.0
000 A(9)=0.0
000 A(10)=0.0
000 GO TO 75
000 V=0.0
000 V=0.0
000 S2=STEPIT(F2,AA,B,THETA,HINTL,HMIN,EPG,N,$100,FS,Sc)
000 S4=STEPIT(F4,AA,B,THETA,HINTL,HMIN,EPG,N,$100,FS,Sc)
000 V=1.0
000 S1=STEPIT(F2,AA,B,THETA,HINTL,HMIN,EPG,N,$100,FS,Sc)
000 V=2.0
000 S=STEPIT(F2,AA,B,THETA,HINTL,HMIN,EPG,N,$100,FS,Sc)
000 V=3.0
000 S7=STEPIT(F2,AA,B,THETA,HINTL,HMIN,EPG,N,$100,FS,Sc)
000 V=4.0
000 S=STEPIT(F2,AA,B,THETA,HINTL,HMIN,EPG,N,$100,FS,Sc)
000 V=5.0
000 S21=STEPIT(F2,AA,B,THETA,HINTL,HMIN,EPG,N,$100,FS,Sc)
000 V=6.0

```

000 C22ECTEPN1(F2,AA,B,THETA,HINTL,HMI,,EPS,N,\$100,FS,CS)
 000 V=7.0
 000 C23ECTEPN1(F2,AA,B,THETA,HINTL,HMI,,EPS,N,\$100,FS,CS)
 000 Z=1.0
 000 C26ECTEPN1(F2,AA,B,THETA,HINTL,HMI,,EPS,N,\$100,FS,CS)
 000 V=6.0
 000 C28ECTEPN1(F2,AA,B,THETA,HINTL,HMI,,EPS,N,\$100,FS,CS)
 000 V=5.0
 000 C24ECTEPN1(F2,AA,B,THETA,HINTL,HMI,,EPS,N,\$100,FS,CS)
 000 V=4.0
 000 C11ECTEPN1(F2,AA,B,THETA,HINTL,HMI,,EPS,N,\$100,FS,CS)
 000 C25ECTEPN1(F4,AA,B,THETA,HINTL,HMIN,EPG,M,\$100,FS,Sc)
 000 V=3.0
 000 C10ECTEPN1(F2,AA,B,THETA,HINTL,HMI,,EPS,N,\$100,FS,CS)
 000 V=2.0
 000 S9ESTEPN1(F2,AA,B,THETA,F,ANTL,HMIN,EPG,N,\$100,FS,SS)
 000 V=1.0
 000 C3ESTEPN1(F2,AA,B,THETA,HINTL,HMIN,EPG,N,\$100,FS,Sc)
 000 Z=2.0
 000 V=2.0
 000 S12ESTEPN1(F2,AA,B,THETA,HINTL,HMI,,EPS,N,\$100,FS,SS)
 000 C18ECTEPN1(F4,AA,B,THETA,HINTL,HMI,,EPS,N,\$100,FS,CS)
 000 V=3.0
 000 C13ECTEPN1(F2,AA,B,THETA,HINTL,HMI,,EPS,N,\$100,FS,CS)
 000 V=4.0
 000 C14ECTEPN1(F2,AA,B,THETA,HINTL,HMIN,FPG,N,\$100,FS,CS)
 000 V=5.0
 000 C27ECTEPN1(F2,AA,B,THETA,HINTL,HMI,,EPS,N,\$100,FS,CS)
 000 V=6.0
 000 C28ECTLPN1(F2,AA,B,THETA,HINTL,HMI,,EPS,N,\$100,FS,CS)
 000 V=7.0
 000 C29ECTEPN1(F2,AA,B,THETA,HINTL,HMI,,EPS,N,\$100,FS,CS)
 000 Z=3.0
 000 C2ECTEPN1(F2,AA,B,THETA,HINTL,HMI,,EPS,N,\$100,FS,CS)
 000 V=6.0
 000 C51ECTEPN1(F2,AA,B,THETA,HINTL,HMI,,EPS,N,\$100,FS,CS)
 000 V=5.0
 000 C30ECTEPN1(F2,AA,B,THETA,HINTL,HMI,,EPS,N,\$100,FS,CS)
 000 V=4.0
 000 C17ECTEPN1(F2,AA,B,THETA,HINTL,HMI,,EPS,N,\$100,FS,CS)
 000 V=3.0
 000 C16ECTEPN1(F2,AA,B,THETA,HINTL,HMI,,EPS,N,\$100,FS,CS)
 000 C16ECTEPN1(F4,AA,B,THETA,HINTL,HMI,,EPS,N,\$100,FS,CS)
 000 Z=4.0
 000 V=4.0
 000 C19ECTEPN1(F2,AA,B,THETA,HINTL,HMI,,EPS,N,\$100,FS,CS)
 000 C20ECTEPN1(F4,AA,B,THETA,HINTL,HMI,,EPS,N,\$100,FS,CS)
 000 V=5.0
 000 C33ECTEPN1(F2,AA,B,THETA,HINTL,HMI,,EPS,N,\$100,FS,CS)
 000 V=6.0
 000 C34ECTEPN1(F2,AA,B,THETA,HINTL,HMI,,EPS,N,\$100,FS,CS)
 000 V=7.0
 000 C35ECTEPN1(F2,AA,B,THETA,HINTL,HMI,,EPS,N,\$100,FS,CS)
 000 Z=5.0
 000 C36ECTEPN1(F2,AA,B,THETA,HINTL,HMI,,EPS,N,\$100,FS,CS)
 000 V=6.0
 000 C37ECTEPN1(F2,AA,B,THETA,HINTL,HMI,,EPS,N,\$100,FS,CS)

```

000 000 V=5,n
000 000 C36=CTPPI (F2,AA,B,THETA,INTL,HMI, EPS,N,SI00,FS,CS)
000 000 S39=STEPPI (F4,AA,B,THETA,INTL,HMI, EPS,N,SI00,FS,SS)
000 000 V=6,n
000 000 C40=CTEPII (F2,AA,B,THETA,INTL,HMI, EPS,N,SI00,FS,CS)
000 000 V=7,n
000 000 S41=STEPPI (F2,AA,B,THETA,INTL,HMI, EPS,N,SI00,FS,SS)
000 000 C42=CTEPII (F4,AA,B,THETA,INTL,HMI, EPS,N,SI00,FS,CS)
000 000 Z=7,n
000 000 C43=CTEPII (F2,AA,B,THETA,INTL,HMI, EPS,N,SI00,FS,CS)
000 000 S44=STEPPI (F4,AA,B,THETA,INTL,HMI, EPS,N,SI00,FS,SS)
000 000 F1=(C1/S2)-(13.14159)/(C1))-(S3/S1)
000 000 F2=(C6/S2)-(S9/S1)
000 000 F3=(C7/S2)-(S10/S1)
000 000 F4=(C8/S2)-(S11/S1)
000 000 F5=(C4/S2)+(4.0*3.14159/(S2))-(S5/C1)
000 000 F6=(C1/S2)-(S9/S6)
000 000 F7=(S6/S2)-(2.0*3.14159/(S6))-(S12/S6)
000 000 F8=(C7/S2)-(S13/S6)
000 000 F9=(C2/S2)-(S14/S6)
000 000 P10=(S4/C2)+(4.0*3.14159/(S2))-(S19/S6)
000 000 P11=(S1/C2)-(S10/S7)
000 000 P12=(S6/C2)-(S13/S7)
000 000 P13=(S7/C2)-(3.0*3.14159/(S7))-(S16/S7)
000 000 P14=(S3/C2)-(S17/S7)
000 000 P15=(S4/C2)+(4.0*3.14159/(S2))-(S16/S7)
000 000 P16=(S1/C2)-(S11/S8)
000 000 P17=(S6/C2)-(S14/S8)
000 000 P18=(S7/C2)-(S17/S8)
000 000 P19=(S8/C2)-(4.0*3.14159/(S8))-(S19/S8)
000 000 P20=(S5/C2)+(4.0*3.14159/(S2))-(S20/S8)
000 000 P21=(S1/C2)-(S24/S21)
000 000 P22=(S1/C2)-(S25/S22)
000 000 P23=(S1/C2)-(S26/S23)
000 000 P24=(S6/S2)-(S27/S21)
000 000 P25=(S6/S2)-(S28/S22)
000 000 P26=(S6/C2)-(S29/S23)
000 000 P27=(S7/S2)-(S30/S21)
000 000 P2A=(S7/S2)-(S31/S22)
000 000 P29=(S7/C2)-(S32/S23)
000 000 P30=(S3/C2)-(S33/S21)
000 000 P31=(S3/S2)-(S34/S22)
000 000 P32=(S6/C2)-(S35/S23)
000 000 P33=(S21/S2)-(S24/S1)
000 000 P34=(S21/S2)-(S27/S6)
000 000 P35=(S21/S2)-(S30/S7)
000 000 P36=(S21/S2)-(S33/S9)
000 000 P37=(S21/S2)-(5.0*3.14159/(S21))-(S36/S21)
000 000 P3A=(S21/S2)-(S37/S22)
000 000 P39=(S21/S2)-(S38/S23)
000 000 P40=(S22/S2)-(S25/S1)
000 000 P41=(S22/S2)-(S28/S6)
000 000 P42=(S22/S2)-(S31/S7)
000 000 P43=(S22/S2)-(S34/S8)
000 000 P44=(S22/S2)-(S37/S21)
000 000 P45=(S22/S2)-(6.0*3.14159/(S22))-(S40/S22)

```

000 r46=(S22/S2)-(S41/S23)
 000 r47=(S23/S2)-(S26/S1)
 000 r48=(S23/S2)-(S29/S6)
 000 r49=(S23/S2)-(S32/S7)
 000 r50=(S23/S2)-(S35/S9)
 000 r51=(S23/S2)-(S38/S21)
 000 r52=(S23/S2)-(S41/S22)
 000 r53=(S23/S2)-(7.0+3.14159/S23)-(S47/S23)
 000 r54=(4.0+3.14159/S2)+(S0/S2)-(S39/r21)
 000 r55=(4.0+3.14159/S2)+(S0/S2)-(S42/r22)
 000 r56=(4.0+3.14159/S2)+(S0/S2)-(S44/S22)
 000 rP1=(P2/r1)-(P7/P6)
 000 rP2=(P3/P1)-(P8/P6)
 000 rP3=(P4/r1)-(P9/P6)
 000 rP4=(P5/r1)-(P10/P6)
 000 rP5=(P2/r1)-(P12/P11)
 000 rP6=(P3/P1)-(P13/P11)
 000 rP7=(P4/r1)-(P14/P11)
 000 rP8=(P5/r1)-(P15/P11)
 000 rP9=(P2/r1)-(P17/P16)
 000 rP10=(P3/P1)-(P18/P16)
 000 rP11=(P4/P1)-(P19/P16)
 000 rP12=(P5/P1)-(P20/P16)
 000 rP13=(P2/P1)-(P24/P21)
 000 rP14=(P2/P1)-(P25/P22)
 000 rP15=(P2/P1)-(P26/P23)
 000 rP16=(P3/P1)-(P27/P21)
 000 rP17=(P3/P1)-(P28/P22)
 000 rP18=(P3/P1)-(P29/P23)
 000 rP19=(P4/P1)-(P30/P21)
 000 rP20=(P4/P1)-(P31/P22)
 000 rP21=(P4/P1)-(P32/P23)
 000 rP22=(P33/P1)-(P34/P6)
 000 rP23=(P33/P1)-(P35/P11)
 000 rP24=(P33/P1)-(P36/P16)
 000 rP25=(P33/P1)-(P37/P21)
 000 rP26=(P33/P1)-(P38/P22)
 000 rP27=(P33/P1)-(P39/P23)
 000 rP28=(P40/P1)-(P41/P6)
 000 rP29=(P40/P1)-(P42/P11)
 000 rP30=(P40/P1)-(P43/P16)
 000 rP31=(P40/P1)-(P44/P21)
 000 rP32=(P40/P1)-(P45/P22)
 000 rP33=(P40/P1)-(P46/P23)
 000 rP34=(P47/P1)-(P48/P6)
 000 rP35=(P47/P1)-(P49/P11)
 000 rP36=(P47/P1)-(P50/P16)
 000 rP37=(P47/P1)-(P51/P21)
 000 rP38=(P47/P1)-(P52/P22)
 000 rP39=(P47/P1)-(P53/P23)
 000 rP40=(P54/P1)-(P54/P21)
 000 rP41=(P54/P1)-(P55/P22)
 000 rP42=(P5/P1)-(P56/P23)
 000 rP43=(P2/r1)-(P6/P6P5)
 000 rP44=(P3/rP1)-(P7/PP5)
 000 rP45=(P4/rP1)-(P8/PP5)
 000 rP46=(P2/rP1)-(P10/PP9)

```

000      u5=(pp3/pp1)-(pp11/pp9)
000      u6=(pp4/pp1)-(pp12/pp9)
000      u7=(pp2/pp1)-(pp10/pp13)
000      u8=(pp2/pp1)-(pp17/pp14)
000      u9=(pp2/pp1)-(pp18/pp15)
000      u10=(pp3/pp1)-(pp19/pp13)
000      u11=(pp3/pp1)-(pp20/pp10)
000      u12=(pp3/pp1)-(pp21/pp15)
000      u13=(pp20/pp1)-(pp23/pp5)
000      u14=(pp20/pp1)-(pp24/pp0)
000      u15=(pp20/pp1)-(pp25/pp13)
000      u16=(pp20/pp1)-(pp26/pp10)
000      u17=(pp22/pp1)-(pp27/pp15)
000      u18=(pp21/pp1)-(pp29/pp5)
000      u19=(pp21/pp1)-(pp30/pp0)
000      u20=(pp20/pp1)-(pp31/pp13)
000      u21=(pp20/pp1)-(pp32/pp14)
000      u22=(pp20/pp1)-(pp33/pp15)
000      u23=(pp34/pp1)-(pp35/pp5)
000      u24=(pp34/pp1)-(pp36/pp0)
000      u25=(pp34/pp1)-(pp37/pp13)
000      u26=(pp34/pp1)-(pp38/pp14)
000      u27=(pp34/pp1)-(pp39/pp15)
000      u28=(pp4/pp1)-(pp40/pp13)
000      u29=(pp4/pp1)-(pp41/pp10)
000      u30=(pp4/pp1)-(pp42/pp15)
000      u01=(u2/u1)-(u5/u4)
000      u02=(u13/u1)-(u14/u4)
000      u03=(u18/u1)-(u19/u4)
000      u04=(u23/u1)-(u24/u4)
000      u05=(u3/u1)-(u6/u4)
000      u06=(u2/u1)-(u10/u7)
000      u07=(u13/u1)-(u15/u7)
000      u08=(u18/u1)-(u20/u7)
000      u09=(u23/u1)-(u25/u7)
000      u010=(u3/u1)-(u28/u7)
000      u011=(u2/u1)-(u11/u8)
000      u012=(u13/u1)-(u16/u8)
000      u013=(u18/u1)-(u21/u8)
000      u014=(u23/u1)-(u26/u8)
000      u015=(u3/u1)-(u29/u8)
000      u016=(u2/u1)-(u12/u9)
000      u017=(u13/u1)-(u17/u9)
000      u018=(u18/u1)-(u22/u9)
000      u019=(u23/u1)-(u27/u9)
000      u020=(u3/u1)-(u30/u9)
000      w1=(u12/u1)-(u07/u06)
000      w2=(u05/u1)-(u08/u06)
000      w3=(u04/u1)-(u09/u06)
000      w4=(u05/u1)-(u010/u06)
000      w5=(u12/u1)-(u012/u011)
000      w6=(u13/u1)-(u013/u011)
000      w7=(u04/u1)-(u014/u011)
000      w8=(u05/u1)-(u015/u011)
000      w9=(u12/u1)-(u017/u016)
000      w10=(u03/u01)-(u018/u016)
000      w11=(u04/u01)-(u019/u016)

```

```

000      W12=(U05/U01)-(U020/U016)
000      W13=(W2/W1)-(W6/W5)
000      W14=(W3/W1)-(W7/W5)
000      W15=(W4/W1)-(W8/W5)
000      W16=(W2/W1)-(W10/W9)
000      W17=(W3/W1)-(W11/W9)
000      W18=(W4/W1)-(W12/W9)
000      A(10)=0.0
000      A(9)=0.0
000      A(8)=(1/W13/W1)-(W16/W14)/((W12/W1)-(W15/W14))
000      A(7)=(W13-A(8)*W12)/W1
000      A(6)=(U04-A(8)*W3-A(7)*W1)/W1
000      A(5)=(U05-A(8)*U04-A(7)*U03-A(6)*U02)/U01
000      A(4)=(U3-A(8)*U23-A(7)*U10-A(6)*U1*-A(5)*U2)/U1
000      A(3)=(PP4-A(8)*PP34-A(7)*PP28-A(6)*PP2-
000      1A(5)+PP3-A(4)*PP2)/PP1
000      A(2)=(P5-A(3)*P47-A(7)*P40-A(6)+P3*-A(5)*P4-
000      1A(4)+P3-A(3)*P2)/P1
000      A(1)=(4.0*3.14159+S4-A(2)*S23-A(7)+S22-A(6)*S21-
000      1A(5)*S8-A(4)*S7-A(3)*S6-A(2)*S1)/S2
000      75 CONTINUE
000      90 FORMAT(
000      WRITE(6,92)
000      92 FORMAT(//,5Y,'COEFFICIENTS')
000      WRITE(6,90)A(1),A(2),A(3),A(4),A(5)
000      WRITE(6,90)A(6),A(7),A(8),A(9),A(10)
000      GO TO 200
000      100 WRITE(6,150)
000      150 FORMAT(5X,'STEP N1 ERROR-HMIN REACHED')
000      200 Z=Z
000      V=V
000      RETURN
000      END

```

TEMP.SERIES

RLI.60-G 07/24-13:32:58

14)

```

000      SUBROUTINE SERIES (A,T1)
000      COMMON Z,DELTA,G,E,V,CCC,CCK,CCH,RI,RO,RF
000      DIMENSION T1(19),A(10)
000      DO 30 J=1,10
000      THETA=FLOAT(J-1)*10.0*3.14159/180.0
000      TT1=(1)+A(2)*COS(THETA)+A(3)*COS(2.0*THETA)
000      TT2=TT1+A(4)*COS(3.0*THETA)
000      T1(J)=(TT2+A(5)*COS(4.0*THETA)
000      1+A(6)*COS(5.0*THETA)+A(7)*COS(6.0*THETA)+A(8)*COS(7.0*THETA)
000      30 CONTINUE
000      RETURN
000      END

```

TEMP.SUAT

RLI.60-G 07/24-10:37:06

09)

```

000      SUBROUTINE SUMT(T1,TF,ICENT)
000      COMMON Z,DELTA,G,E,V,CCC,CCK,CCH,RI,RO,RF
000      DIMENSION T1(10),TF(19)
000      DO 30 J=1,10
000      TF(J)=T1(J)-1.0
000      30 CONTINUE

```

```

000      IF (F)50,50,40
000      40 GO TO 60
000      50 TFCENT=TF(1)
000      60 RETURN
000      END
TEMP,HFLUX
ALIN69-G 07/24-13:37:10
15)
000      SUBROUTINE HFLUX(A,OWCENT,OW)
000      COMMON 7,DELRIG,EIV,CCC,CKK,CCH,RI,RO,RF
000      DIMENSION US(19),A(10),OW(19)
000      DO 40 J=1,19
000      DEG=FLOAT(J-1)*10.0*3.14159/180.0
000      C1(J)=2.0-A(2)*COS(DEG)-2.0+A(3)*COS(2.0*DEG)
000      C2(J)=3.0-A(4)*COS(3.0*DEG)
000      C3(J)=4.0-A(5)*COS(4.0*DEG)
000      C4(J)=5.0-A(6)*COS(5.0*DEG)-6.0*A(7)*COS(6.0*DEG)
000      C5(J)=7.0-A(8)*COS(7.0*DEG)
000      40 CONTINUE
000      DO 45 J=1,19
000      OW(J)=US(J)*RF/RO
000      45 CONTINUE
000      IF (F)50,50,60
000      50 OWCENT=OW(1)
000      60 RETURN
000      END
TEMP,TCLAD
ALIN69-G 07/24-13:37:15
14)
000      SUBROUTINE TCLAD(TC,CCH,RO,A,FCENT,E)
000      DIMENSION TC(19),A(10)
000      RDR=1.0/(CCH+RO)
000      DO 30 J=1,19
000      DEG=FLOAT(J-1)*10.0*3.14159/180.0
000      T1=A(2)*COS(DEG)-A(3)*2.0*COS(2.0*DEG)
000      T2=T1+A(4)*3.0*COS(3.0*DEG)-A(5)*4.0*COS(4.0*DEG)
000      T3=T2+A(6)*5.0*COS(5.0*DEG)-A(7)*6.0*COS(6.0*DEG)
000      T4=T3+A(8)*7.0*COS(7.0*DEG)
000      TC(J)=507*T4
000      30 CONTINUE
000      IF (F)60,60,70
000      60 TCENT=TC(1)
000      70 RETURN
000      END
TEMP,TMAX
ALIN69-G 07/24-13:37:22
04)
000      SUBROUTINE TMAX(A,TM,SQU)
000      DIMENSION A(10)
000      TM=0.0
000      DO 20 J=1,1001
000      SQU=J-1
000      RU=FLOAT(SQU)
000      CSQU=RU*0.001
000      T1=(CSQU**2.0)+A(1)-A(2)*SQU+A(3)+SQU*SQU
000      T2=T1-A(4)*(SQU**3.0)+A(5)*(SQU**4.0)
000      T3=T2-A(6)*(SQU**5.0)+A(7)*(SQU**6.0)-A(8)*(SQU**7.0)

```

```

000      TF(T*-T) 10.20,20
000      10 T=T
000      CQU=CQU1
000      20 CONTINUE
000      T=T+T
000      RETURN
000      END
TELEP,PRFL
07/24-13:33:24
061

```

```

000      SUBROUTINE PRFL(A,TP)
000      DIMENSION A(10),TP(21)
000      DO 30 J=1,11
000      .J=J-1
000      R=FLOAT(J)
000      CQ=1.0-R**0.1
000      TP(J)=A(1)+A(2)*SQ+(A(3)-1.0)*SQ*SQ+A(4)*(CQ**3.0)+A(5)*(SQ**4.0)
000      1-A(6)*(SQ**5.0)+A(7)*(SQ**6.0)+A(8)*(SQ**7.0)
000      30 CONTINUE
000      DO 40 J=12,21
000      .J=J-11
000      R=FLOAT(J)
000      CQ=K**0.1
000      TP(J)=A(1)-1(2)*SQ+(A(3)-1.0)*SQ*SQ-A(4)*(CQ**3.0)+A(5)*(SQ**4.0)
000      1-A(6)*(SQ**5.0)+A(7)*(SQ**6.0)-A(8)*(SQ**7.0)
000      40 CONTINUE
000      RETURN
000      END

```

```

TRAP,PRINT
ALLIAG-6 07/24-13:37:28
35)
000 CURCONTI,E,PRINT,TF,QW,TFCENT,QWCENT,TC,TM,SQU,TP,TCCENT)
000 COMMON Z,DELR,G,E,V,CCC,CK,CCH,RI,EO,PF
000 DIMENSION TC(10),TF(19),TF(21),QW(19)
000 WRITE(6,5)
000 5 FORMAT(2Y,1,-----)
000 WRITE(6,10)
000 10 FORMAT(2Y,1,PARAMETER DATA,/)
000 WRITE(6,12)CCC,TFCENT
000 12 FORMAT(10,12)K GAS/K FUEL =,F 12.6,15X,TFCENT =,F12.6)
000 WRITE(6,13)CK,TCCENT
000 13 FORMAT(10,13)K CLAD/K FUEL =,F12.6,14X,TCCENT =,F12.6)
000 WRITE(6,14)CCH,QWCENT
000 14 FORMAT(10,14)WALL/K FUEL =,F12.6,14X,QWCENT =,F12.6)
000 WRITE(6,15)DELR
000 15 FORMAT(10,15)DELR =,F12.6)
000 WRITE(6,16)G
000 16 FORMAT(10,16)G =,E14.6)
000 WRITE(6,20)E
000 20 FORMAT(10,20)E =,F10.6)
000 WRITE(6,100)
000 100 FORMAT(12Y,1,-----)
000 WRITE(6,110)
000 110 FORMAT(10,110)
000 1,1C,12X,TC/TCCENT,10X,1,1W/QWCENT,10X,1,1NU,TC/QWCENT)
000 DO 150 J=1,19
000 J1=(J-1)*10

```

```

000      TTT=TF(J)/TCENT
000      QQQ=QV(J)/QCENT
000      TTTC=TC(J)/TCENT
000      DELG=FLDQAT(J)*3.14159/180.0
000      QN=RE*TF(J)/(RO*(1+(DELR+G-E*COS(DELG))/CCC)+
000      1*(ALDQ(RO/RI)/CCK)+1.0/(CCH*RO)))
000      QN=QV/JQCENT
000      WRITE(6,120)J1,TF(J),TTT,TC(J),TTTC,QQQ,QN,
120  FORMAT(5Y,14,5X,F12.6,5Y,F12.6,5X,F12.6,5X,
000      F12.6,5X,F12.6,5X,F12.6)
000      150  CONTINUE
000      WRITE(6,200)TH
000      200  FORMAT(//,5X,'THE MAXIMUM TEMPERATURE = ',F14.7)
000      WRITE(6,250)SQ
000      250  FORMAT(5Y,'AT THETA = 180 AND RADIUS = ',F14.7)
000      WRITE(6,255)
000      255  FORMAT(//,1,'- - - - -')
000      WRITE(6,260)
000      260  FORMAT(15X,'TEMPERATURE PROFILE THROUGH FUEL')
000      WRITE(6,265)
000      265  FORMAT(//,8X,'RADIUS',15X,'TEMP',//)
000      DO 300 J=1,21
000      RE=LDAT(J-1)
000      SQ=1.0-R*0.1
000      WRITE(6,270)SQ,TP(J)
000      270  FORMAT(5Y,F10.6,10X,F10.6)
000      300  CONTINUE
000      RETURN
000      END

```

TEMP.TMAP

NLI1109-G

07/24-13:33:39

16)

```
000      SUBROUTINE TMAP(TF,A,TM)
000      DIMENSION TF(13),A(10),C(11,19),TTc(11),N(19)
000      PARAMETER
000      M=19
000      E=0.00001
000      T1=TF
000      T2=TF(19)
000      T3=T1-T2
000      T4=T3/6.0
000      DO 30 J=1,6
000      RJ=FLOAT(J)
000      TG=RJ*T4
000      T61=T1-TG
000      T16(J)=T61
000      X=RJ/6.0
000      DO 20 JJ=1,19
000      DEG=FLOAT(JJ-1)*10.0*3.14159/180.0
000      K=0
000      NN=0
000      1 FAP=(A(1)-TG)+A(2)*X*COS(DEG)+(A(3)+COS(2.0*DEG)-1.0)*X*X
000      FAX=FY+A(4)*COS(3.0*DEG)+(X**3.0)+A(5)*COS(4.0*DEG)*(X**4.0)
000      1+A(6)*COS(5.0*DEG)*(X**5.0)+A(7)*COS(6.0*DEG)*(X**6.0)
000      2+A(8)*COS(7.0*DEG)*(X**7.0)
000      FXP=A(2)*COS(DEG)+2.0*(A(3)*COS(2.0*DEG)-1.0)*X
000      FAXP=-FXP+3.0*(A(4)*COS(3.0*DEG)*X*X+0.0+A(5)*COS(4.0*DEG)*(X**3.0)
```

```

1+5.0+A(6)*COS(5.0*DEG)*(X**4.0)+6.0*A(7)*COS(6.0*DEG)*(X**5.0)
2+7.0*A(8)*COS(7.0*DEG)*(X**6.0)
  CALL NEWT1(X,FX,FXP,E,M,K)
  GO TO(1,2,3,4,4,4),K
2  C(J,J)=X
20 CONTINUE
30 GO,TINUE
50 LMM=MM+1
  MM=3
  TG=TF(5)
  TTG(MM)=TG
  DO 60 L=1,M
  DEG=FLOAT(L-1)*10.0+3.14159/160.0
  X=0.2
  K=0
  M=00
5  FX=(A(1)-TG)+A(2)*X*COS(DEG)+A(3)*COS(2.0*DEG)-1.0)*X
  FX=FX+A(4)*COS(3.0*DEG)*(X**3.0)+A(5)*COS(4.0*DEG)*(X**4.0)
  1+A(6)*COS(5.0*DEG)*(X**5.0)
  2+A(7)*COS(6.0*DEG)*(X**6.0)
  3+A(8)*COS(7.0*DEG)*(X**7.0)
  FXP=A(2)*COS(DEG)+2.0*(A(3)*COS(2.0*DEG)-1.0)*X
  FXP=FXP+3.0*A(4)*COS(3.0*DEG)*X+4.0*A(5)*COS(4.0*DEG)*(X**3.0)
  1+5.0*A(6)*COS(5.0*DEG)*(X**4.0)
  2+7.0*A(7)*COS(6.0*DEG)*(X**5.0)
  3+7.0*A(8)*COS(7.0*DEG)*(X**6.0)
  CALL NEWT1(X,FX,FXP,E,M,K)
  GO TO(5,6,3,4,4,4),K
6  S(MM,L)=X
60 CONTINUE
  IF(MMM-1)50,100,100
3  KJ=TE(6,200)
4  KJ=TE(6,210)K
200 FORMAT(5X,'NON-CONVERGENCE WITH 60 ITERATIONS')
210 FORMAT(5X,'ERROR RETURN- ERROR INDICATOR K=',I5)
100 KJ=TE(6,260)
260 FORMAT(10L,'DATA FOR TEMPERATURE MAPS')
  KJ=TE(6,280)
280 FORMAT(10X,'RADII FOR GIVEN TEMPERATURES AND ANGLES',/)
  DO 290 L=1,19
  H(L)=(L-1)*10
290 CONTINUE
  DO 400 J=1,11
  KJ=TE(6,300)TTG(J)
300 FORMAT(5X,'TEMPERATURE=',F10.6)
  KJ=TE(6,310)H(1),S(J,1),H(7),S(J,7),H(13),S(J,13)
  KJ=TE(6,310)H(2),S(J,2),H(8),S(J,8),H(14),S(J,14)
  KJ=TE(6,310)H(3),S(J,3),H(9),S(J,9),H(15),S(J,15)
  KJ=TE(6,310)H(4),S(J,4),H(10),S(J,10),H(16),S(J,16)
  KJ=TE(6,310)H(5),S(J,5),H(11),S(J,11),H(17),S(J,17)
  KJ=TE(6,310)H(6),S(J,6),H(12),S(J,12),H(18),S(J,18)
310 FORMAT(5X,I3,5X,F10.6,10X,I3,5X,F10.6,10X,I3,5X,F10.6)
  KJ=TE(6,320)H(19),S(J,19)
320 FORMAT(61X,I3,5X,F10.6,/)
400 CONTINUE
  RETURN
  END

```

```

TEMP.DAT
07/24-13:33:46
000 1 1
000 2.0 0.16 8.0 3.261E-5 0.0
000 0.016 5.0E-4
000 4.0 4.0
TEMP.MDG
07/24-13:33:53
000 IN TEMP.MAIN
000 IN TEMP.F2
000 IN TEMP.F4
000 IN TEMP.INTEG
000 IN TEMP.SERIES
000 IN TEMP.SUMT
000 IN TEMP.HEATX
000 IN TEMP.TCIAD
000 IN TEMP.TMAX
000 IN TEMP.PREL
000 IN TEMP.PRINT
000 IN TEMP.TMAP
000 LIR SYSTEM**MATHSTAT

```

THIS LISTING PRODUCED ON JULY 24, 1974

*** PLEASE RETURN THIS LISTING TO:
NEMDG

* * *
 RUN: NUMBER 6- 9

COEFFICIENTS
 1.6776 -4.20017 -7.96592-03 -5.27759-04 -4.43761-05
 -5.02966-06 -1.04329-07 -8.45095-06 0.00000 0.00000

 PARAMETER DATA

K GAS/K FUEL = .000000 TFCENT= .711175
 K CLAD/K FUEL = 4.000000 TCCENT= .005518
 H WALL/K FUEL = 25000.000000 GWCENT= 1.741177
 DELR= .024324
 G1+G2= .164938-02

E= .010011

THETA	TF	TF/TFCENT	TC	TC/TCCENT	QW/QWCENT	NU*TC/QWCENT
0	.488806	.687473	.005010	1.108975	1.108975	1.108975
10	.492496	.692549	.005000	1.106023	1.106023	1.106023
20	.503143	.707521	.004970	1.100539	1.100539	1.100573
30	.520397	.731656	.004927	1.090579	1.090579	1.090610
40	.543195	.763842	.004864	1.077568	1.077568	1.077561
50	.570317	.802694	.004795	1.062207	1.062207	1.062165
60	.602050	.846634	.004722	1.045246	1.045246	1.045225
70	.635699	.893921	.004642	1.027453	1.027453	1.027480
80	.670570	.942957	.004561	1.009548	1.009548	1.009586
90	.705432	.992121	.004480	.992122	.992122	.992121
100	.739554	1.039962	.004407	.975616	.975616	.975578
110	.771710	1.086181	.004330	.960374	.960374	.960349
120	.801181	1.126422	.004277	.946701	.946701	.946720
130	.827253	1.161285	.004233	.934560	.934560	.934096
140	.849343	1.194348	.004179	.923032	.923032	.923035
150	.866993	1.219157	.004144	.912297	.912297	.917263
160	.879858	1.237259	.004119	.911696	.911696	.911670
170	.887086	1.248256	.004103	.908284	.908284	.908705
180	.890314	1.251961	.004088	.907135	.907135	.907183

THE MAXIMUM TEMPERATURE = 1.7075491
 AT THETA = 180 AND RADIUS = .0990000

TEMPERATURE PROFILE THROUGH FUEL

RADIUS	TEMP
1.000000	.488886
.900000	.700582
.800000	.892082
.700000	1.063393
.600000	1.214519
.500000	1.345464
.400000	1.456232
.300000	1.546827
.200000	1.617253
.100000	1.667513
.000000	1.697611
-.100000	1.707549
-.200000	1.697331
-.300000	1.666959
-.400000	1.616438
-.500000	1.545769
-.600000	1.454955
-.700000	1.344000
-.800000	1.212906
-.900000	1.061676
-1.000000	.890314

DATA FOR TEMPERATURE MAPS

RADII FOR GIVEN TEMPERATURES AND ANGLES

TEMPERATURE= 1.571343

0	.266290	60	.309357	120	.409772
10	.269444	70	.323670	130	.425752
20	.272900	80	.339611	140	.439792
30	.278660	90	.356764	150	.451327
40	.286700	100	.374599	160	.459902
50	.296970	110	.392493	170	.465182
				180	.466969

TEMPERATURE= 1.435137

0	.420530	60	.465607	120	.565950
10	.421840	70	.483652	130	.581049
20	.425749	80	.497066	140	.594177
30	.432209	90	.514371	150	.604877
40	.441119	100	.532017	160	.612786
50	.452327	110	.549412	170	.617635
				180	.619276

TEMPERATURE= 1.293932

0	.537339	60	.584505	120	.684777
10	.538732	70	.599917	130	.699431
20	.542882	80	.616563	140	.712100
30	.549711	90	.633935	150	.722380
40	.559077	100	.651477	160	.729953
50	.570770	110	.668614	170	.734590
				180	.736153

TEMPERATURE= 1.162726

0	.635807	60	.684414	120	.784615
10	.637259	70	.700072	130	.798971
20	.641577	80	.716869	140	.811333
30	.648064	90	.734280	150	.821332
40	.658344	100	.751746	160	.828682
50	.670370	110	.768706	170	.833177
				180	.834691

TEMPERATURE= 1.026520

0	.722553	60	.772283	120	.872413
10	.724052	70	.789127	130	.886543
20	.728503	80	.805036	140	.898671
30	.735792	90	.822471	150	.908459
40	.745718	100	.839875	160	.915642
50	.758002	110	.856697	170	.920031
				180	.921509

TEMPERATURE= .890314					
0	.800974	60	.851636	120	.951695
10	.802512	70	.867631	130	.965641
20	.807075	80	.884629	140	.977582
30	.814533	90	.902080	150	.987198
40	.824663	100	.919430	160	.994247
50	.837160	110	.936138	170	.998552
				180	1.000001

TEMPERATURE= .866993					
0	.813726	60	.864537	120	.964580
10	.815269	70	.880551	130	.978499
20	.819851	80	.897563	140	.990410
30	.827336	90	.915017	150	1.000000
40	.837499	100	.932358	160	.000000
50	.850029	110	.949048	170	.000000
				180	.000000

TEMPERATURE= .801181					
0	.848786	60	.899986	120	1.000000
10	.850346	70	.916067	130	.000000
20	.854976	80	.933115	140	.000000
30	.862533	90	.950574	150	.000000
40	.872763	100	.967891	160	.000000
50	.885404	110	.984533	170	.000000
				180	.000000

TEMPERATURE= .705532					
0	.897544	60	.949275	120	.000000
10	.899126	70	.965440	130	.000000
20	.903822	80	.982535	140	.000000
30	.911477	90	1.000000	150	.000000
40	.921839	100	.000000	160	.000000
50	.934578	110	.000000	170	.000000
				180	.000000

TEMPERATURE= .602050					
0	.947734	60	1.000000	120	.000000
10	.949340	70	.000000	130	.000000
20	.954101	80	.000000	140	.000000
30	.961953	90	.000000	150	.000000
40	.972336	100	.000000	160	.000000
50	.985195	110	.000000	170	.000000
				180	.000000

TEMPERATURE= .520307					
0	.985741	60	.000000	120	.000000
10	.987364	70	.000000	130	.000000
20	.992174	80	.000000	140	.000000
30	1.000000	90	.000000	150	.000000
40	.000000	100	.000000	160	.000000
50	.000000	110	.000000	170	.000000
				180	.000000

APPENDIX D

DATA FOR CHAPTER V

* * *
 RUN NUMBER 3- 46

COEFFICIENTS
 2.1317 -.46735 -4.0198E-02 -5.48289-03 -9.29361-04
 -1.77302-04 -2.56528-05 -1.61237-04 0.00000 0.00000

 PARAMETER DATA

K GAS/K FUEL = .044000 TFCENT= 1.217775
 K CLAD/K FUEL = 4.000000 TCENT= .045176
 H WALL/K FUEL = 2500.000000 QWCENT= 1.791177
 DELR= .024324
 G1+G2= .212021-03

E= .016216

THETA	TF	TF/TFCENT	TC	TC/TCENT	QW/QWCENT	NU*TC/QWCENT
0	.617326	.506929	.058054	1.285045	1.285045	1.285045
10	.627985	.513682	.057690	1.276965	1.276965	1.276965
20	.638957	.541115	.055663	1.254266	1.254266	1.254266
30	.707000	.581060	.055142	1.220589	1.220589	1.220589
40	.770429	.632653	.053298	1.179769	1.179769	1.179769
50	.843739	.692993	.051266	1.134795	1.134795	1.134795
60	.923032	.759622	.049159	1.088163	1.088163	1.088163
70	1.007109	.827007	.047094	1.042438	1.042438	1.042438
80	1.090332	.895347	.045171	.999084	.999084	1.000000
90	1.170948	.961547	.043441	.961634	.961584	.961584
100	1.247125	1.024101	.041894	.927339	.927339	.926700
110	1.317437	1.081840	.040510	.896697	.896697	.896291
120	1.380552	1.133667	.039300	.869934	.869934	.870284
130	1.435250	1.179694	.038302	.847829	.847829	.847871
140	1.480670	1.215693	.037524	.830622	.830622	.830717
150	1.516490	1.245295	.036934	.817546	.817596	.817721
160	1.542466	1.266626	.036499	.807890	.807890	.807396
170	1.558325	1.279649	.036209	.801508	.801508	.801741
180	1.563675	1.284043	.036106	.799223	.799223	.799085

THE MAXIMUM TEMPERATURE = 2.1842082
 AT THETA = 180 AND RADIUS = .2250000

* * *
 RUN NUMBER 4- 46

COEFFICIENTS
 2.0898 -.47385 -4.15846-02 -5.80953-03 -1.01083-04
 -1.96966-04 -2.52533-05 -2.19822-04 0.00000 0.00000

 PARAMETER DATA

K GAS/K FUEL = .044000 TFCENT= 1.177116
 K CLAD/K FUEL = 4.000000 TCCENT= .004513
 H WALL/K FUEL =25000.000000 CWCENT= 1.741177
 DELK= .024324
 G14G2= .212821-03

E= .016216

THETA	TF	TF/TFCENT	TC	TC/TCCENT	GW/GWCENT	NU*TC/CWCENT
0	.567359	.481993	.005830	1.290463	1.290463	1.290463
10	.574303	.491288	.005799	1.281098	1.281098	1.281657
20	.610046	.518253	.005655	1.258378	1.258378	1.259209
30	.659752	.560481	.005528	1.223699	1.223699	1.224552
40	.723705	.614498	.005340	1.182012	1.182012	1.181772
50	.798115	.678281	.005133	1.135191	1.135191	1.135213
60	.879873	.747482	.004914	1.085612	1.085612	1.088187
70	.964467	.819347	.004707	1.041991	1.041991	1.042653
80	1.048843	.891027	.004513	.993874	.993874	.990736
90	1.130413	.960324	.004330	.960382	.960382	.960325
100	1.207418	1.025742	.004163	.926032	.926032	.925106
110	1.278506	1.086133	.004004	.895106	.894107	.894549
120	1.342320	1.143346	.003921	.867054	.867954	.869442
130	1.397563	1.187277	.003820	.845650	.846650	.846539
140	1.443384	1.226186	.003743	.828548	.828548	.828679
150	1.479414	1.255812	.003685	.815672	.816692	.816097
160	1.505618	1.277373	.003641	.805929	.806929	.805246
170	1.521877	1.292718	.003611	.799291	.799291	.799613
180	1.527110	1.297331	.003600	.796861	.796861	.797773

THE MAXIMUM TEMPERATURE = 2.1437486
 AT THETA = 180 AND RADIUS = .2200000

RUN NUMBER 5- 60

COEFFICIENTS
 2.3759 -1.48842 -4.24286-02 -5.73254-03 -9.54093-04
 -1.77045-04 -3.22667-05 -8.04009-05 0.00000 0.00000

PARAMETER DATA

A GAS/K FUEL = .026400 TCPCNT= 1.477480
 A CLAD/K FUEL = 4.000000 TCPCNT= .045498
 A WALL/K FUEL = 2500.000000 CXCNT= 1.743553
 HEIKZ .016216
 G1402Z .164938-02

Ez .910811

THETA	TF	TF/TCPCNT	TC	TC/TCPCNT	QC/CXCNT	QC/TC/TCPCNT
0	.838109	.567250	.959068	1.297463	1.297963	1.297523
10	.849211	.574770	.955678	1.298705	1.299705	1.298507
20	.861562	.584653	.957612	1.296075	1.296075	1.296525
30	.872844	.631119	.956049	1.291033	1.291033	1.291312
40	.890341	.675706	.954048	1.147043	1.147043	1.147043
50	1.075173	.707707	.951842	1.146651	1.146651	1.146257
60	1.150904	.704433	.949674	1.091203	1.091800	1.091631
70	1.245006	.843350	.947549	1.044212	1.044212	1.044417
80	1.333085	.902270	.945445	.999721	.999721	1.000009
90	1.417446	.969308	.943369	.959475	.959375	.959308
100	1.497102	1.013201	.942210	.920454	.920354	.920303
110	1.570466	1.062936	.940563	.891441	.891541	.891347
120	1.636201	1.107427	.939313	.864462	.864062	.864216
130	1.693147	1.145997	.938274	.840440	.841200	.841530
140	1.740612	1.178086	.937455	.820125	.820125	.820171
150	1.777903	1.213390	.936801	.804402	.804902	.804937
160	1.805027	1.221694	.936306	.799293	.799293	.799004
170	1.821443	1.232797	.936001	.795043	.795043	.795103
180	1.826900	1.236525	.935933	.790888	.790888	.791179

THE MAXIMUM TEMPERATURE = 2.4332192
 AT THETA = THU AND RADII'S = .2350000

* * *
 RUN NUMBER 6- 50

COEFFICIENTS
 2.3337 --.49456 -4.37432-02 -5.03603-03 -1.02102-04
 -1.76021-04 -3.53140-05 -1.02007-04 0.00000 0.00000

 PARAMETER DATA

K GAS/K FUEL = .026000 TFCENT= 1.436532
 K CLAD/K FUEL = 4.000000 TCCEMTE= .004550
 H WALL/K FUEL = 25000.000000 QWCENT= 1.753555
 DELR= .016216
 G1+G2= .164938-02

E= .010011

THETA	TF	TF/TFCENT	TC	TC/TCCEMTE	QW/QWCENT	NU*TC/QWCENT
0	.780012	.548552	.005929	1.303001	1.303001	1.302604
10	.799357	.556456	.005890	1.294531	1.294531	1.294780
20	.832400	.579451	.005780	1.270349	1.270349	1.270676
30	.884342	.615600	.005615	1.234140	1.234140	1.234510
40	.951424	.662306	.005415	1.190121	1.190121	1.190730
50	1.029548	.716600	.005195	1.141824	1.141824	1.141910
60	1.114666	.775943	.004969	1.092220	1.092220	1.092727
70	1.202976	.837417	.004740	1.043886	1.043886	1.044152
80	1.291134	.899786	.004545	.998043	.998043	.999233
90	1.376456	.958197	.004360	.958199	.958199	.958107
100	1.456965	1.014224	.004185	.921659	.921659	.921504
110	1.531075	1.065813	.004029	.889914	.889914	.889566
120	1.597453	1.112021	.003893	.862201	.862201	.862400
130	1.654956	1.152050	.003781	.839241	.839241	.839622
140	1.702767	1.185332	.003673	.821116	.821116	.821176
150	1.740433	1.211552	.003573	.807324	.807324	.806983
160	1.767685	1.230523	.003487	.797275	.797275	.796980
170	1.784242	1.242049	.003409	.790923	.790923	.791064
180	1.789807	1.245922	.003358	.788713	.788713	.789111

THE MAXIMUM TEMPERATURE = 2.3023745
 AT THETA = 180 AND RADIUS = .2375000

* * *
 RUN NUMBER 3- 64

COEFFICIENTS
 2.7830 -.64756 -7.12655-32 -1.19094-02 -2.40451-03
 -5.42677-04 -1.25186-04 -1.74216-04 0.00000 0.00000

 PARAMETER DATA

K GAS/K FUEL = .026000 TFCENT= 1.98892
 K CLAD/K FUEL = 4.000000 TCENT= .045175
 H WALL/K FUEL = 2500.000000 OCWCENT= 1.741177
 DELR= .024324
 G1+G2= .212821-03

E= .016216

THETA	TF	TF/TFCENT	TC	TC/TCENT	OW/OCWCENT	NU*TC/OCWCENT
0	1.054001	.529569	.064153	1.420064	1.420754	1.410405
10	1.070666	.538044	.063522	1.406254	1.406254	1.406044
20	1.110802	.562234	.051789	1.367722	1.367722	1.369146
30	1.193497	.699771	.059251	1.311548	1.311548	1.312051
40	1.298307	.647416	.054271	1.245502	1.245502	1.245513
50	1.396041	.701857	.053101	1.176076	1.176076	1.175516
60	1.512464	.760062	.050026	1.107345	1.107345	1.107042
70	1.630506	.819382	.047103	1.042644	1.042644	1.043009
80	1.746422	.877634	.044467	.984290	.984290	.984037
90	1.856964	.933185	.042157	.933173	.933173	.933185
100	1.959911	.986019	.040152	.888774	.888774	.888233
110	2.053578	1.032040	.038410	.850219	.850219	.849937
120	2.136918	1.073371	.036924	.817328	.817328	.817507
130	2.208458	1.109826	.035712	.789504	.789504	.789074
140	2.267552	1.139518	.034774	.766717	.766737	.766041
150	2.313356	1.162787	.034007	.749154	.750154	.750650
160	2.347264	1.179576	.033555	.742759	.740759	.742314
170	2.367546	1.189770	.033224	.735432	.735432	.735536
180	2.374357	1.193196	.033107	.732845	.732845	.733936

THE MAXIMUM TEMPERATURE = 2.8441514
 AT THETA = 180 AND RADIUS = .1047000

* * *
 RUN NUMBER 3- B2

COEFFICIENTS
 6.1571 -1.0652 -.16416 -3.56492-02 -8.96849-04
 -2.45365-03 -7.11329-04 -2.89988-04 0.00000 0.00000

 PARAMETER DATA

K GAS/K FUEL = .008000 TFCENT= 6.236766
 K CLAD/K FUEL = 4.000000 TCENT= .045176
 H WALL/K FUEL = 2500.000000 CWCENT= 1.741177
 DELR= .024324
 G1+G2= .212821-03

E= .016216

THETA	TF	TF/TCENT	TC	TC/TCENT	OW/OWCENT	NU*TC/OWCENT
0	3.879735	.622079	.080298	1.777443	1.777443	1.777509
10	3.914114	.627591	.078795	1.744165	1.744165	1.744047
20	4.012073	.643298	.074684	1.653166	1.653166	1.652988
30	4.160165	.667043	.067940	1.526023	1.526023	1.526207
40	4.341527	.695123	.062626	1.386247	1.386247	1.386562
50	4.540465	.728020	.056499	1.250641	1.250641	1.250529
60	4.744684	.760757	.050006	1.127483	1.127483	1.127380
70	4.945315	.792034	.046065	1.019666	1.019666	1.019610
80	5.136140	.823531	.041920	.927908	.927908	.928317
90	5.313047	.851497	.038474	.851546	.851546	.851897
100	5.473539	.877646	.035641	.789924	.789924	.789629
110	5.616696	.903578	.033304	.737194	.737194	.736774
120	5.741311	.928565	.031384	.694691	.694691	.694750
130	5.846983	.952509	.029851	.650772	.650772	.651228
140	5.933320	.975352	.028683	.63-920	.634920	.635103
150	6.000351	.992101	.027826	.615931	.615931	.615571
160	6.048312	.998790	.027216	.602434	.602434	.602045
170	6.077212	.994423	.026633	.593066	.593066	.594105
180	6.086884	.975974	.026700	.591015	.591015	.591499

THE MAXIMUM TEMPERATURE = 6.4039504
 AT THETA = 180 AND RADIUS = .4660000

 RUN NUMBER 3- 42

COEFFICIENTS

1.8071 -.34893 -2.36953-02 -2.64096-03 -3.73182-04
 -5.88627-05 2.29465-06 -1.37403-04 0.00000 0.00000

 PARAMETER DATA

K CAS/K FUEL = .044000 TFCENT= .849976
 K CLAD/K FUEL = 4.000000 TCCENT= .045408
 H WALL/K FUEL = 2500.000000 QACENT= 1.751565
 DELR= .016216
 G1+G2= .212421-03

E= .010811

THETA	TF	TF/TFCENT	TC	TC/TCCENT	QW/QACENT	NU*TC/QACENT
0	.431277	.907397	.054754	1.203491	1.204491	1.202734
10	.438558	.915964	.054527	1.199340	1.198340	1.198101
20	.449301	.945956	.053851	1.183816	1.182816	1.184401
30	.473435	.980527	.052869	1.162030	1.160030	1.162627
40	.537402	.932254	.051841	1.135030	1.135030	1.134050
50	.589462	.693002	.050244	1.104317	1.104317	1.103429
60	.647226	.761462	.048744	1.071357	1.071357	1.071073
70	.708177	.833170	.047229	1.038050	1.038050	1.038520
80	.769905	.905794	.045734	1.006234	1.006234	1.006476
90	.830433	.977004	.044454	.977057	.977057	.977005
100	.888279	1.047080	.043230	.950332	.950332	.949718
110	.942225	1.108928	.042126	.925898	.925898	.925522
120	.991072	1.165094	.041138	.904187	.904107	.904520
130	1.033695	1.216143	.040313	.886044	.886044	.886650
140	1.069291	1.262022	.039655	.871804	.871804	.871886
150	1.097461	1.291164	.039170	.860934	.860934	.860388
160	1.117987	1.315312	.038794	.852755	.852755	.852291
170	1.130962	1.330107	.038551	.847331	.847331	.847554
180	1.134814	1.335109	.038463	.845381	.845381	.846006

THE MAXIMUM TEMPERATURE = 1.8368585
 AT THETA = 180 AND RADIUS = .1710000

APPENDIX E

NOMENCLATURE

a_v	Constants obtained from Equation (A.20)
e	Degree of eccentricity
$g_1 + g_2$	Temperature jump distance
G	Normalized temperature jump distance ($g_1 + g_2 / R_f$)
$h_c(\theta)$	Contact heat-transfer coefficient
K_c	Thermal conductivity of cladding
K_f	Thermal conductivity of fuel
K_g	Thermal conductivity of gas in gap
q_s''	Fuel surface heat flux
q_w''	Cladding surface heat flux
$q_w''(\text{conc})$	Cladding surface heat flux for concentric fuel pellet
q'''	Volumetric heat generation
r	Radius
R_f	Radius of fuel
R_i	Cladding inner radius
R_o	Cladding outer radius
T_c	Cladding surface temperature
T_f	Fuel surface temperature
$T_c(\text{conc})$	Cladding surface temperature for concentric fuel pellet
$T_f(\text{conc})$	Fuel surface temperature for concentric fuel pellet
$\Delta r / R_f$	Normalized radial difference ($(R_i - R_f) / R_f$)

ϵ	Normalized eccentricity (e/R_f)
ξ	Normalized radius (r/R_f)
ϕ	Normalized temperature $\left(\frac{T - T_b}{q''' R_f^2 / 4K_f} \right)$
ϕ_c	Normalized cladding surface temperature
ϕ_f	Normalized fuel surface temperature
$\phi_c(\text{conc})$	Normalized cladding surface temperature for concentric fuel pellet
$\phi_f(\text{conc})$	Normalized fuel surface temperature for concentric fuel pellet
θ	Angular measurement

BIBLIOGRAPHY

1. Duncomb, E., C. M. Friedrich, and J. K. Fischer: "CYGRO-3-A Computer Program to Determine Temperature, Stresses, and Deformation in Oxide Fuel Rods," WAPD-TM-961 (1970).
2. "FIGRO- Fortran IV Digital Computer Program for the Analysis of Fuel Swelling and Calculation of the Temperature in Bulk-oxide Cylindrical Fuel Elements," WAPD-TM-618 (1966).
3. Homan, F. J., W. J. Lackey, and C. M. Cox: "FMODEL- A Fortran IV Computer Code to Predict In-Reactor Behavior of LMFBR Fuel Pins," ORNL-4835 (1973).
4. "TAFY, Fuel Pin Temperatures and Gas Pressure Analysis," BAW-311 (1966).
5. Marlowe, M. O.: "Predicting In-Reactor Densification Behavior of UO_2 ," Trans. Am. Nucl. Soc., 17, 166 (1973).
6. Rubenstein, L. S., and D. F. Ross: "Impact of Fuel Densification on the U.S. LWR Industry," Trans. Am. Nucl. Soc., 18, 120 (1974).
7. Nijsing, R.: "Temperature and Heat Flux Distribution in Nuclear Fuel Element Rods," Nuclear Engineering and Design, 4, 1-20 (1966).
8. Brook, A. J.: "The Problem of Eccentrically Mounted Fuel Pellets," Nuclear Engineering and Design, 4, 429-431 (1966).
9. Grillo, P. and G. Testa: "Dependence of Heat Flux Distributions on Fissile Material Distribution in Fuel," Nuclear Applications, 5, 130-139 (1968).
10. Wolf, Lothar and Klaus Johannsen: "An Analysis of the Two-dimensional Temperature Distribution in Eccentrically Mounted Cylinders with Special Application to Sodium-bonded Reactor Fuel Elements," Fourth International Heat Transfer Conference Proceedings 1970, 1, Cu. 1.7 (1970).
11. Nijsing, R.: "Temperature and Heat Flux Distribution in Nuclear Fuel Element Rods," Nuclear Engineering and Design, 4, 1-20 (1966).
12. Ross, A. M. and R. L. Stoute: "Heat Transfer Coefficient Between Uranium Dioxide and Zircaloy 2," AECL-1552 (1962).

13. Tong, L. S. and J. Weisman: Thermal Analysis of PWR, Am. Nucl. Soc., Hinsdale, Illinois (1970).
14. Dean, R. A.: "Thermal Contact Conductance," M.S. Thesis, University of Pittsburgh (1963).
15. Wassiljewa, A.: Phys. Z., 5, 737 (1904).
16. Hirschfelder, Joseph O., Charles F. Curtis, and R. Byron Bird: Molecular Theory of Gases and Liquids, John Wiley and Sons, New York, 534 (1954).
17. Lindsay, Alexander L. and LeRoy A. Bromley: "Thermal Conductivity of Gas Mixtures," Industrial and Engineering Chemistry, 42, 1508-1511 (1950).
18. Srivastava, B. N. and S. C. Saxena: "Thermal Conductivity of Binary and Ternary Rare Gas Mixtures," Proc. Phys. Soc. B, 70, 369-378 (1957).
19. Srivastava, B. N. and S. C. Saxena: "Formulas for Thermal Conductivity of Ternary Gas Mixtures," J. Chem. Phys., 27, 583-584 (1957).
20. Von Ubisch, H., S. Hall, and R. Srivastav: "Thermal Conductivities of Mixtures of Fission Product Gases with Helium and Argon," Proceedings of the Second United Nations International Conference on the Peaceful Uses of Atomic Energy, 7, 698-700 (1958).
21. Zysin, Yu A., A. A. Ibov, and L. I. Sel'chenkov: Fission Product Yields and their Mass Distributions, Consultant's Bureau Enterprises, Inc., New York (1964).
22. El-Wakil, M. M.: Nuclear Heat Transport, International Textbook Company, Scranton, Pennsylvania (1971).
23. Nijsing, R.: "Temperature and Heat Flux Distribution in Nuclear Fuel Element Rods," Nuclear Engineering and Design, 4, 1-20 (1966).
24. Carslaw, H. S. and J. C. Jaeger: Conduction of Heat in Solids, Clarendon Press, Oxford, 339 (1947).
25. Fagan, J. R. and J. O. Mingle: "The Effect of Axial Heat Conduction in Fuel Plates in Maximum Heat Flow Rates and Temperatures," Nuclear Science and Engineering, 18, 443-447 (1964).
26. Thorpe, J. F.: "Axial Heat Conduction in Reactor Fuel Elements," Nuclear Science and Engineering, 23, 329 (1965).
27. Ozisik, M. Necati: Boundary Value Problems of Heat Conduction, International Textbook Company, Scranton, Pennsylvania, 181 (1968).